SCALABLE COLUMN GENERATION MODELS AND ALGORITHMS FOR OPTICAL NETWORK PLANNING PROBLEMS

Hai Anh Hoang

A thesis
in
The Department
of
Computer Science

Presented in Partial Fulfillment of the Requirements
For the Degree of Doctor of Philosophy
Concordia University
Montréal, Québec, Canada

August 2014

Concordia University
School of Graduate Studies

This is to certify that the thesis prepared

By: **Mr. Hai Anh Hoang**

Entitled: **Scalable Column Generation Models and Algorithms for Optical Network Planning Problems**

and submitted in partial fulfillment of the requirements for the degree of

Doctor of Philosophy (Computer Science)

complies with the regulations of this University and meets the accepted standards with respect to originality and quality.

Signed by the final examining commitee:

____________________ Chair

____________________ Dr. Didier Colle, External Examiner

____________________ Dr. Brigitte Jaumard, Thesis Supervisor

____________________ Dr. Jaroslav Opatrny, Examiner

____________________ Dr. Hovhannes A. Harutyunyan, Examiner

____________________ Dr. John Xiupu Zhang, Examiner

Approved ______________________________
Chair of Department or Graduate Program Director

__________ 20 _____ ____________________________

Dr. Christopher W. Trueman, Interim Dean
Faculty of Engineering and Computer Science

Abstract

Scalable Column Generation Models and Algorithms for Optical Network Planning Problems

Hai Anh Hoang, Ph.D.
Concordia University, 2014

Column Generation Method has been proved to be a powerful tool to model and solve large scale optimization problems in various practical domains such as operation management, logistics and computer design. Such a decomposition approach has been also applied in telecommunication for several classes of classical network design and planning problems with a great success.

In this thesis, we confirm that Column Generation Methodology is also a powerful tool in solving several contemporary network design problems that come from a rising worldwide demand of heavy traffic (100Gbps, 400Gbps, and 1Tbps) with emphasis on cost-effective and resilient networks. Such problems are very challenging in terms of complexity as well as solution quality. Research in this thesis attacks four challenging design problems in optical networks: design of p-cycles subject to wavelength continuity, design of dependent and independent p-cycles against multiple failures, design of survivable virtual topologies against multiple failures, design of a multirate optical network architecture. For each design problem, we develop a new mathematical models based on Column Generation Decomposition scheme.

Numerical results show that Column Generation methodology is the right choice to deal with hard network design problems since it allows us to efficiently solve large scale network instances which have been puzzles for the current state of art. Additionally, the thesis reveals the great flexibility of Column Generation in formulating design problems that have quite different natures as well as requirements.

Obtained results in this thesis show that, firstly, the design of p-cycles should be under a wavelength continuity assumption in order to save the converter cost since the difference between the capacity requirement under wavelength conversion vs. under wavelength continuity is insignificant. Secondly, such results which come from our new general design model for failure dependent p-cycles prove the fact that

failure dependent p-cycles save significantly spare capacity than failure independent p-cycles. Thirdly, large instances can be quasi-optimally solved in case of survivable topology designs thanks to our new path-formulation model with online generation of augmenting paths. Lastly, the importance of high capacity devices such as 100Gbps transceiver and the impact of the restriction on number of regeneration sites to the provisioning cost of multirate WDM networks are revealed through our new hierarchical Column Generation model.

Acknowledgments

First and foremost, I would like to express my sincerest and earnest gratitude to my supervisor, Dr. Brigitte Jaumard for her guidance, support, and enthusiasm throughout my PhD study at Concordia University. Her immense knowledge, helpful suggestions and comments as well as encouragements make this research possible. I am grateful to her for the valuable time she puts in the discussions on my research projects. I would like to thank to Dr. Christine Tremblay for her suggestions and close collaboration on chapter 7.

I deeply appreciate my thesis committee for their prompt evaluation and comments. Their valuable feedbacks and questions improve my thesis work. I also would like to thank my lab mates for the delightful environment that they have provided me with.

Last but not least, I would like to extend the deepest gratitude to my dear family for their moral support and inspiration. I am greatly indebted to my mother and my brother for their unconditional encouragement and love and to my fiance for her understanding, patience, and care during all these years.

Contents

List of Figures **x**

List of Tables **xi**

List of Acronyms **xii**

List of Publications **xiv**

1 Introduction **1**

1.1 Background 1

1.2 Research projects 3

1.2.1 Design of p-cycles subject to wavelength continuity 4

1.2.2 Design of dependent and independent p-cycles against multiple failures 5

1.2.3 Design of survivable virtual topologies against multiple failures 6

1.2.4 Design of a multirate optical network architecture 7

1.3 Contributions 8

1.4 Plan of thesis 10

2 Optical network background **11**

2.1 Equipment and physical aspects 11

2.2 Cross-layer design 14

2.3 Survivability and main protection schemes 15

2.4 Column generation methodology 18

2.4.1 A single pricing CG algorithm 18

2.4.2 A multiple pricing CG algorithm 19

3 Literature review **21**
3.1 The RWA problem with p-cycles and wavelength conversion 21
3.2 Multiple link failures in WDM networks 24
3.3 Survivable logical topology design 27
3.4 Multirate cross-layer optical network design 30
3.5 Conclusion 33

4 Design of p-cycles subject to wavelength continuity **34**
4.1 Problem statement 34
4.2 Notion of configuration 36
4.3 Definitions and notations 37
4.4 Decomposition model for p-cycles with wavelength continuity assumption 39
4.4.1 Master problem 39
4.4.2 Pricing problem 40
4.5 Decomposition model for p-cycles without wavelength continuity assumption 42
4.5.1 Master problem 42
4.5.2 Working path pricing problem 42
4.5.3 p-Cycle pricing problem 43
4.6 Decomposition model for FIPP p-cycles with wavelength continuity assumption 43
4.7 Decomposition model for FIPP p-cycles without wavelength continuity assumption 45
4.7.1 Master problem 45
4.7.2 FIPP p-cycles pricing problem 46
4.8 Numerical results 47
4.9 Conclusion 50

5 Design of dependent and independent p-cycles against multiple failures **51**
5.1 Definitions and notations 52
5.2 FDPP p-cycle decomposition model 55
5.2.1 Master problem 55
5.2.2 Pricing problem 55

5.3 Solution enhancements 57
5.3.1 Speed up pricing problem 57
5.3.2 Memory management 58
5.4 Insights into the proposed model 59
5.4.1 Compare with the previously proposed model 59
5.4.2 As a node protection framework 60
5.4.3 An example where FDPP solution exists but FIPP solution does not 61
5.5 Numerical results 62
5.5.1 Network and data instances 63
5.5.2 Performance of the FDPP p-cycle model: single link failure . . 63
5.5.3 Performance of the FDPP p-cycle model: dual link failure . . 64
5.5.4 FDPP p-cycle model: node protection 66
5.5.5 FDPP p-cycle model: triple & quadruple link failure 67
5.6 Conclusion 68

6 Design of survivable virtual topologies against multiple failures 69
6.1 The decomposition model 73
6.1.1 Definitions and notation 73
6.1.2 Variables 75
6.1.3 Master problem 76
6.1.4 Pricing problem 78
6.1.5 Solving multi-level ILP objective 80
6.1.6 Computing the required spare capacity for a successful IP restoration 81
6.2 Numerical results 82
6.2.1 Data instances 82
6.2.2 Transport capacity and link dimensioning 83
6.2.3 Quality of solutions 86
6.2.4 Networking performances 87
6.3 Conclusion 89

7 Design of a multirate optical network architecture 91
7.1 Problem description 92

7.2 Cost model 94
7.3 Decomposition model 95
7.3.1 Definitions and notations 96
7.3.2 Master model 98
7.3.3 Pricing I: generation of wavelength configurations (γ) 99
7.3.4 Pricing II: generation of multi-hop path configuration (π) . . . 100
7.3.5 Adaptation to undirected model 101
7.4 Solution of the models 101
7.5 Numerical experiments 102
7.5.1 Data instances 103
7.5.2 Impact of traffic volume and physical constraints on CAPEX . 107
7.6 Conclusion 113
7.7 Future work 113

8 Conclusion and future works **115**
8.1 Conclusion 115
8.2 Future works 116

Bibliography **118**

List of Figures

2.1 Multiplexer and demultiplexer. 12
2.2 A model of optical switch where a wavelength is either bypassed, converted, added or dropped 13
2.3 A single pricing CG algorithm 19
2.4 A multiple pricing CG algorithm 20
4.1 An unfeasible protection solution 35
4.2 Configuration decomposition of a WDM network 36
5.1 ILP & column generation algorithm 58
5.2 A backup cycle 60
5.3 A node failure 61
5.4 Transformation of a node failure into a link failure 61
5.5 FDPP vs FIPP 62
5.6 Number of selected/generated configurations 65
5.7 R_2 ratio vs. capacity redundancy 66
6.1 A survivable mapping example 70
6.2 Explain why redundancy ratio is a significantly large number. 88
7.1 A simple multirate optical network 94
7.2 Outline of the solution process 102
7.3 Traffic demand distribution 105
7.4 US-24 network 106
7.5 Average of transceiver percentages of 750km, 1500km and 3000km . . 107
7.6 Average of transceiver percentages of 10Gbps, 40Gbps and 100Gbps . 109
7.7 Comparison of percentages of transceivers grouped by bit-rate that is made between the case of maximum 12 regenerable sites and of maximum 24 regenerable sites 111
7.8 Cost comparison between different amount of maximum regenerable sites112

List of Tables

3.1 Characteristics of studies in the static p-cycle RWA problem 24
3.2 Characteristics of studies in multiple link failures 27
3.3 Characteristics of studies in survivable virtual topology 29
3.4 Characteristics of studies in multirate cross-layer optical network design 32
4.1 Characteristics of the data sets tested with the p-cycle model 47
4.2 Results obtained under a joint-optimization scheme with/without wavelength conversion capacity for the p-cycle model 48
4.3 Results obtained under a joint-optimization scheme with/without wavelength conversion capacity for the FIPP p-cycle model 49
5.1 Description of Network Instances 63
5.2 Comparison of FIPP p-cycle models vs. FDPP p-cycle models. 64
5.3 Accuracy of the Solutions 65
5.4 Node protection solutions 67
5.5 High order link protection scenario description 67
5.6 Higher order link protection scenario 68
6.1 Routing bandwidth and additional bandwidth 72
6.2 Network Topologies 83
6.3 Performance of the decomposition model 84
6.4 Existence and dimensioning of a survivable logical topology (single-link failures) 85
6.5 Multiple failure set scenarios 88
6.6 Existence and dimensioning of a survivable logical topology (multiple-link failures & $|V_{\text{P}}| = 1/2|V_{\text{L}}|$) 89
7.1 Cost model (MTD = Maximum Transmission Distance). 95
7.2 Traffic load vs. co 104
7.3 Statistics of the percentage average 108

List of Acronyms

CG Column Generation

LP Linear Programming

ILP Integer Linear Programming

MP Master Problem

RMP Restricted Master Problem

OC Optical Carrier

Gbps Gigabits per second

Tbps Terabits per second

WDM Wavelength-Devision Multiplexing

OXC Optical Cross Connect

RWA Routing Wavelength Assignment

IP Internet Protocol

LSP Label Switching Path

MPLS Multi-Protocol Label Switching

FDPP Failure-Dependent Path Protection

FIPP Failure-Independent Path Protection

SRLG Shared Risk Link Group

MTR Maximum Transmission Reach

CAPEX Capital Expenditure

OPEX Operating Expense

List of Publications

Manuscripts to be submitted

[Jaumard and **Hoang Hai Anh**] Brigitte Jaumard and **Hoang Hai Anh**. **Design and Dimensioning of Logical Survivable Topologies against Multiple Failures**. In *Journal of Optical Communications and Networking*.

[**Hoang Hai Anh** and Jaumard] **Hoang Hai Anh** and Brigitte Jaumard. **Design of a multirate optical network architecture**. In *Journal of Optical Communications and Networking*.

Published manuscripts

[Jaumard et al., 2013] Brigitte Jaumard, **Hoang Hai Anh**, and Do Trung Kien. **Robust FIPP p-cycles against dual link failures**. *Telecommunication Systems*, pages 1–12, 2013.

[Jaumard and **Hoang Hai Anh**, 2013] Brigitte Jaumard and **Hoang Hai Anh**. **Design and Dimensioning of Logical Survivable Topologies Against Multiple Failures**. In *Journal of Optical Communications and Networking*, pages 23–36, 2013.

[Jaumard et al., 2012] Brigitte Jaumard, **Hoang Hai Anh**, and Bui Nguyen Minh. **Path vs. Cutset approaches for the design of logical survivable topologies**. In *IEEE International Conference on Communications (ICC)*, pages 3061–3066, 2012.

[Jaumard and **Hoang Hai Anh**, 2012] Brigitte Jaumard and **Hoang Hai Anh**. **Design of Survivable IP-over-WDM Networks (invited)**. In *The Fourth International Conference on Communications and Electronics*, pages 13–18, 2012.

[**Hoang Hai Anh** and Jaumard, 2011a] **Hoang Hai Anh** and Brigitte Jaumard. **RWA and p-Cycles**. In *Ninth Annual Communication Networks and Services Research Conference (CNSR)*, pages 195–201, May 2011a.

[**Hoang Hai Anh** and Jaumard, 2011b] **Hoang Hai Anh** and Brigitte Jaumard. **Design of p-Cycles under a Wavelength Continuity Assumption**. In *IEEE International Conference on Communications (ICC)*, pages 1–5, June 2011b.

[**Hoang Hai Anh** and Jaumard, 2011c] **Hoang Hai Anh** and Brigitte Jaumard. **A New Flow Formulation for FIPP p-Cycle Protection subject to Multiple Link Failures (Best Paper Award)**. In *3rd International Congress on Ultra Modern Telecommunications and Control Systems and Workshops (ICUMT)*, pages 1–7, October 2011c.

[Jaumard et al., 2011] Brigitte Jaumard, **Hoang Hai Anh**, and Bui Nguyen Minh. **Using decomposition techniques for the design of survivable logical topologies**. In *5th International Conference on Advanced Networks and Telecommunication Systems (ANTS)*, pages 1–6, December 2011.

Chapter 1

Introduction

1.1 Background

The growth rate of traffic over the global IP backbone network is expected to be increased by approximately a factor of 12 over next decade [Korotky, 2012; Cisco, 2013]. To answer to the significant traffic demand that is coming, a new generation of high-speed optical devices (100Gbps, 400Gbps, and 1Tbps) has been intensively studied and start being commercialized. Heavy traffic volume and a wide range of new optical equipment are two complexity factors that make the mission of planning a reasonable road map to upgrade the current backbone infrastructure more difficult.

Optical backbone networks are built on wavelength-devision multiplexing (WDM) technology which allows transmission of multiple non-overlapped wavelengths over a single-mode fiber, thus increases the transmission capacity. Currently, commercial optical fibers can support over a hundred wavelength channels, each of which can have transmission speeds of a few units to few tens of gigabits per second such as OC-48 (2.5 Gbps), OC-192 (10 Gbps), OC-768 (40 Gbps), and recently 100 Gigabit Ethernet [Higginbotham]. Theoretically, the potential bandwidth of a single mode fiber is about 50 terabits per second (Tbps) [Zheng and Mouftah, 2004]. Certainly, this potential bandwidth is still far from the current available electronic processing speed of up to hundreds gigabits per second (Gbps).

Provisioning cost and network reliability are often the most concerns of a network designer. Such criteria are not treated separately but as a whole guideline. Since recent optical devices operate at a very rapid speed of optical processing, they provide network operators the strength to cope with the ongoing heavy traffic demands. However, those new devices are very expensive. Rebuilding the whole backbone network with the new optical equipment is a financially unfeasible solution. Instead, a trade-off between the old, slow but cheap technology and the new, high-speed but expensive one has to be found while the rapid traffic growth need to be supported.

Network reliability is the second concern of any network designer. As people have been more connected than ever, many daily activities such as banking, gaming, social communication have been taken place in Internet whose infrastructure consists of optical backbone networks. Thus, to provide a good user experience, those optical systems have to be resilient to failures and able to be self-healing within a very short time-frame (∼50-150ms). Plus, a higher link/node failure protection level rather than single link failure need to be provided for a better protection quality [Guangzhi *et al.*, 2012]. To address such a multiple link/node failure problem, technology availability, network topology, and recovery mechanisms have to be taken into account. The traditional protection mechanisms which are based on path or link protection were developed for point-to-point or ring systems. Particularly, line-switched self-healing rings have been the standards in survivable SONET/SDH ring networks [Wu and Lau, 1992]. The most important feature of these methods is their very fast recovery speed (∼50ms). However, the amount of dedicated spare capacity needed to provide a full protection against a single link failure is at least 100% or even more (over protected capacity). The reason for this high percentage of dedicated protection capacity is due to the ring topology. When it comes to WDM mesh networks, a smaller spare capacity ratio than the one obtained with ring networks can be achieved. Link protection has a high spare capacity ratio, but a short recovery downtime, on the contrary, path protection has a long recovery downtime, but a small spare capacity ratio. Thus, both traditional link and path protection methods have been failing to offer a rapid and cost-effective recovery solution to mesh WDM networks. Cycle-based protection schemes are attractive solutions in that case.

Network dimensioning with the above two criteria (provisioning cost and reliability) is a NP-Complete problem and it always is a challenge to get a good solution for such a problem for large-size network instances. Most existing approaches in literature are heuristic ones whose solution quality is questionable. Authors often compare the heuristic solutions with the optimal ones for very small networks (6-10 nodes) to show that the gap between them is very small, then extrapolates that such a result still holds for bigger networks. That assumption overestimates what heuristics can bring to the table and that the performance of heuristics may change drastically when the size of the data instances increases. This research proves that it is possible to get ε-optimal solutions which are significantly better than heuristic solutions, at least for medium size problems. It might be still difficult to solve fully realistic instances with decomposition techniques. However, their combination with heuristics can reach far better solutions for large-size data instances than heuristics alone.

This thesis attacks several WDM network design problems from a different perspective: provide ε-optimal solutions whose accuracy ε is often less than 1%, therefore more than what is required, taking into account the accuracy of the traffic patterns that are used for network design and planning problems. It is worth to note that even a small percentage of cost saving has a huge benefit for operators. This ambitious mission is achieved by extensively applying Column Generation (CG) methodology [Dantzig and Wolfe, 1960; Lasdon, 1970; Chvatal, 1983; Lübbecke and Desrosiers, 2005] which is a large scale linear programming optimization technique, with its strength unfolding in solving decomposable integer programming problems.

Research in this thesis is an attempt to popularize CG technique in optical network design domain. With the obtained results, CG has been proved to be the most powerful tool for the time being if we aim at both scalability and ε-optimality. Besides, our proposed CG models allow us to understand the rationale of wavelength continuity assumption in simple/non-simple p-cycles, to study the accuracy of FDPP p-cycles solutions and evaluate spare capacity advantage of FDPP p-cycles in comparison with FIPP p-cycles, to generalize multiple link/node failure problem in survivable virtual topologies, and to study impact of long-range high-capacity transceivers in multirate WDM networks.

1.2 Research projects

Four design problems are studied in the thesis: design of p-cycles subject to wavelength continuity, design of dependent and independent p-cycles against multiple failures, design of survivable virtual topologies against multiple failures, design of a multirate optical network architecture. Each problem relates to a different aspect of a WDM network and the contribution of the thesis is to design original column generation models to solve them efficiently, and then draw accurate conclusions of the cost-efficiency design of various optical network aspects. We define those problems in the following sections.

1.2.1 Design of p-cycles subject to wavelength continuity

Resilient network provisioning consists in establishing a set of working paths and a set of protection paths. While the set of working paths is used to accommodate the requests in the operational mode, the set of protection paths are activated when some link failure occurs.

For a given traffic demand matrix, the offline RWA problem [Jaumard *et al.*, 2009] takes care of the wavelength assignment of working paths while minimizing the bandwidth requirements or another objective. Each established working path is assigned to a wavelength so that two working paths going through the same link have to be assigned to two different wavelengths. Another often studied objective for the RWA problem is the minimization of the number of required wavelengths.

With respect to protection paths, different types of pre-configured protection structures exist, such as shared backup path/link protection [Ramamurthy *et al.*, 2003], p-cycles [Grover and Stamatelakis, 1998], p-trees [Grue and Grover, 2007], h-trees [Shah-Heydari and Yang, 2004] or p-structures [Sebbah and Jaumard, 2010]. In particular, p-cycles and their generalization with p-structures received a lot of attention as they not only correspond to a pre-configured, but also to a pre-cross-connected protection scheme for single link failures. Among them, p-cycles have been widely studied since they are the first proposed p-structure. The central concept of this protection scheme is a cycle, called p-cycle, that provides one protection unit for every on-cycle link that belongs to this cycle and two protection units for every straddling link that has its endpoints on the cycle, but that is not on the cycle. Each p-cycle acts similarly to an unit line-switched self-healing ring, thus achieves the ring-like restoration speed. Unlike line switched ring, each p-cycle protects not only its on-cycle links but also its straddling links, hence a significant amount of capacity redundancy can be achieved [Grover and Doucette, 2002]. p-Cycle protection scheme obtains a good trade-off between mesh-based capacity efficiency and ring-based restoration time, therefore, it has emerged as a very promising protection scheme in WDM mesh networks.

In the first research project, for the first time the RWA and p-cycle design problem under wavelength continuity assumption has been investigated in order to answer the question whether such an assumption results in significant additional bandwidth requirements. We develop an exact method that jointly solves the RWA and p-cycle design problem. Particularly, an exact estimate of the consequences of the wavelength continuity assumption on the spare capacity requirements and on the provisioning cost is obtained.

1.2.2 Design of dependent and independent *p*-cycles against multiple failures

Protection schemes are based on either (end-to-end) path, segment or link protection. Path-based protection consumes less protection capacity but has longer restoration times than link protection. Thus, when it comes to spare capacity, in particular for WDM mesh networks where bandwidth is quite costly, path-based protection schemes are preferred.

Line-switched self-healing rings have been the standard in SONET/SDH ring networks due to their very fast recovery speed. This led to p-cycles, the particular class of pre-configured pre-crossed connection scheme based on link protection. In case of path protection, the so-called FIPP protection scheme has been studied [Kodian and Grover, 2005]. FIPP p-cycles have been shown to offer a path protection within backup ring structures, which provide a rapid restoration service while requiring an economic amount of reserved capacity [Kodian and Grover, 2005; Kodian *et al.*, 2005; Jaumard *et al.*, 2007]. However, failure dependent path protection (FDPP), which is an extension of FIPP by using shared path protection instead of independent path protection, can have a significantly better redundancy ratio than FIPP. However, FDPP has a slower recovery rate since it has a more complex signaling than in the case of FIPP [Tapolcai *et al.*, 2013]. This point of view will be proved in this thesis.

Up to now, most previous publications have focused on using a path protection scheme to protect network traffic against single link failures. However, path-based protection design against single link failures turns out not to be always sufficient to keep the WDM networks away from many down-time cases as other kinds of failures, such as node failures, dual link failures, triple link failures which have a common name: *shared risk link groups* [Shen *et al.*, 2005]. Several works partially dealt with this issues [Choi *et al.*, 2002; Schupke *et al.*, 2004; Sebbah and Jaumard, 2009; Clouqueur and Grover, 2005a; Huang *et al.*, 2007]. However, the models proposed in those works cannot be generalized for multiple link failures or are far from being scalable.

The second research project aims to develop a generic model which can be customized to represent whatever path protection structures. It needs to be efficiently solved and combined with either heuristics or a branch-and-price method in order to derive an integer solution. The developed model is equivalent to the model of [Orlowski and Pióro, 2011], but new in the case of FDPP p-cycle. In order to adapt the generic model to FDPP p-cycle, bandwidth sharing constraints need to be moved to pricing problems, and then, the master problem looses its decomposability structure and the pricing problem is no more polynomially solvable. An algorithm that can efficiently solve the pricing problem will be proposed. Our purpose is to determine how much spare capacity is saved if FDPP p-cycles replace FIPP p-cycles as a protection mechanism.

1.2.3 Design of survivable virtual topologies against multiple failures

Network operators have to cope with frequent failures at or below the IP-layer: fiber cuts, router hardware/software failures, malfunctioning of optical equipment, protocol mis-configurations, etc. While most failures result from dig-up cables arising in construction works and account for about 60% of failure events in optical networks [Cholda and Jajszczyk, 2010], there are also multiple failures, which usually have a common cause (e.g., they share a common component which fails and causes all links to go down together). As mentioned in [Markopoulou *et al.*, 2008] where the authors studied the characterization of failures in an operational Sprint IP backbone network, such multiple failures do occur, and need to be addressed in the design of a survivable logical topology, throughout a backup mechanism which must ensure network connectivity in case of any, or at least some, multiple link/node failure.

The IP layer is referred to as the logical/virtual layer where each logical link (called LSP - Label Switch Path in the context of MPLS - Multi-Protocol Label Switching) is mapped onto a lightpath in the optical/physical layer. Therefore, a network failure, such as, e.g., a fiber cut, results in several logical broken links because the physical resource (e.g., a duct hosting several fibers) can be shared by several optical lightpaths, and those logical broken links, in turn, can make the logical topology disconnected. However, a necessary condition for the existence of a restoration scheme in the IP layer is that the logical topology remains connected (survivable) when some failures occur.

In the third study, we investigate further the logical survivable topology design problem with a new mathematical model which is much more scalable than previously published ones. Multiple link failures (including the so-called Shared Risk Link Group (SRLG), see, e.g., [Strand *et al.*, 2001]) have to be considered. The motivation of this research project is to investigate the proper link dimensioning in order to ensure successful IP restoration, and evaluate the resulting redundancy ratio, i.e., protection/restoration over primary ratio for the bandwidth requirements in the optical layer.

1.2.4 Design of a multirate optical network architecture

As the cost of high speed (such as 40 Gbps, 100 Gbps) optical transceivers and regenerators is still very expensive, the cost-effective design problem becomes crucial to industry. Besides, CAPEX and OPEX of supporting equipment such as cooling system cannot be ignored. In order to reduce such additional cost, a helpful rule of thumb is to restrict the number of nodes where regenerators can be deployed. Such a rule keeps regenerators around few nodes, thus expensive supporting devices can be shared among those regenerators. However, a constraint on the number of regenerator-deployable nodes makes the network design process difficult since we have to find a selective set of nodes where regenerators are deployed. Moreover, such a constraint results in the number of long range transceivers, such as 3000km transceivers, increases.

In the fourth research, we estimate the impact on the network dimensioning cost when the amount of regenerator-deployable nodes is restricted. To have an exact estimate on that impact, several physical constraints (such as maximum physical hops, fiber arm limitation, maximum transmission reach) are considered in our design problem. When those physical constraints are included, the problem becomes very computationally challenging. In the thesis, we come up with a cost model of the most dominant devices in market and also propose a tractable CG technique. Again, CG approach will be proved to be an effective tool to solve highly complicated but decomposable problems.

1.3 Contributions

This thesis revisited four network design problems with a focus on a wide-range of criteria such as cost-effective, cycle-based protection, multiple failures, and multirate devices. Column Generation approach has been intensively applied as a generic framework to deal with the highly exponential nature of network optimization problems. Indeed, most proposed Integer Linear Programming (ILP) models become intractable when the size of optical networks gets significant. Heuristic is the common path that researchers use to design scalable solutions. However, those solutions are often ad-hoc and difficult to be generalized. Also, quality evaluation of heuristic solutions is often ignored. In this study, for the first time, ε-optimal solutions of several difficult problems are obtained with realistic instances thanks to the recourse to CG techniques. In this thesis, an original CG model and a scalable solution process have been developed for all four design problems. In the following, the contribution to networking aspects of the four design problems will be discussed.

RWA problem with and without wavelength continuity assumption in context of simple p-cycles (cycles where nodes cannot be repeated) and non-simple p-cycle (nodes can be revisited many times) is thoroughly investigated. By developing exact methods, we have an accurate estimate of the consequences of that assumption on the spare capacity requirements and on the provisioning cost. In addition, joint-optimization of routing and protection schemes as well as online p-cycle generation are carried out, thus reduce spare capacity redundancy. Numerical results show that the difference between the capacity requirement under wavelength conversion vs. under wavelength continuity is meaningless. Consequently, in view of the reduced provisioning cost (saving at least on the converters), the design of p-cycles under a wavelength continuity assumption is supported.

The thesis proposed a new generic flow formulation for FDPP p-cycle. The generality of that model is that it can be customized for whatever path protection structures. The proposed model, even if equivalent to the model of [Orlowski and Pióro, 2011], is new in case of FDPP p-cycle. Since the pricing problem in this case is not polynomially solvable, a hierarchical decomposition algorithm (similar to the one of [Rocha and Jaumard, 2012]) has been employed. Performance evaluation is made in the case of FDPP p-cycle subject to dual failures. For small to medium size networks, the proposed model remains fairly scalable for increasing percentages of dual failures, and requires much less bandwidth than p-cycle protection schemes (ratio varies from 2 to 4). For larger networks, heuristics are required in order to keep computing times reasonable. In the particular case of single link failures, it compares very favorably (5 to 10% of bandwidth saving) to the previously proposed column generation ILP model of [Rocha *et al.*, 2012] for FIPP protection. Such an evidence proves the fact that FDPP saves more spare capacity than FIPP in practice.

In the thesis, a decomposition model is proposed to solve the logical survivable topology problem, under the wavelength continuity assumption, subject to multiple failures including single node failures and SRLGs, on arbitrary networks in the context of directional physical and logical topologies. The most important contribution is, instead of using cutset-based formulations and exploiting some special graph structures to gain some scalability as other authors [Modiano and Narula-Tam, 2001, 2002; Todimala and Ramamurthy, 2007; Thulasiraman *et al.*, 2009b, 2010], we introduce a path-based formulation with online generation of augmenting paths. Such a path-based formulation solves several network instances which cannot be solved by cutset-based formulations. Moreover, that path-based formulation considers multiple link/node failures under the wavelength continuity assumption for the primary routing, and investigates the proper dimensioning of the physical links in order to guarantee a successful IP restoration, if no connectivity issues prevent it. Those features are not able to be realized in cutset-based formulations.

The last contribution of the thesis is to introduce a CG model for optimizing optical equipment in multirate networks. Some researchers have already studied this subject, but to best of our knowledge, no work takes into account the maximum number of hops per lightpath which is introduced in our study. As it is impossible for 3R regenerators to synchronize concurrent optical channels, such a constraint need to be applied in order to make a network design realistic. Besides, in our model, one important constraint is applied: the number of nodes that can deploy regenerators is limited. The need of that constraint comes from the fact that in reality regenerators are gathered in just some nodes for being effectively managed as well as minimizing the overall cost of supporting equipment such as cooling system. Those two constraints are often missing in previously proposed models and are our important contributions to this subject. Impact of those constraints on the network cost is thoroughly investigated and becomes a helpful source of information for network designers.

Those contributions are detailed in Chapter *List of Publications* (see page xiv).

1.4 Plan of thesis

The thesis is organized as follows. Chapter 2 provides a brief information about the physical aspects of dominant optical equipment, in particular, characteristics as well as limitations of those equipment are given. The relationship between the optical layer and the physical layer, especially how the attributes of the physical layer impacts on the optical layer and vice-versa are discussed. This chapter also presents the definition of survivability and classical protection schemes.

Chapter 3 reviews recent researches on the studied subjects. It indicates what has been studied and what is missing from the current literature, thus, provides us a clear picture of what is going on in the subject and also shows that the research of that thesis is indeed the state of art. Chapter 3 consists of four sections: design of p-cycles subject to wavelength continuity, design of dependent and independent p-cycles against multiple failures, design of survivable virtual topologies against multiple failures, design of a multirate optical network architecture.

The four next chapters: Chapter 4, 5, 6, 7 presents the introduction, the proposed model, the numerical results and the conclusion of each research project previously presented.

Finally, the overall conclusion of the research conducted in the thesis is given in Chapter 8.

Chapter 2

Optical network background

This chapter reviews essential knowledge that is needed to comprehend the research subjects. Section 2.1 presents the main optical equipment that have major impact on the deployment cost and the performance as well. Section 2.2 indicates the common physical impairments in cross-layer design. It mentions several impairments that need to be focused on when working on such a cross-layer problem. Next, we provide definitions of the survivability and main protection schemes in Section 2.3. Finally, Section 2.4 briefly introduces the Column Generation (CG) methodology.

2.1 Equipment and physical aspects

Main equipment in an optical networks consist of:

1. Transmitters and receivers
2. Multiplexers and demultiplexers
3. Optical switches
4. Amplifiers
5. Regenerators

Transmitters and receivers are cross-points between the electrical layer and the optical layer. Each transmitter encodes electrical signal into optical signal. Actually, each optical signal of a transmitter is transfered by a specific wavelength that is assigned to that transmitter. The destination of such an optical signal is a receiver where that optical signal is converted back to the original electrical forms. Hence, transmitters and receivers are often called E/O and O/E devices, respectively.

Transmission medium for optical signal is optical fiber. At the beginning, each optical fiber was able to transfer only one wavelength. Such a way of transmission is a huge waste of resource since an optical fiber can accommodate an approximation of 50Tps while bandwidth of an optical wavelength is limited by electrical modulation speed of transceivers (transmitter/receiver) which is up to 100Gbps nowadays. In order to effectively exploit the huge capacity of optical fibers, WDM technology has been developed. That technology allows sharing a same optical fiber for a bundle of different wavelengths, thus fiber bandwidth becomes the bandwidth accumulation of each wavelength going through that fiber. Such a way dramatically improves optical throughput.

WDM technology is implemented by using multiplexers and demultiplexers where the former are responsible for combining different wavelengths into a single optical signal and the latter do the opposite function, that is to split original wavelengths from that single optical signal. In Fig. 2.1, the device on the left is a multiplexer because the signals come from multiple ports to one port. On the contrary, the device on the right is a demultiplexer because the signals come from one port to multiple ports.

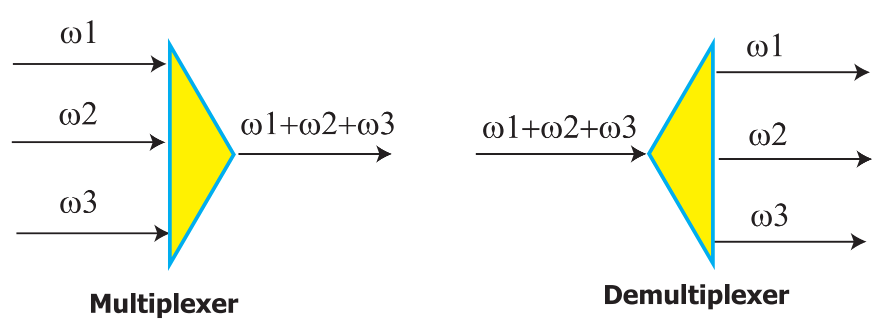

Fig. 2.1: Multiplexer and demultiplexer.

WDM mesh networks, thanks to their mesh topology, save more working and spare capacities than WDM ring networks. They also provide a greater flexibility in network dimensioning. The principal equipment in WDM mesh network is optical switch which routes incoming and outgoing wavelengths in a proper way to satisfy traffic demands. In a mesh topology, nodes represent optical switches and links represent optical fibers that are plugged into those nodes. Incoming (outgoing) composite optical signals in optical fibers are extracted (combined) by multiplexers (demultiplexers) before coming in (out) of optical switches. Each optical switch has many slots that can accommodate transmitters (to generate optical signals), receivers (to convert optical signals to electrical ones), or to connect incoming wavelength channel to the right outgoing channel. Those optical switches can be viewed as routers which define network traffic. Fig. 2.2 shows the general structure of an optical switch. Wavelength converters in Fig. 2.2 are an optional design choice which allows or does not allow an optical lightpath having different wavelengths.

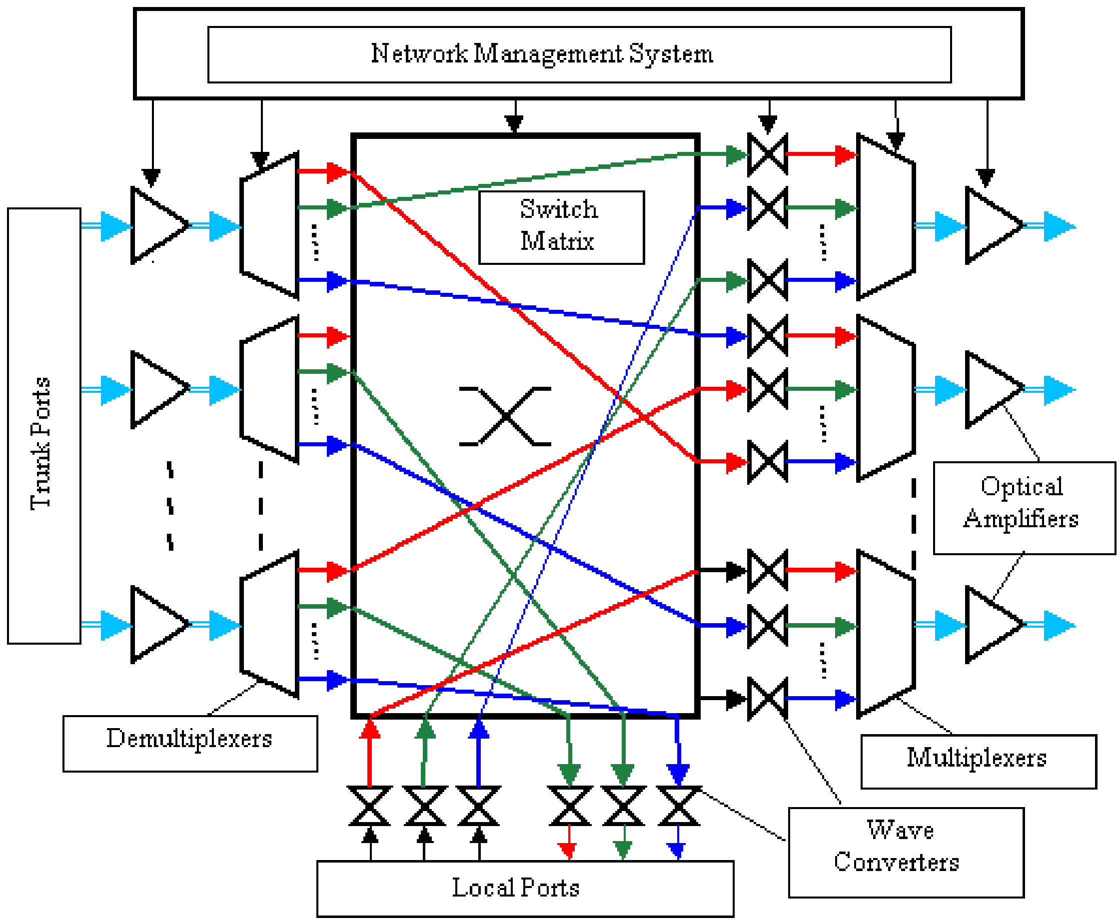

Fig. 2.2: A model of optical switch where a wavelength is either bypassed, converted, added or dropped

Dominant physical aspects in optical equipment are: power attenuation, chromatic dispersion, and timing delay. Power attenuation refers to the fact that an optical signal loses its power while it propagates through a fiber. It also loses a small amount of power when bypassing an optical switch. Chromatic dispersion is the phenomenon of the broadening of optical signals which results in the difference in the arriving moments of different spectral components. Timing delay is defined as the propagation time of a signal from source to destination. Propagation time in optical domain can be neglected as every optical signal travels at the speed of light. But whenever such an optical signal goes through an O/E/O conversion, a delay is added to the transmission duration. Those described physical aspects may make an optical transmission infeasible, thus need to be considered in any network design solution.

Other optical amplifiers, that boost the optical power, or regenerators, that reproduces the optical signal, can be used to deal with power attenuation. Those optical amplifiers are deployed along the fiber (in-line optical amplifiers) and at entrance points of optical switches (pre-amplifiers). An amplifier boosts every passing wavelength with a same amount of power. On the contrary, a regenerator only regenerates one wavelength and is deployed at optical switches. A regenerator that produces a different wavelength than the input one is called a wavelength converter.

An optical amplifier does not restore the signal shape, thus does not deal with chromatic dispersion. That is why regenerators have to be installed at some lightpath intermediate nodes since they remedy the signal shape. Combination of optical amplifiers and regenerators certainly extends the length of feasible optical lightpaths. However, each regenerator adds an extra timing delay to the transmission duration. Hence, any lightpath has an upper bound on the number of regenerators that can be installed in order to guarantee the accumulated timing delay being below a certain threshold.

2.2 Cross-layer design

The majority of researches on the optical network design problem ignores the physical impairments such as chromatic dispersion, power attenuation and timing delay. The reason is that physical impairments are not a big issue with 2.5 Gbps optical links, i.e., the popular bit rate that is still very much used today, but that are becoming slowly replaced by higher optical links such as 10, 40, and 100 Gbps. Nowadays, with wavelength bandwidth ranges up to 40 Gbps or even 100 Gbps, physical impairments are not negligible. At very a high bit rate, physical impairments degrade significantly the bit error rate (BER) of WDM networks, thus the extra cost for mitigating physical impairments in WDM network becomes meaningful. That is why combining the design of the physical layer with the design of the optical layer is a key feature in implementing very high bit rate WDM networks.

In our study, the optical layer design takes into account physical impairments such as chromatic dispersion, power attenuation and timing delay. Impact of those impairments depend on bit-rate per lightpath. To cope with power attenuation, optical amplifiers and regenerators are used. For chromatic dispersion, regenerators are the solution. Since timing delay caused by O/E/O conversion cannot be compensated, an upper bound on the number of regenerators per lightpath is given as an input parameter.

The three physical impairments that are mentioned above contributes the most to the optical transmission quality. Some other impairments such as ASE noises, cross-talk noises, four-wave mixing, etc. (see [Ramaswami *et al.*, 2009]) also degrade that quality so that maximum transmission reach (MTR) is introduced as an upper bound on the distance between two consecutive regenerators in order to keep the impact of those impairments under an acceptable level. MTR has to be considered in any cross-layer design.

2.3 Survivability and main protection schemes

In this section, we define the survivability as well as main protection schemes in optical WDM networks.

Survivability

For a given optical network with logical and physical topologies, a mapping from the logical layer to the physical layer is called *survivable* against a collection of sets of physical link and/or node failures if the occurrence of any failure set belonging to that collection does not make the logical topology disconnected. In other words, under any failure set, there always exists a path linking the source to the destination of every logical link.

Protection vs. Restoration

Both network protection and network restoration refer to mechanisms that a network uses to cope with network failure. In a network protection mechanism, a proactive backup lightpath is configured for each network failure while, in case of a network restoration mechanism, such a backup lightpath is determined after failure occurrence.

Shared vs. Dedicated Protection

Shared protection refers to protection mechanisms where backup resources are shared between primary lightpaths. On the contrary, a mechanism is called dedicated protection if each primary lightpath has its own backup capacity. Obviously, shared protection has a smaller reduction ratio but a more complicated network management mechanism than dedicated protection.

Link-based Protection

A link-based protection mechanism reserves backup paths for each working link failure. When a link fails, its two end nodes re-route the disrupted traffic to the backup path around the failed link.

Path-based Protection

A path-based protection mechanism reserves a backup path for each working path. A working path failure refers to any link failure or node failure that disrupts the traffic of that working path. When a working path fails, its two end nodes switch the disrupted traffic to the planned backup path. Certainly, the working path and the corresponding backup path need to be link/node disjoint in order to guarantee the correctness of the path-based protection approach.

Segment-based Protection

Segment protection divides a working lightpath into several segments, each of them is a subset of consecutive links on a path. For each working segment, a disjoint backup lightpath is established between the two end nodes of that segment. Such a backup lightpath is used to route disrupted traffic whenever the corresponding segment fails.

Link-based protection, path-based protection, and segment-based protection can be either shared or dedicated. Those protections can be sorted in a descending order of redundancy ratio as:

$$RR_{\text{link-based protection}} > RR_{\text{segment-based protection}} > RR_{\text{path-based protection}},$$

where RR stands for *redundancy ratio*, while in an ascending order of recovery time, they can be sorted as:

$$RT_{\text{link-based protection}} < RT_{\text{segment-based protection}} < RT_{\text{path-based protection}},$$

where RT stands for *recovery time*.

p-Cycle Protection

p-Cycle-protection ([Grover and Stamatelakis, 1998]) is a shared link-based protection approach where backup lightpaths are circles (a special form of a line where two end points are the same). Each p-cycle unit provides one protection unit for each on-cycle working link and two protection units for each straddle working link which has two end points in the cycle but does not belong to that cycle.

Those p-cycle-protections can be categorized into simple p-cycle-protection or non-simple p-cycle-protection depending on whether backup circles are node-disjoint or not [**Hoang Hai Anh** and Jaumard, 2011]. p-Cycle-protection has the shortest recovery time in comparison to the above protection schemes since the backup layer in this case do not need to be re-configured after any failure occurrence.

FIPP p-cycles Protection

FIPP p-cycles protection ([Kodian and Grover, 2005]) is an extension of p-cycle protection where independent path protection is used instead of link-based protection. Each FIPP p-cycle can only provide backup protection for end-to-end working paths between nodes on the cycle. But, such a cycle is able to protect a group of working paths whose routes are all mutually disjoint.

FDPP p-cycles Protection

FDPP p-cycles protection acts in the same way as FIPP p-cycles protection except that the protected working paths do not need to be mutually disjoint. In other words, FDPP p-cycles employ shared-path protection scheme while FIPP p-cycles use independent path protection scheme.

FDPP p-cycles protection has a better redundancy ratio than FIPP p-cycles protection, but has a slower recovery time since a node may need to be re-configured in order to support the backup lightpaths. In comparison to FIPP p-cycles protection, a more complicated signaling management need to be developed in case of FDPP p-cycles protection.

2.4 Column generation methodology

Column Generation (CG) is a large scale linear programming optimization technique [Dantzig and Wolfe, 1960; Lasdon, 1970; Lübbecke and Desrosiers, 2005]. It is useful to remember that CG is a solution scheme to solve large linear programs (LP), that needs to be combined with other techniques in order to get ILP solutions [Barnhart *et al.*, 1998]. We outline a simple CG algorithm with a single pricing problem in Section 2.4.1 and a simple multi pricing CG algorithm in Section 2.4.2. Such an algorithm in combination with the standard ILP methods is a baseline for other mathematical model developments in this thesis.

2.4.1 A single pricing CG algorithm

Consider a Master Problem which is actually a minimization problem with a huge set of variables such that it is impractical to solve that problem [Vanderbeck, 1994; Barnhart *et al.*, 1998]. First, some initial columns (configurations) are used to form the Restricted Master Problem (RMP) that is a subset of the columns of the Master Problem. The RMP is optimally solved and its optimal dual variables are used to feed the pricing problem, whose objective is minimization of the reduced cost of a generic variable in the RMP. Next, the pricing problem is solved and its optimal solution, i.e., a new configuration, is added to the RMP if its corresponding reduced cost is negative, i.e., it is an augmented configuration meaning its addition will improve the value of the current LP solution. Note that although solving *exactly* those pricing problems would lead to the best one step ahead improvement of the objective function of the RMP problem, it is a common practice to stop their solution as soon as a solution with a negative reduced cost has been reached (it has to do with the compromise between the required time to get an optimal solution and the number of times pricing problems are solved: it is more efficient, in practice, to solve pricing problems more often while only using their first solutions associated with a negative reduced cost instead of their optimal solutions). The RMP is optimally solved again and so on until the reduced cost of the pricing problem is positive, meaning that the optimal solution of the continuous relaxation (i.e., linear programming (LP) relaxation) of the master problem has been obtained.

In order to generate an optimal ILP solution of the master problem, one should use

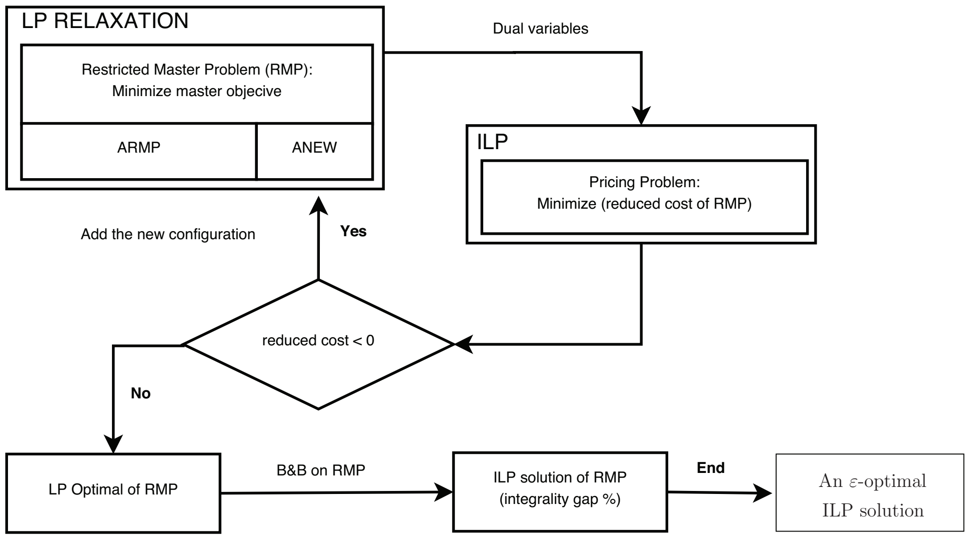

Fig. 2.3: A single pricing CG algorithm

a branch-and-price algorithm, which is often computationally expensive, see [Barnhart *et al.*, 1998]. Instead, we use a branch-and-bound method (the one embedded in CPLEX IBM [2011a]) on the constraint matrix (Restricted Master Problem) made of the columns generated in order to reach the optimal solution of the LP relaxation. The integrity gap between the optimal ILP solution of the RMP and the optimal solution of the LP relaxation of the MP measures the accuracy of the ILP solution. The solution diagram of the CG is given in Fig. 2.3, see [Chvatal, 1983] and [Barnhart *et al.*, 1998] for more details.

2.4.2 A multiple pricing CG algorithm

Large scale linear programming problems with a block-diagonal structure can benefit from a decomposition technique for their efficient solution [Dantzig and Wolfe, 1960; Lasdon, 1970; Lübbecke and Desrosiers, 2005]. Such a technique decomposes a linear programming problem into a master problem with several subproblems. Each subproblem is associated with a diagonal block of the master constraint matrix, whose columns define the subproblem columns. In a block-diagonal matrix, every element is null except the elements of the diagonal blocks. A generic pricing problem can be designed to generate the sub-columns of any subproblem. However, this generic pricing problem can be broken into several pricing problems, e.g., Pricings I and II. Each pricing problem generates a kind of columns (configurations) of that the RMP

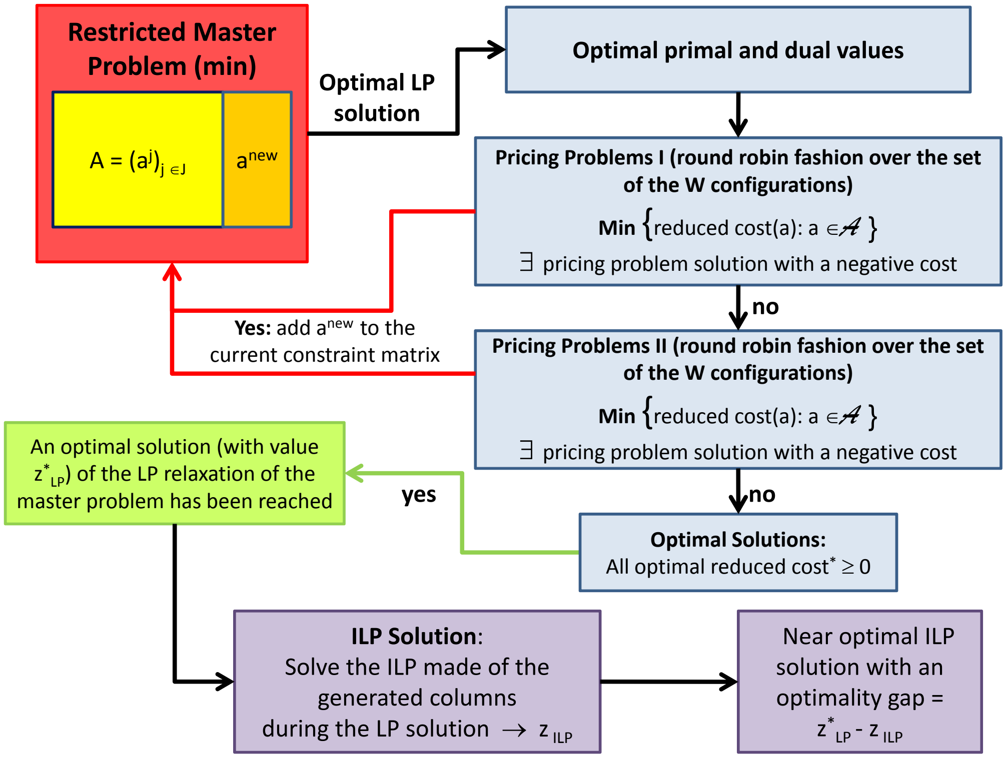

Fig. 2.4: A multiple pricing CG algorithm

is made.

Similar to the single pricing CG algorithm, first, some initial columns are generated in order to set a first RMP. Then, the current RMP is optimally solved, and the optimal values of the dual variables become available. These values are input parameters for the pricing problems. So next, each pricing problem (i.e., Pricings I and II) is solved to get an augmented configuration. The pricing problems are solved in sequence, first pricing problems I in a round robin fashion, and then pricing problems II as pricing problems II are more costly to solve. The process is repeated until the reduced cost of all pricing problems (I and II) is not negative anymore, in which case we can conclude that the optimal solution of the LP relaxation of the Master Problem has been reached. The solution scheme is summarized in the diagram of Fig. 2.4.

As indicated in Section 2.4.1, the branch-and-bound method provided by [IBM, 2011a] is used to get the ILP solution.

Chapter 3

Literature review

This chapter reviews studies that relate to the thesis. Section 3.1 outlines the researches on the routing and wavelength assignment (RWA) problem with p-cycles and wavelength conversion. Section 3.2 gives a summary of studies in the multiple failure problem with FIPP p-cycle. Section 3.3 highlights works in survivable logical topology design. Section 3.4 overviews significant studies in cross-layer design on multirate networks. Section 3.5 concludes this chapter.

3.1 The RWA problem with *p*-cycles and wavelength conversion

The RWA problem has received a lot of attention in the last two decades. This problem is to assign bandwidth unit (working and/or backup) a relevant wavelength in order to attain a certain objective. Such an objective is either to minimize the deployment cost (for e.g., bandwidth capacity or dollar cost) or to minimize the blocking rate (equivalently to maximize system throughput) depending on whether the traffic demand is static or dynamic. A solving process is called sequential-optimization (joint-optimization) if it generates working paths and p-cycles separately (jointly). Wavelength conversion means a lightpath or a p-cycle may change the assigned wavelength at an intermediate node by deploying wavelength converters. A RWA network holds the wavelength continuity assumption if and only if it does not have wavelength conversion capacity.

Dynamic traffic and blocking rate

[Subramaniam *et al.*, 1999; Xiao and Leung, 1999; Chu *et al.*, 2003; Xiao *et al.*, 2004; Xi *et al.*, 2005; Houmaidi and Bassiouni, 2006] study the RWA problem with the blocking rate objective and dynamic traffic demand. Blocking rate can be reduced by deploying wavelength converters at certain nodes, however those converters are expensive. Thus, those studies investigate the relationship between the blocking rate and the wavelength converter cost, in particularly, how many and where the network should deploy those converters. Several analytical models have been propose to estimate the blocking rate research the blocking rate of networks that are protected by p-cycles [Clouqueur and Grover, 2005b; Cholda and Jajszczyk, 2007; Mukherjee *et al.*, 2006; Szigeti and Cinkler, 2011]. In particular, [Clouqueur and Grover, 2005b] shows that the size of p-cycles plays a vital role in improving network availability. The shorter the p-cycle length is, the higher the network availability is.

Sequential optimization

[Schupke *et al.*, 2002; Li and Wang, 2004; Tianjian and Bin, 2006; Wu *et al.*, 2010b] investigate the static RWA problem with p-cycles. In those studies, the solving process generates the working paths and the backup p-cycles in separate steps. In the first step, the shortest path algorithm routes working paths. An ILP selects the best p-cycles from a set of p-cycle candidates in the second step. A breath-first search or an ILP algorithm pre-enumerates a set of p-cycle candidates with certain conditions, for e.g., a restriction on p-cycle length. [Schupke *et al.*, 2002] conducts the research with and without wavelength conversion and discovers that, in both cases, the long p-cycles result in a smaller spare capacity ratio than the short p-cycles.

Joint optimization

[Grover and Doucette, 2002; Schupke *et al.*, 2003; Mauz, 2003; Stidsen and Thomadsen, 2004; Nguyen *et al.*, 2006; Eshoul and Mouftah, 2009; Nguyen *et al.*, 2010; Pinto-Roa *et al.*, 2013] study sequential optimization versus joint optimization. Numerical results show that, in comparison to sequential optimization, joint optimization saves a significant amount of of working and spare capacities. In those researches, the solving process selects p-cycles from a set of pre-enumerated candidates, except that in [Stidsen and Thomadsen, 2004] p-cycles are not necessary to be pre-enumerated. To best of our knowledge, only [Stidsen and Thomadsen, 2004] applies column generation to the joint optimization RWA problem and successfully obtains ε-optimal solutions.

Wavelength conversion

[Schupke *et al.*, 2002, 2003; Li and Wang, 2004; Tianjian and Bin, 2006; Tran and Killat, 2008] investigate wavelength conversion in RWA networks. [Schupke *et al.*, 2002, 2003] indicate that wavelength converters improve the spare over working ratio up to 0.71. [Li and Wang, 2004; Tianjian and Bin, 2006] minimize the wavelength converter cost in WDM networks that guarantee 100% protection against single link failure. [Tran and Killat, 2008] studies how wavelength converter configuration, for e.g., full-range converters or partial wavelength converter, impacts on the per-node probability that such a node exists in a set of feasible working path.

***p*-Cycle pre-enumeration**

Since the set of possible p-cycles is extremely huge, the solving process has to select p-cycles from a small subset of p-cycles [Schupke *et al.*, 2002; Grover and Doucette, 2002; Schupke *et al.*, 2003; Mauz, 2003; Li and Wang, 2004; Nguyen *et al.*, 2006; Tianjian and Bin, 2006; Eshoul and Mouftah, 2009; Nguyen *et al.*, 2010; Wu *et al.*, 2010b; Pinto-Roa *et al.*, 2013]. The authors use a breadth-first search or a ILP with certain restrictions in order to generate such a subset. Those restrictions eliminates p-cycles that are unlikely to be in the expected solution. E.g., [Schupke *et al.*, 2003] restrict the p-cycle length and [Nguyen *et al.*, 2006, 2010] propose a stricter definition of p-cycles, so called fundamental p-cycles. Only [Stidsen and Thomadsen, 2004] generates p-cycles during the solution process.

Table 3.1 describes the characteristics of the important studies. Column *"Optimization"* indicates that such a study routes the working paths and designs the backup plan either sequentially, jointly, or considers only the working path. The next column denotes whether a work needs a p-cycle pre-enumeration process or not. Column *"Instance size"* shows the largest instance the work solves. Column *"Wavelength conversion"* indicates whether a study takes into account the wavelength conversion or not. The last column shows network traffics in terms of number of demand connections between node pairs.

First, to best of our knowledge, no work treats joint-optimization, wavelength conversion, and elimination of p-cycle pre-enumeration together in the static RWA problem (see Table 3.1). Joint optimization and elimination of p-cycle pre-enumeration

Study	Optimization	*p*-Cycle pre-enumeration	Instance size	Wavelength conversion	Traffic demand (connections)
[Schupke *et al.*, 2002]	sequential	✓	11 nodes 26 edges	✓	348
[Schupke *et al.*, 2003]	joint	✓	11 nodes 26 edges	✓	176
[Li and Wang, 2004; Tianjian and Bin, 2006]	sequential	✓	14 nodes 21 edges	✓	50
[Tran and Killat, 2008]	working path		17 nodes 26 edges		35
[Wu *et al.*, 2010a]	sequential		11 nodes 26 edges		45
[Eshoul and Mouftah, 2009]	joint	✓	20 nodes 64 edges		∼242
[Grover and Doucette, 2002]	joint	✓	11 nodes 26 edges		176
[Mauz, 2003]	joint	✓	28 nodes 60 edges		∼242
[Stidsen and Thomadsen, 2004]	joint		43 nodes 71 edges		4043
[Nguyen *et al.*, 2006, 2010]	joint	✓	28 nodes 45 edges		41
[Pinto-Roa *et al.*, 2013]	working path		14 nodes 21 edges		∼1274

Table 3.1: Characteristics of studies in the static p-cycle RWA problem

are the guarantee for the solution accuracy, thus need to be considered. Secondly, Table 3.1 shows that most of the current works solve a few small network instances, except for [Stidsen and Thomadsen, 2004] who solve a network of 43 nodes and 71 edges, other works only solve up to networks of 28 nodes 60 edges.

3.2 Multiple link failures in WDM networks

Two important topics in multiple link failures are network availability and spare capacity design. The first topic is to derive analytical estimation of the network availability with knowledge of network failure pattern. Such an estimation allows the service-level agreement (SLA) between a network providers with its clients. The second topic is to find the most economic solution that is resilient to certain multiple link failures, i.e., dual link failures. Notice that, node failure is a special case of multiple link failure since a node failure is equivalent to a failure set of all adjust edges to that node.

Network availability against multiple link failures

[Mukherjee *et al.*, 2006; Huang *et al.*, 2007; Cholda and Jajszczyk, 2007; Yuan and Wang, 2011] investigate the availability against network failures. A mathematical concept, which is similar to the one of serial and parallel electronic circuits, is applied in order to derive an analytical term that represents such an availability. In those studies, the network traffic is characterized as a stochastic process that is simulated in experiments. The authors used the simulation to prove the correctness of their availability formulation. [Mukherjee *et al.*, 2006] studies the availability of p-cycle protection networks against single link failures. [Huang *et al.*, 2007; Yuan and Wang, 2011] conducts the research on such an availability against multiple link failures, but with path protection. [Cholda and Jajszczyk, 2007] evaluates the availability as a function of Mean Time to Failure (MTTF). This approach is not only more precise than other studies but also considers node failures. Surprisingly, according to this work, the reliably of p-cycle protection is outside the desired bound thus p-cycles should not be used in wide-area networks.

Dual link failure and spare capacity

Double link failures in optical networks have been intensively investigated in [Choi *et al.*, 2002; Schupke *et al.*, 2004; Clouqueur and Grover, 2005a; Ramasubramanian and Chandak, 2008; Sebbah and Jaumard, 2009; Eiger *et al.*, 2012]. They proposed each an ILP model to deal with dual link failures, assuming either p-cycle or path protection scheme.

[Choi *et al.*, 2002; Clouqueur and Grover, 2005a] study dual link failure with path-based protection. [Choi *et al.*, 2002] proposed three loop-back link protection heuristics for recovering from double link failures. The first two heuristics consists primarily in computing two link disjoint backup paths for each link thus is link-dependence, while the third one consists in computing a backup path p_ℓ^{B} for each link ℓ, such that the backup path of the links of p_ℓ^{B} does not contain ℓ. The authors also observe that it is possible to achieve almost 100% recovery from double link failures with a modest increase of the backup capacity, a conclusion that is quite surprising taking into account the results reported by other studies. [Clouqueur and Grover, 2005a] offered three ILP models to deal with dual link failures in a particular situation. The first model is to provide 100% protection against dual link failures. As opposed to [Choi *et al.*, 2002], such a protection can require up three times the spare capacity. The second model maximizes the dual failure restoration average with respect to a specified total capacity. The third model allows to customize the dual failure restoration effort on a per-demand basis. [Ramasubramanian and Chandak, 2008] investigates dual link failure resiliency through link protection. The authors established a sufficient condition for the existence of a solution which has to satisfy the backup link mutual exclusion requirement. Such a requirement states that the backup paths of two links which may fail simultaneously have to be disjoint. In this work, both ILP and heuristic are proposed. [Eiger *et al.*, 2012] developed a heuristic method to fully protect WDM networks against single and dual link failures using FIPP p-cycles. Candidate FIPP p-cycles are pre-enumerated by an ad-hoc procedure.

Multiple link failure and spare capacity

[Liu and Ruan, 2006a; Orlowski and Pióro, 2011] studies multiple link failure resilience. Those works use path-based protection against multiple link failures except that [Liu and Ruan, 2006a] use p-cycle protection. The technical challenge for the problem is that there is a huge number of protection plan candidates. To deal with that, [Liu and Ruan, 2006a] proposes a particular kind of p-cycle, so-called a basic p-cycles, which is a p-cycle that survives against any multiple link failure. Certainly, such basic p-cycles are a smaller subset of the whole p-cycle candidates. Consequently, in that work, the optimality is sacrificed for the scalability. Several decomposition models of path protection are proposed in [Orlowski and Pióro, 2011] in order to protect WDM networks against multiple link failures. The study primarily focuses on the complexity analysis without providing any numerical experiment. In those models, a column is an optical path while our concept of column is a traffic flow associated with one or more paths. This way, we expect to generate less columns than using path-based columns and then have a faster solution process. There is no comparative performance between the proposed models of [Orlowski and Pióro, 2011] and the other path-based protection models.

Table 3.2 describes the characteristic of studies in multiple link failures. Column *Spare capacity* indicates that a work optimizes the spare capacity against link failures. The next column lets us know whether a work estimates the network availability or not. Column *"Failure degree"* denotes that a study solves single link failure (degree=1), double link failure (degree=2), or the general multiple link failure (degree=*). MTTF is a special failure metric that is the average amount of time before the system fails. Column *"Protection"* shows which protection mechanism that is considered. Column *"Instance size"* is the size of the largest instance that is solved. The last column shows a round estimation of protected quantity.

To best of our knowledge, multiple link failure with path-based p-cycles has not been studied yet. The works that use p-cycle protection have to use a subset of p-cycle candidates to ease the solving process. That satisfies the optimality. Additionally, except that [Eiger *et al.*, 2012] and [Yuan and Wang, 2011] solve the network of 30 nodes and 40 edges and the one of 40 nodes and 3.0 node degree, respectively, other studies can solve up to a network of 24 nodes and 44 edges.

Study	Spare capacity	Network availability	Failure degree	Protection	Instance size	Failure protected quantity
[Choi *et al.*, 2002]	✓		2	path	24 nodes 44 edges	992 single links
[Schupke *et al.*, 2004]	✓		2	*p*-cycle	11 nodes 26 edges	100% dual-link failure protection
[Clouqueur and Grover, 2005a]	✓		2	path	16 nodes 26 edges	100% dual-link failure protection
[Liu and Ruan, 2006b]	✓		*	*p*-cycle	14 nodes 21 edges	300 demands 3372 SRLGs
[Mukherjee *et al.*, 2006]		✓	1	*p*-cycle	12 nodes 30 edges	∼660 connection demands
[Huang *et al.*, 2007]		✓	*	path	16 nodes 25 edges	N/A
[Cholda and Jajszczyk, 2007]		✓	MTTF	*p*-cycle	11 nodes 14 edges	N/A
[Ramasubramanian and Chandak, 2008]	✓		2	link	20 nodes 32 edges	100% dual-link failure protection
[Sebbah and Jaumard, 2009]	✓		2	*p*-cycle	15 nodes 24 edges	100% dual-link falure protection
[Orlowski and Pióro, 2011]	✓		*	path		N/A
[Yuan and Wang, 2011]		✓	*	path	40 nodes 3.0 nodal degree	10 SRLGs
[Eiger *et al.*, 2012]	✓		2	FIPP *p*-cycle	30 nodes 40 edges	57 connection demands

Table 3.2: Characteristics of studies in multiple link failures

3.3 Survivable logical topology design

In IP-over-WDM networks, IP layer and optical layer are called the logical (virtual) layer and the physical layer, respectively. Each logical link is mapped on one or several physical lightpaths. A single physical link failure probably makes a set of logical links broken, thus such a failure can make the logical topology disconnected. A mapping is called survivable if and only if the logical topology is resilient to any single physical link failure. The problem of finding a survivable mapping, or in some case finding the one with the cheapest cost, is referred to as the survivable logical topology design problem. Up to now, cutset-based and subgraph-based are the two approaches that have been used to attach the problem.

Cutset-based approach

The main idea of the cutset-based approach based on the spirit of Menger's theorem which states that, in a undirected graph, the minimum cutset for a pair of vertexes equals the maximum number of pairwise edge-independent of that pair [Modiano and Narula-Tam, 2001, 2002; Todimala and Ramamurthy, 2007; Kan *et al.*, 2009; Thulasiraman *et al.*, 2009a,b, 2010]. Most of those models propose several logical cutset requirements in order to guarantee the logical topology survivability against a single physical link failure, except that in [Todimala and Ramamurthy, 2007; Thulasiraman *et al.*, 2009a] multiple link failures are considered.

[Modiano and Narula-Tam, 2001, 2002; Todimala and Ramamurthy, 2007; Liu and Ruan, 2007; Kan *et al.*, 2009] propose a model that generates the least expensive survivable mapping. However, in some cases such a survivable mapping does not exist. Hence, [Liu and Ruan, 2007; Thulasiraman *et al.*, 2009a; Lin *et al.*, 2011] consider adding more spare capacity to make sure that a survivable mapping exists. Studies in Thulasiraman *et al.* [2009b,a, 2010] do not care about the capacity optimization. They aim to get a survivable mapping.

The proposed cutset-based models generate cut-sets between each node pair. Amount of such cutset is quite huge so that it is infeasible to manage them. To deal with that problem, many studies deal only with a particular class of logical topologies. This way, the number of generated cut-sets starts making sense. E.g., [Modiano and Narula-Tam, 2001, 2002] conducted numerical results on ring logical topologies. [Todimala and Ramamurthy, 2007] considered planar cyclic graphs (i.e., if it has a drawing of simple cyclic graphs connecting all the vertexes and having chords that do not cross). [Thulasiraman *et al.*, 2009a] investigates chordal graphs. [Thulasiraman *et al.*, 2009b, 2010] conducted experiments on regular graphs.

[Thulasiraman *et al.*, 2009a,b, 2010] shows the duality between the cutset-based approach with the subgraph-based one, thus the corresponding algorithms have the same algorithmic natures. Based on that observation, the authors come up with a new concept of cutset cover as well as of circuit cover. They introduce a new family of cutset-based and circuit-based algorithms which are far more efficient than the previously proposed ones.

Subgraph-based approach

The subgraph-based approach introduces the concept of piecewise survivable mapping, i.e., a survivable mapping of the logical topology on the physical topology exists if and only if there exists a survivable mapping for a contracted logical topology, that is, a logical topology where a specified subset of edges is contracted [Kurant and Thiran, 2005, 2006, 2007; Javed *et al.*, 2006, 2007; Thulasiraman *et al.*, 2009a,b, 2010] . Consequently, a family of SMART algorithms (Survivable Mapping Algorithm by Ring Trimming) are proposed. The idea of such an algorithm is to build subgraphs that satisfy a certain survivability requirement, then merge them into a bigger one. One advantage of such an approach is that it can locate the critical region where, when failure happens, makes the network disconnected. The subgraph-based researches do not optimize the capacity, i.e., the number of wavelength in the physical layer. [Kurant and Thiran, 2005, 2006, 2007] study the possibility to provide additional capacity to guarantee the existence of survivable mappings. Among them, only [Kurant and Thiran, 2006] take into account multiple link failures.

To date, most proposed ILP models are based on cut-set constraints, and consequently, have scalability issues. Indeed, most ILP models become intractable when the size of the logical networks is getting significant. A great effort has been used in order to reduce the number of generated cut-set constraints by exploiting some special graph structures. However, so far, there is not yet clear tools to identify the useful cut-sets without jeopardizing the optimality of the solutions, although it allowed the design of efficient heuristics. Also, nearly all studies (indeed all except [Kan *et al.*, 2009] in the above cited studies) consider unit demands only, i.e., consider the input of a set of logical links (or lightpaths when they have been mapped to a physical path) with a unit demand. While it can be justified in a context of unlimited physical link capacities, it is restrictive in the context of a limited number of wavelengths. Subgraph-based studies can solve very large instances, however those instances have to be regular graphs. Moreover, their objective is to find a survivable mapping rather than the most economical one.

Table 3.3 describes the characteristics of studies in survivable virtual topology. Column *"protection level"* indicates whether a study consider single or multiple physical link failure. Column *"optimization"* shows whether capacity optimization is taken into account. The possibility of providing additional spare capacity is presented in Column *"additional capacity"*. Other columns are straightforward. Table 3.3 shows that no study yet takes into account multiple link failures, capacity optimization, and additional capacity possibility together. Few can solve very large instances, but those instances have to possess a certain special graph structure. The largest general graph that can be solved is 24 nodes and 44 edges network.

Study	**Protection level**	**Optimization**	**Additional capacity**	**Algorithm**	**Physical topology**	**Logical topology**
[Modiano and Narula-Tam, 2001, 2002]	single failure	✓		cutset-based	14 nodes 21 edges	14 nodes 5-degree
[Kurant and Thiran, 2005, 2007]	single failure		✓	subgraph-based	14 nodes 21 edges	25 nodes f-latices
[Kurant and Thiran, 2006]	multiple failure		✓	subgraph-based		
[Javed *et al.*, 2006]	single failure			subgraph-based	50 nodes 150 edges regular graph	50 nodes 225 edges
[Javed *et al.*, 2007]	single failure			subgraph-based	1000 nodes 8-degree regular graph	800 nodes 2000 edges
[Todimala and Ramamurthy, 2007]	multiple failure	✓		cutset-based	24 nodes 44 edges	20 edges planar cycle
[Liu and Ruan, 2007]	single failure	✓	✓	cutset-based	14 nodes 21 edges	14 nodes 21 edges
[Kan *et al.*, 2009]	single failure	✓		cutset-based	12 nodes 18 edges	12 nodes 5-degree
[Thulasiraman *et al.*, 2009b]	single failure			subgraph+cutset-based	200 nodes 4-degree regular graph	150 nodes 4-degree
[Thulasiraman *et al.*, 2009a]	multiple failure		✓	subgraph+cutset-based		
[Thulasiraman *et al.*, 2010]	single failure			subgraph+cutset-based	200 nodes 4-degree regular graph	150 nodes 4-degree
[Lin *et al.*, 2011]	single failure	✓	✓	cutset-based	25 nodes	12 nodes

Table 3.3: Characteristics of studies in survivable virtual topology

3.4 Multirate cross-layer optical network design

Multirate optical networks recently attracted the attention of researchers due to its tremendous capacity in combining old low speed optical technology together with new very high speed one that is currently being deployed. As the cost of high speed (such as 40 Gbps, 100 Gbps) optical transceivers and regenerators is still very expensive, the cost-effective design problem becomes crucial to industry. Dealing with the cost factor of multirate networks is the key feature to make high-speed optical networks accessible to public.

[Batayneh *et al.*, 2006, 2011b,a] studied the multirate optical network design problem with the constraint of maximum number of ports in mind. [Batayneh *et al.*, 2006] is one among first works on multirate optical networks. Its objective is to optimize the cost of optical ports deployed at nodes. Here, each node is an opaque OXC where every optical bypass is an O/E/O regenerator. This work considers the practical situation in that ports are fabricated as bundles of ports on a single line card. An heuristic is proposed in order to solve such a design problem, and experiments show that 6% cost reduction is achieved with their algorithm for 24-nodes US network. However, many important constraints such as wavelength continuity, transmission reach limits, etc. are missing in that study. [Batayneh *et al.*, 2011b] minimizes interface cost of multirate networks with Ethernet interface at add/drop ports while trying its best to satisfy traffic requests of E-VPNs. Each E-VPN is a virtual private network where multipoint-to-multipoint protocol is used. In order to efficiently exploit multirate networks, E-VPN connections are reorganized by aggregating low bandwidth connections onto larger capacity demands. An important contribution of authors is that protection is taken into account. They use dedicated protection among different E-VPNs while sharing protection within an E-VPN. Therein, the constraint of maximum number of hops in a multi-hop lightpath is not presented.

[Batayneh *et al.*, 2008; Nag *et al.*, 2010; Batayneh *et al.*, 2011a; Liu *et al.*, 2011; Eira *et al.*, 2012; Xie *et al.*, 2012; Santos *et al.*, 2012; Zhao *et al.*, 2013] take into account the transmission reach constraint when solving the multirate optical network design problem. [Batayneh *et al.*, 2008] proposed an optical network where every add/drop interface is an Ethernet device, then focused on reducing the cost of interfaces, that are employed to provision traffic demands, while satisfying physical constraints such as wavelength continuity, maximum number of ports, maximum interface number. Moreover, transmission reach that depends on its corresponding bit-rate is included in their model. Their proposed heuristic successfully solved the Germany network of 17 nodes, with demands between every node pairs. Even if O/E/O regenerators help to restore the shape of optical signal which is distorted during transmission, they are not able to make concurrent optical channels synchronized, thus, an optical signal cannot be sent over optical fibers for an unlimited distance. That is why maximum number of regenerators on a multi-hop lightpath need to be applied in order to make the model more realistic, but, such a constraint is not introduced in the work of [Batayneh *et al.*, 2008]. Multirate optical networks with trade-off between transmission reach and implementation cost of modulation formats (i.e., transceiver cost) are studied in [Nag *et al.*, 2010]. As opposed to other works, the authors used BER to validate the feasibility of an optical lightpath.

A comparison in terms of transponder cost is given in [Liu *et al.*, 2011]. Results show that multirate networks carry more traffic and achieve significant cost reduction (up to 32%) than single rate ones. This study considers BER impairment as well as maximum number of ports in a link, but, many important constraints such as wavelength continuity, transmission reach, etc. are missing in their model. [Eira *et al.*, 2012] proposed a framework to optimize transponder and regenerator costs in optical WDM networks. Authors took into account optical reach, channel width and signal modulation format as input parameters. However, they did not consider grooming in their study. Maximum number of regenerator sites as well as limits on number of available wavelengths and on number of hops are completely ignored in that research.

Regenerator allocation problem is partly solved in [Zhao *et al.*, 2013; Xie *et al.*, 2012] as a preprocessing step to their proposed grooming RWA algorithm. Optimization of regenerator based only on transmission reach, neither CAPEX nor OPEX. Besides, they studied on dynamic traffic with a focus on the blocking connection rate. [Santos *et al.*, 2012] introduce a hybrid approach between integer linear programming (ILP) and graph coloring heuristics to solve the multirate WDM network design problem where maximum number of wavelengths, optical reach as well as cost of transceivers and regenerators are taken into account. Hereby, back-to-back regenerator structure is employed since the authors assume that the regenerator cost is double of the transceiver cost. Actually, the regenerator nodes are pre-enumerated in their model and there is no restriction on the number of segments in multi-hop lightpaths as well as on the number of possible regenerator nodes. Additionally, grooming is not included in their model thus the heterogeneity of optical devices is not fully exploited for cost-effective purpose.

Only [Batayneh *et al.*, 2011a] considered both the transmission reach and maximum number of port constraints. Relationship between transmission reach and network cost (in terms of Ethernet interfaces) in a multirate network is thoroughly studied in [Batayneh *et al.*, 2011a]. Here, traffic consists of Ethernet tunnels which are connections in the electrical layer, and those Ethernet tunnels are aggregated onto Ethernet paths which are lightpaths in the optical layer. As an extension of [Batayneh *et al.*, 2008], the work took into account wavelength continuity, maximum number of ports per link, maximum number of interfaces per node, transmission reach, and node throughput constraints. But again, maximum number of hops per lightpaths is not considered in this model. An interesting feature of this work is that traffic demands are generated between every node-pair and are proportional to population per node.

Citation	**Transmisstion Reach**	**Maximum number of port**	**Instance size**	**Traffic demand** (connections)
[Batayneh *et al.*, 2006]		✓	24 nodes 44 edges	2208
[Batayneh *et al.*, 2008]	✓		17 nodes 26 edges	272
[Nag *et al.*, 2010]	✓		14 nodes 21 edges	182
[Batayneh *et al.*, 2011b]		✓	17 nodes 26 edges	120
[Batayneh *et al.*, 2011a]	✓	✓	24 nodes 44 edges	~3312
[Liu *et al.*, 2011]	✓		14 nodes 21 edges	182
[Eira *et al.*, 2012]	✓		75 nodes 99 edges	~560
[Xie *et al.*, 2012]	✓		75 nodes 99 edges	600
[Santos *et al.*, 2012]	✓		24 nodes 43 edges	552
[Zhao *et al.*, 2013]	✓		28 nodes 39 edges	N/A

Table 3.4: Characteristics of studies in multirate cross-layer optical network design

Table 3.4 describes the characteristics of studies in the multirate cross-layer optical network design problem. Column *"Transmission Reach"* and *"Maximum number of port"* denote studies that consider the transmission reach constraint and the maximum number of port constraint, respectively. Column *"Instance size"* shows the largest instance that the study solves. The last column is the traffic demands that were used in their experiments.

Table 3.4 shows that no work studies the multirate problem with a limit on number of regenerable site constraint. Only [Batayneh *et al.*, 2011a] considers both transmission reach and maximum number of ports per node constraint. In our thesis, we propose a model for the three constraints: transmission reach, maximum number of port and a limit on number of regenerable sites, together. In particular, we study the impact of a limit on number of regenerable sites over the network cost.

3.5 Conclusion

Firstly, the major part of literature have been focusing on one or two realistic network instances. The most popular instances for experiments are NSFNET and US-Network. Numerical results on other popular network instances should be conducted in order to have more evidence to support their conclusions. Secondly, most of proposed ILP models can solve only small network instances of 10 to 24 nodes. For larger instances, a heuristic has to be applied. Since each problem needs a specified heuristic, no work proposes a universal framework to solve a class of problems and their proposed solutions are not easily to be generalized. Besides, there is no quality guarantee on heuristic solution. Finally, few proposed heuristics can solve extremely large network instances, but those heuristics exploit a certain structure that is required for the instances.

Chapter 4

Design of p-cycles subject to wavelength continuity

4.1 Problem statement

While there has been many studies on the efficient design of p-cycles and FIPP p-cycles focusing on optimizing their spare capacity efficiency, few of them consider such p-cycle-based designs under the wavelength continuity assumption, i.e., no wavelength converter at any node. Consequently, few authors look at the routing and wavelength assignment in the context of p-cycles, where all links defining the same p-cycle have to be assigned to the same wavelength.

In case of wavelength conversion, since under a wavelength continuity assumption, a p-cycle and its protected working units must be assigned to the same wavelength. Due to the implicit node conversion assumption, most p-cycle design works only require that the link protection capacity be not smaller than the link working capacity. Under the wavelength continuity assumption, such a requirement is insufficient. Look at the example depicted in Fig. 4.1. Assume that two disjoint lightpaths p and p' are assigned wavelength λ, and have each, one of their link protected by one of the two p-cycles c and c'. Without wavelength converter, λ has to be assigned to p-cycles c and c', but it is not possible as these p-cycles share a link.

In this paper, we propose to investigate thoroughly the issue of wavelength conversion vs. wavelength continuity for p-cycles and FIPP p-cycles, with large scale optimization tools (decomposition techniques) in order to get an exact estimate of

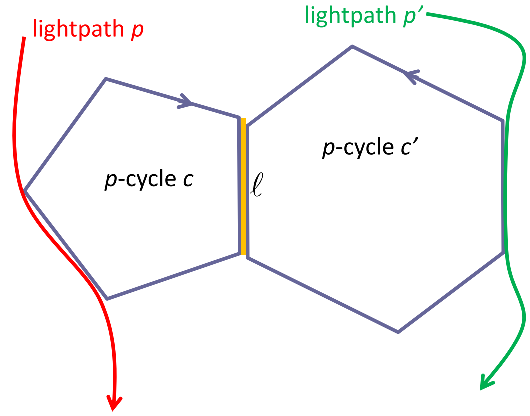

Fig. 4.1: An unfeasible protection solution

the consequences of the wavelength continuity assumption on the spare capacity requirements and consequently on the provisioning cost.

The recourse to decomposition techniques allows the design of exact efficient scalable models contrarily to heuristics which ensure scalability but no accuracy guarantee. In particular, it allows an online generation of improving p-cycle-based configurations, one after the other with respect to the objective, instead of a costly computing time offline generation of p-cycles or FIPP p-cycles as in previous studies, a key issue for a scalable solution.

We describe the definition of configurations as well as mathematical notations in Section 4.2 and 4.3. Next, we introduce our model for p-cycles with and without wavelength continuity assumption in Section 4.4 and 4.5, respectively. Numerical results show that the difference between the capacity requirement under wavelength conversion vs. under wavelength continuity is meaningless (see Table 4.2). Consequently, in view of the reduced provisioning cost (saving at least on the converters), we advocate the design of p-cycles under a wavelength continuity assumption.

We extend our model for FIPP p-cycles without and with wavelength continuity assumption in Section 4.6 and 4.7, respectively. With the obtained numerical results in Table 4.3, we draw the same conclusion as in the case of p-cycles that is the impact of wavelength continuity assumption on capacity requirement is insignificant.

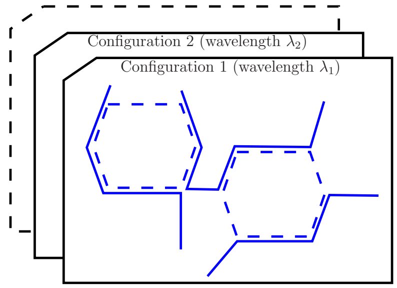

Fig. 4.2: Configuration decomposition of a WDM network

4.2 Notion of configuration

Column generation has been shown to be an efficient and scalable method to solve the static RWA ILP problem, see [Jaumard *et al.*, 2009]. To apply this technique again to the design of p-cycles under the wavelength continuity assumption, we need to devise a decomposition of the initial problem, called master problem, into subproblems, so-called pricing problems in the column generation terminology [Chvatal, 1983]. At each iteration of the solution process, an augmented configuration γ is generated. Such a configuration γ is defined as follows:

Definition 4.1. A configuration γ consists of: *(i)* all the selected working paths and p-cycles that are assigned to an identical wavelength; *(ii)* the set of requests which are routed on the selected working paths; and *(iii)* the set of requests which are protected by the selected p-cycles.

Let Γ denote the set of all possible configurations.

Using a column generation decomposition, a WDM network can be viewed as a partition of pairwise disjoint configurations, where each configuration is associated with a specific wavelength (see an illustration on Fig. 4.2, plain lines are link disjoint working paths and dash circles are link disjoint p-cycles). Assuming all wavelengths to be uniformly available on all links, we do not need to care about which configuration is associated with which wavelength. It thus allows a CG ILP model to get rid of the annoying wavelength symmetry problem, as indicated in [Jaumard *et al.*, 2009].

In the particular case of the design of p-cycles under the wavelength continuity assumption, note that each working path and each p-cycle is embedded in a single configuration. In addition, in each configuration, due to its pairing with a unique wavelength, all working paths are pairwise link disjoint, as well as p-cycles. In the present work, we assume (as in best network design practices) that the protection and working capacity are provided by distinct fibers, so that a p-cycle and its protected working capacity can share the same link with the same wavelength.

In next section, we propose a joint optimization model that takes care simultaneously of the routing and wavelength assignment (RWA) of both the working paths and of the p-cycles. We have the following interesting property:

Theorem 4.2. *If two p-cycle c_1 and c_2 have a node in common, then they can be replaced by a p-cycle c that protects the same working capacity with the same spare capacity as the sum of the two corresponding capacities, with the potential to protect additional requests.*

Proof. Let G_{12} be the subgraph obtained by merging cycles c_1 and c_2. Firstly, as c_1 and c_2 share one node, subgraph G_{12} is connected. Secondly, indegrees and outdegrees of each node in the subgraphs associated with c_1 and c_2 are equal, so does those in subgraph G_{12}. Thus, we can establish a p-cycle c that is an Euler circuit of G_{12}. p-cycle c requires the same amount of protection bandwidth as the bandwidth sum of c_1 and c_2. However, requests with one endpoint on c_1 and another on c_2 (distinct from the shared nodes by the two cycles) can be potentially protected by c, provided that there is enough spare capacity. □

A consequence of Theorem 4.2 is that every feasible protection solution can be represented by a set of node disjoint p-cycles.

When we consider wavelength conversion capacity, we can generate working paths and cycle-based protections from two independent pricings: working path pricing and p-cycle (FIPP p-cycle) pricing. In this case, we have two types of configurations, i.e., one consists of working paths and another consists of cycle-based protections.

4.3 Definitions and notations

We assume the WDM network to be represented by a directed graph $G = (V, L)$ where V denotes the set of nodes (generic index v) and L denotes the set of links (generic index ℓ) with each a wavelength capacity of W. Traffic is described by a set of demands, with a granularity equal to the transport capacity of a wavelength, between node pairs $\mathcal{SD}$:

$$\mathcal{SD} = \{\{v_s, v_d\} : d_{sd} > 0\},$$

where d_{sd} corresponds to the number of unit demand requests from v_s to v_d.
Parameters:

W Number of available wavelengths.

$\mathcal{P}$ Set of working paths, indexed by $p \in \mathcal{P}$.

$\mathcal{C}$ Set of protection configurations, indexed by $c \in \mathcal{C}$.

Γ Set of configuration which contain both working paths and cycle-based protections, indexed by $\gamma \in \Gamma$.

COST_p Cost of working path p.

COST_c Cost of protection configuration c.

COST_γ Cost of configuration γ.

a_ℓ^γ $= 1$ if link ℓ belongs to working capacity of configuration γ, and 0 otherwise.

a_ℓ^p $= 1$ if link ℓ belongs to working path p, and 0 otherwise.

a_ℓ^{sd} $= 1$ if link ℓ belongs to a working path from v_s to v_d, and 0 otherwise.

a_ℓ amount of working capacity routed through ℓ.

b_ℓ^γ $= 1$ if link ℓ belongs to protection configuration γ, and 0 otherwise.

b_ℓ^c $= 1$ if link ℓ belongs to protection configuration c, and 0 otherwise.

b_ℓ amount of protection capacity on ℓ.

m_ℓ^c $= 1$ if link ℓ is protected by protection configuration c, and 0 otherwise.

$\delta^+(.)$ Overall set of incoming links operator.

$\delta^-(.)$ Overall set of outgoing links operator.

Variables:

w_γ number of times configuration γ is repeated.

w_p number of times working path p is repeated.

w_c number of times protection configuration c is repeated.

y_v $= 1$ if node v is on p-cycles, and 0 otherwise.

d_v input/output degree of node v.

α_{sd}^γ number of connections between v_s and v_d routed (working path) in configuration γ.

β_{sd}^c amount of protected working capacity that configuration c provided from v_s to v_d.

4.4 Decomposition model for *p*-cycles with wavelength continuity assumption

The master problem expresses the relationship among the configurations while the pricing problem contains the constraints in order to establish a new configuration. The unit cost of a configuration γ is denoted by COST_γ, and is set to the bandwidth capacity in this study, i.e., the sum of the lengths of the working paths and of the p-cycles associated with γ.

4.4.1 Master problem

The master problem contains only one set of variables: $w_\gamma \in \mathbb{Z}^+$ with w_γ equal to the number of selected copies of configuration γ. It is written as follows.

$$\min \sum_{\gamma \in \Gamma} \text{COST}_\gamma w_\gamma$$

subject to:

$$\sum_{\gamma \in \Gamma} w_\gamma \leq W \tag{4.1}$$

$$\sum_{\gamma \in \Gamma} \alpha_{sd}^\gamma w_\gamma \geq d_{sd} \qquad (v_s, v_d) \in \mathcal{SD} \tag{4.2}$$

$$w_\gamma \in \mathbb{Z}^+ \qquad \gamma \in \Gamma$$

Constraint (4.1) limits the number of configurations to the number of available wavelengths. Constraints (4.2) are the demand constraints.

4.4.2 Pricing problem

We need 4 sets of variables in order to set the constraints for establishing a configuration, which are divided in the constraints for the working scheme and those for the protection scheme. Let u^1 and u_{sd} are the dual values of constraints (4.1) and (4.2), respectively, and $\text{COST}_\gamma = \sum\limits_{\ell \in L}(a_\ell^\gamma + b_\ell^\gamma)$. The objective of the pricing is defined as follows.

$$\min \quad \bar{r}(w_\gamma) = \text{COST}_\gamma + u^1 - \sum_{(v_s,v_d) \in \mathcal{SD}} u_{sd} \alpha_{sd}^\gamma$$

subject to:

(working part)

$$\sum_{(v_s,v_d) \in \mathcal{SD}} a_\ell^{sd} = a_\ell^\gamma \qquad \ell \in L \tag{4.3}$$

$$\sum_{\ell \in \delta^+(v_i)} a_\ell^{sd} = \sum_{\ell \in \delta^-(v_i)} a_\ell^{sd} \qquad (v_s, v_d) \in \mathcal{SD}, \; v_i \in V \setminus \{v_s, v_d\} \tag{4.4}$$

$$\sum_{\ell \in \delta^-(v_s)} a_\ell^{sd} = \sum_{\ell \in \delta^+(v_d)} a_\ell^{sd} = 0 \qquad (v_s, v_d) \in \mathcal{SD} \tag{4.5}$$

$$\sum_{\ell \in \delta^+(v_s)} a_\ell^{sd} = \alpha_{sd}^\gamma \qquad (v_s, v_d) \in \mathcal{SD} \tag{4.6}$$

(protection part)

$$\sum_{\ell \in \delta^+(v)} b_\ell^\gamma = \sum_{\ell \in \delta^-(v)} b_\ell^\gamma \geq y_v \qquad v \in V \tag{4.7}$$

$$a_\ell^\gamma + b_\ell^\gamma \leq y_v \qquad v \in V, \ell \in \delta^+(v) \cup \delta^-(v) \tag{4.8}$$

$$\sum_{\ell \in \delta^+(S)} b_\ell^\gamma \geq a_{(v,v')}^\gamma \qquad S \subset V,\ v \in S, v' \in V \setminus S$$

$$2 \leq |S| \leq |V| - 2. \tag{4.9}$$

The working part is made of *network flow* constraints in order to generate a set of link disjoint working paths. It consists in generating so-called *maximum independent set configuration* as in [Jaumard *et al.*, 2009].

For the protection part, using Theorem 4.2, we can narrow our search of node disjoint p-cycles to the search of a set of pairwise node disjoint p-cycles.

Constraints (4.7) express that the number of incoming and outgoing protection links are equal at every node. Thus, the protection capacity, represented by t_ℓ, is composed of node disjoint p-cycles.

Constraints (4.8) allow fulfilling: *(i)* that nodes of every protection and protected links have to be on p-cycles, and *(ii)* that an *on-cycle* link ℓ cannot protect itself.

Constraints (4.9), inspired from the classical Generalized Subtour Elimination Constraints, imply that every working link is protected within a p-cycle. They also imply that no working link acts like a *bridge* link between two separate p-cycles. If such a working link exists and supposes that it is a *bridge* between p-cycles A and B. Let C denote the p-cycle that protects this link. Obviously, C has common nodes (source and destination of the working link) with both A and B, thus, those p-cycles have to be merged into one p-cycle.

Constraints (4.9) are very numerous, thus adding all of them in the pricing problem could make the solving process performance inefficient. Instead, constraints (4.9) have been implemented in CPLEX as so-called lazy constraints, meaning that these constraints are only added if we notice that they are violated by the current solution. In practice, two solution rounds suffice before all constraints are satisfied even if not embedded explicitly in the set of constraints at the outset.

4.5 Decomposition model for p-cycles without wavelength continuity assumption

In this model, we assume that wavelength converters are installed at every node. Thus, we do not care about wavelength assignment, but put a limit on the working and protection capacity of a link. We use two Pricings, one for generating working paths and other for a set of separate p-cycles. We define a set of separate p-cycles a protection configuration. We apply a multi-pricing column generation algorithm to solve this problem.

4.5.1 Master problem

$$\min \sum_{p \in \mathcal{P}} \text{COST}_p w_p + \sum_{c \in \mathcal{C}} \text{COST}_c w_c$$

subject to:

$$\sum_{p \in \mathcal{P}} a_\ell^p w_p \leq W \qquad \ell \in L \tag{4.10}$$

$$\sum_{c \in \mathcal{C}} b_\ell^c w_c \leq W \qquad \ell \in L \tag{4.11}$$

$$\sum_{p \in \mathcal{P}_{sd}} w_p \geq d_{sd} \qquad (v_s, v_d) \in \mathcal{SD} \tag{4.12}$$

$$\sum_{p \in \mathcal{P}} a_\ell^p w_p \leq \sum_{c \in \mathcal{C}} m_\ell^c w_c \quad \ell \in L \tag{4.13}$$

Constraints (4.10), (4.11), and (4.12) express the number of available wavelengths and the request demands. Constraints (4.13) imply that, on each link, amount of protected capacity has to be greater or equal to amount of working capacity.

We define u_ℓ^1, u_ℓ^2, u_{sd}^3, and u_ℓ^4 the dual values of constraints (4.10), (4.11), (4.12), and (4.13) respectively.

Working path pricing is used to generate a working path, and is defined as follows.

4.5.2 Working path pricing problem

$$\min \bar{r}(w_{p \in \mathcal{P}_{sd}}) = \text{COST}_p + \sum_{\ell \in L} u_\ell^1 a_\ell^p - u_{sd}^3 + \sum_{\ell \in L} u_\ell^4 a_\ell^p$$

We define COST_p the length of working path p. Thus, $\text{COST}_p = \sum_{\ell \in L} a_\ell^p$. The objective function of this pricing problem becomes:

$$\min \bar{r}(w_{p \in \mathcal{P}_{sd}}) = \sum_{\ell \in L} a_\ell^p (1 + u_\ell^1 + u_\ell^4) - u_{sd}^3$$

Actually, this pricing is a Shortest Path Problem and can be easily solved by a classical algorithm such as Dijkstra algorithm. p-Cycle pricing problem is responsible for producing a set of separate p-cycles, and is defined as follows.

4.5.3 p-Cycle pricing problem

$$\min \bar{r}(w_c) = \text{COST}_c + \sum_{\ell \in L} u_\ell^2 b_\ell^c - \sum_{\ell \in L} u_\ell^4 m_\ell^c$$

We define COST_c the length of all p-cycles in configuration c. Thus, $\text{COST}_c = \sum_{\ell \in L} b_\ell^c$. The objective function of this pricing problem becomes:

$$\min \bar{r}(w_c) = \sum_{\ell \in L} (1 + u_\ell^2) b_\ell^c - \sum_{\ell \in L} u_\ell^4 m_\ell^c$$

subject to:

$$\sum_{\ell \in \delta^+(v)} b_\ell^c = \sum_{\ell \in \delta^-(v)} b_\ell^c = d_v \geq y_v \qquad v \in V \tag{4.14}$$

$$m_\ell^c + b_\ell^c \leq y_v \qquad v \in V, \; \ell \in \delta^+(v) \cup \delta^-(v) \tag{4.15}$$

$$\sum_{\ell \in \delta^+(S)} b_\ell^c \geq m_{(v,v')}^c \qquad S \subset V, \; v \in S, v' \in V \setminus S, \; 2 \leq |S| \leq |V| - 2 \tag{4.16}$$

4.6 Decomposition model for FIPP p-cycles with wavelength continuity assumption

We keep the same master problem as in Section 4.4.1 but use the following pricing problem which simultaneously generates working paths and FIPP p-cycles instead of p-cycles, where $\text{COST}_\gamma = \sum_{\ell \in L} (a_\ell^\gamma + b_\ell^\gamma)$.

$$\min \quad \bar{r}(w_\gamma) = \text{COST}_\gamma + u^1 - \sum_{(v_s,v_d)\in\mathcal{SD}} u_{sd}\alpha^\gamma_{sd}$$

subject to:

(working part)

$$\sum_{(v_s,v_d)\in\mathcal{SD}} a^{sd}_\ell = a^\gamma_\ell \qquad \ell \in L \tag{4.17}$$

$$\sum_{\ell\in\delta^+(v_i)} a^{sd}_\ell = \sum_{\ell\in\delta^-(v_i)} a^{sd}_\ell \qquad (v_s,v_d) \in \mathcal{SD} \tag{4.18}$$

$$v_i \in V \setminus \{v_s, v_d\} \tag{4.19}$$

$$\sum_{\ell\in\delta^-(v_s)} a^{sd}_\ell = \sum_{\ell\in\delta^+(v_d)} a^{sd}_\ell = 0 \qquad (v_s,v_d) \in \mathcal{SD} \tag{4.20}$$

$$\sum_{\ell\in\delta^+(v_s)} a^{sd}_\ell = \alpha^\gamma_{sd} \qquad (v_s,v_d) \in \mathcal{SD} \tag{4.21}$$

(protection part)

$$\max_{(v_s,v_d)\in\mathcal{SD}} b^{sd}_\ell = b^\gamma_\ell \qquad \ell \in L \tag{4.22}$$

$$\sum_{\ell\in\delta^+(v_i)} b^{sd}_\ell = \sum_{\ell\in\delta^-(v_i)} b^{sd}_\ell \qquad (v_s,v_d) \in \mathcal{SD} \tag{4.23}$$

$$v_i \in V \setminus \{v_s, v_d\} \tag{4.24}$$

$$\sum_{\ell\in\delta^-(v_s)} b^{sd}_\ell = \sum_{\ell\in\delta^+(v_d)} b^{sd}_\ell = 0 \qquad (v_s,v_d) \in \mathcal{SD} \tag{4.25}$$

$$\sum_{\ell\in\delta^+(v_s)} b^{sd}_\ell = \beta_{sd} \qquad (v_s,v_d) \in \mathcal{SD} \tag{4.26}$$

(cycle constraints)

$$\sum_{\ell\in\delta^+(v_i)} b_\ell = \sum_{\ell\in\delta^-(v_i)} b_\ell \qquad v_i \tag{4.27}$$

$$\sum_{\ell\in\delta^+(v_i)} b_\ell + \sum_{\ell\in\delta^-(v_i)} b_\ell \leq 2 \qquad v_i \tag{4.28}$$

(relationship between protection part and working part)

$$b_\ell^{sd_1} + b_\ell^{sd_2} \leq 3 - \max_{\ell'}(a_{\ell'}^{sd_1} + a_{\ell'}^{sd_2}) \qquad sd_1, sd_2 \in \mathcal{SD}, \ell, \ell' \tag{4.29}$$

$$\beta_{sd} \geq a_\ell^{sd} \qquad (v_s, v_d) \in \mathcal{SD}, \ell \in \delta^-(v_s) \tag{4.30}$$

$$a_\ell^{sd} + b_\ell^{sd} \leq 1 \qquad \ell \in L \qquad (v_s, v_d) \in \mathcal{SD} \tag{4.31}$$

Besides constraints that are described in the previous pricings, we introduce three additional sets of constraints. Constraints (4.29) imply that two working paths that share a same link have to be protected by disjoint FIPP p-cycles. Constraints (4.30) express that all working paths have to be protected. Constraints (4.31) imply that working paths and FIPP p-cycles are link-disjoint.

4.7 Decomposition model for FIPP p-cycles without wavelength continuity assumption

We use the following master problem which is almost identical to the one in Section 4.5, except that we replace Constraint (4.13) by Constraint (4.35) which express that we protect the whole working capacity between v_s and v_d.

4.7.1 Master problem

$$\min \sum_{p \in \mathcal{P}} \text{COST}_p w_p + \sum_{c \in \mathcal{C}} \text{COST}_c w_c$$

subject to:

$$\sum_{p \in \mathcal{P}} a_\ell^p w_p \leq W \qquad \ell \in L \tag{4.32}$$

$$\sum_{c \in \mathcal{C}} b_\ell^c w_c \leq W \qquad \ell \in L \tag{4.33}$$

$$\sum_{p \in \mathcal{P}_{sd}} w_p \geq d_{sd} \qquad (v_s, v_d) \in \mathcal{SD} \tag{4.34}$$

$$\sum_{p \in \mathcal{P}_{sd}} w_p \leq \sum_{c \in \mathcal{C}} \beta_{sd}^c w_c \quad (v_s, v_d) \in \mathcal{SD} \tag{4.35}$$

We define u_ℓ^1, u_ℓ^2, u_{sd}^3, and u_{sd}^4 the dual values of constraints (4.32), (4.33), (4.34), and (4.35) respectively.

We use the multi-pricing column generation algorithm with the same working path pricing problem as in Section 4.5. However, we use the following pricing problem instead of the p-cycle pricing one to generate FIPP p-cycles.

4.7.2 FIPP p-cycles pricing problem

$$\min \bar{r}(w_c) = \textsc{cost}_c + \sum_{\ell \in L} u^2_\ell b^c_\ell - \sum_{sd \in \mathcal{SD}} u^4_{sd} \beta^c_{sd}$$

We define $\textsc{cost}_c$ the length of all FIPP p-cycles in configuration c. Thus, $\textsc{cost}_c = \sum\limits_{\ell \in L} b^c_\ell$. The objective function of this pricing problem becomes:

$$\min \bar{r}(w_c) = \sum_{\ell \in L} (1 + u^2_\ell) b^c_\ell - \sum_{sd \in \mathcal{SD}} u^4_{sd} \beta^c_{sd}$$

subject to:

(protection part)

$$\max_{(v_s,v_d) \in \mathcal{SD}} b^{sd}_\ell = b^\gamma_\ell \qquad \ell \in L \tag{4.36}$$

$$\sum_{\ell \in \delta^+(v_i)} b^{sd}_\ell = \sum_{\ell \in \delta^-(v_i)} b^{sd}_\ell \qquad (v_s, v_d) \in \mathcal{SD} \tag{4.37}$$

$$v_i \in V \setminus \{v_s, v_d\} \tag{4.38}$$

$$\sum_{\ell \in \delta^-(v_s)} b^{sd}_\ell = \sum_{\ell \in \delta^+(v_d)} b^{sd}_\ell = 0 \qquad (v_s, v_d) \in \mathcal{SD} \tag{4.39}$$

$$\sum_{\ell \in \delta^+(v_s)} b^{sd}_\ell = \beta_{sd} \qquad (v_s, v_d) \in \mathcal{SD} \tag{4.40}$$

(cycle constraints)

$$\sum_{\ell \in \delta^+(v_i)} b_\ell = \sum_{\ell \in \delta^-(v_i)} b_\ell \qquad v_i \tag{4.41}$$

$$\sum_{\ell \in \delta^+(v_i)} b_\ell + \sum_{\ell \in \delta^-(v_i)} b_\ell \leq 2 \qquad v_i \tag{4.42}$$

Table 4.1: Characteristics of the data sets tested with the p-cycle model

Network instance	$\lvert V\rvert$	$\lvert L\rvert$	Node degree	$\lvert W\rvert$	$\lvert\mathcal{SD}\rvert$	$\overline{D}_{sd}$
DFN-BWIN	10	90	9.00	42	90	20.60
DFN-GWIN	11	94	8.54	240	110	20.03
PDH	11	68	6.18	24	24	25.29
POLSKA	12	36	3.00	200	66	20.92
ATLANTA	15	44	2.93	800	210	19.48
GERMANY	17	52	3.06	560	121	19.95
SUN	27	102	3.78	260	67	21.03

4.8 Numerical results

This section describes the dataset that is used to test our models and the obtained results.

The optimality gap evaluates the solution quality/accuracy. It is defined as follows: $(|z^\star - z^\star_{\text{LP}}|)/z^\star_{\text{LP}}$ (%) where $z^\star$ is the optimal ILP solution of the RMP and $z^\star_{\text{LP}}$ is the optimal solution of the LP relaxation of MP. It turns out that, we achieve a reasonable small gap for benchmark instances.

Algorithms were implemented in C++ using Concert Technology library of CPLEX 11.100. The computational experiments were performed on a 2.2 GHz AMD Opteron 64-bit processor with 16GB of RAM.

In order to validate the models developed, we use the benchmark network instances listed in Table 4.1. Therein, for each network, we provide the number of nodes, the number of directed links, the average node degree, the number of node pairs with traffic, and the average number of connections per node pair (with traffic). All network instances are taken from [Orlowski *et al.*, 2007], traffic instances have been generated using an uniform distribution. Note that we could not directly use the traffic instances from [Orlowski *et al.*, 2007] as they consist of symmetrical traffic data, but we did generated traffic for the same node pairs, using a uniform distribution.

Table 4.2: Results obtained under a joint-optimization scheme with/without wavelength conversion capacity for the p-cycle model

Wavelength continuity					
Network instances	Total capacity	%W	GAP	CPU	# configs
DFN-BWIN	2,312	83	3.72	1h-17m-43s	39
DFN-GWIN	3,769	68	1.67	2h-26m-57s	240
PDH	1,036	74	0.78	50s	24
POLSKA	5,210	54	0.02	5m-16s	200
ATLANTA	19,488	55	0.48	2h-06m-42s	727
GERMANY	14,372	46	0.05	1h-19m-46s	551
SUN	8,431	52	0.00	4h-09m-12s	252
No wavelength continuity					
DFN-BWIN	2,233	83	0.18	7m-41s	39
DFN-GWIN	3,561	71	0.03	22s	141
PDH	1,028	74	0.00	2s	24
POLSKA	5,171	54	0.00	2s	200
ATLANTA	19,303	55	0.00	7s	561
GERMANY	14,246	46	0.00	4s	526
SUN	8,224	53	0.00	2m-31s	169

Table 4.2 and Table 4.3 shows the characteristics of the solutions obtained with our new ILP model of p-cycles and FIPP p-cycles under a joint-optimization scheme with/without wavelength conversion capacity, respectively. For each solved instance, the total capacity, the optimality gap, the computing time, and the number of used wavelengths are given.

Numerical results show that although the bandwidth is slightly higher under the wavelength continuity assumption, the difference is not significant in view of the efficiency and the cost of single hop lightpaths, as we, at least, save the expense cost of wavelength converters.

Solving time relatively depends on amount of bandwidth demands and topology size. Amount of bandwidth demands has a great impact on the solving time of Master problem. Otherwise, the solving time of Pricing problem depends heavily on topology size. Since amount of bandwidth demands and topology size of both PDH

Table 4.3: Results obtained under a joint-optimization scheme with/without wavelength conversion capacity for the FIPP p-cycle model

Network instances	Total capacity	%W	GAP	CPU	# configs
Wavelength continuity					
DFN-BWIN	1,549	87	4.3	04h:37m:23s	20
DFN-GWIN	2,641	71	2.6	11h:29m:47s	36
PDH	,536	65	0.9	00h:00m:27s	11
POLSKA	3,400	61	0.9	00h:20m:05s	55
ATLANTA	13,483	59	0.9	05h:14m:53	181
GERMANY	10,559	46	0.8	03h:49m:13s	107
SUN	5,495	59	0.9	13h:36m:41s	54
No wavelength continuity					
DFN-BWIN	1,541	87	4.3	01h:23m:35s	16
DNF-GWIN	2,590	72	2.3	04h:25m:26s	44
PDH	,535	65	0.7	00h:00m:29s	9
POLSKA	3,393	60	0.7	06h:50m:28s	64
ATLANTA	13,481	59	0.9	22h:50m:25s	169
GERMANY	10,556	46	0.9	41h:45m:38s	121
SUN	5,462	59	0.3	14h:17m:12s	64

and POLSKA instances are small, their total solving times are pretty low.

4.9 Conclusion

We developed two decomposition models that jointly optimize the capacity of working paths with p-cycles and FIPP p-cycles. It has three original features. Firstly, our models address WDM networks that do not have any wavelength conversion capability. Secondly, our models jointly optimize the working and the protection capacity. Thirdly, working paths and p-cycles as well as FIPP p-cycles are generated on fly, and added to the master problem only if they improve the current value of the objective. We tested the proposed model on several medium-size networks. We compared the required bandwidth with/without the wavelength continuity assumption and observed that the difference is meaningless, so that, due to their cost, node converters are not justified.

Chapter 5

Design of dependent and independent *p*-cycles against multiple failures

We propose a new generic flow formulation for Failure-Dependent Path-Protecting (FDPP) p-cycles subject to multiple failures. While our new model resembles the decomposition model formulation proposed by [Orlowski and Pióro, 2011] in the case of classical shared path protection, its originality lies in its adaptation to FDPP p-cycle. When adapted to that last pre-configured pre-cross connected protection scheme, the bandwidth sharing constraints must be handled in a different way in order to take care of the sharing along the FDPP p-cycle. It follows that, instead of a polynomial-time solvable pricing problem as in the model of [Orlowski and Pióro, 2011], we end up with a more complex pricing problem, which is no more polynomially solvable. We therefore focused on speeding up the iterative solution process of the pricing problems using a hierarchical decomposition of the original pricing problem. Moreover, a very useful mathematical technique is applied to keep the size of the master problem reasonably small so that it is efficiently solvable.

Performance evaluation is made in the case of FDPP p-cycle subject to dual link failures and some higher-order link failures as well. The proposed model remains fairly scalable for increasing percentages of dual link failures, and requires much less bandwidth than p-cycle protection schemes (ratio varies from 2 to 4). In the particular case of single link failures, it compares favorably to the previously proposed column generation ILP model of [Rocha *et al.*, 2012] for FIPP p-cycle. Several experiments with higher-order failures such as triple link failures, quadruple link failures are conducted to show the generality of our model. We will also explain how easy it is to implement node protection schemes on the model, thus imply that node protection problem is just a special case of link protection problem.

We introduce the concepts and notations in Section 5.1, and then we set the newly proposed column generation model for multiple link failure protection in Section 5.2. We propose an approach to speed up the solution process in Section 5.3. Section 5.4 gives some insights to our proposed model. Section 5.5 presents the numerical results. Finally, Section 5.6 draws the conclusion.

5.1 Definitions and notations

We assume the WDM network to be represented by an undirected graph $G = (V, L)$ where V denotes the set of nodes (indexed by v) and L denotes the set of links (indexed by ℓ), each with a fiber capacity of W wavelengths. We denote by $\delta(v)$ the set of adjacent links of node v, $v \in V$.

Under a multiple link failure scenario, let $\mathcal{F}$ be the set of all possible link failure sets, indexed by F. We assume that all dominated failure sets have been eliminated, i.e., for any F, F' belonging to $\mathcal{F}$, we assume that $F \not\subseteq F'$ and $F' \not\subseteq F$.

We assume that the primary (working) routing of the requests has been done, e.g., along the shortest paths between source and destination nodes. Let wp working path index and $\mathcal{WP}$ set of working paths. For each working path wp, let v_s and v_d the source and the destination of that path, respectively. We assume that the generated working paths are able to be protected by a certain set of backup paths. Such an assumption is guaranteed by a pre-processing step that eliminates sets of working paths that are unable to be protected.

In our model, the protection solution is provided by a set of configurations, where each configuration γ is defined as follows:

Definition 5.1. A configuration $\gamma = (\varphi, p)$ is represented by a pair of vectors φ and p such that $\varphi = (\varphi_{wp}^{F,\ell})$ and $p = (p_{wp}^{F})$, for $F \in \mathcal{F}$, $wp \in \mathcal{WP}$ and $\ell \in L$, where:

$\varphi_{wp}^{F,\ell}$ is the number of protection units on link ℓ which are used for protecting part of all the traffic going through working path wp against failure set F.

p_{wp}^{F} is the number of protected units provided by configuration γ for the traffic going through working path wp against failure set F.

Let Γ denote the set of all possible configurations.

Note that, with such a configuration definition, each configuration can be selected more than once. Moreover, in general, a given configuration only protects a fraction of the working capacity. By aggregating several configurations, the overall network is then protected. Indeed, for a given set of configurations $\{\gamma_1, \gamma_2, \dots, \gamma_n\}$, we can build a new configuration γ as an aggregate configuration defined by a linear combination (with coefficients $\alpha_1, \alpha_2, \dots, \alpha_n$) of the protection elements $\varphi_{wp}^{F,\ell}$ and p_{wp}^{F} of each of the *elementary* configurations as follows:

For all $F \in \mathcal{F}, wp \in \mathcal{WP}$,

$$\varphi_{sd}^{F,\ell,\gamma} = \sum_{i=1..n} \alpha_i \, \varphi_{wp}^{F,\ell,\gamma_i} \qquad \ell \in L \tag{5.1}$$

$$p_{wp}^{F,\gamma} = \sum_{i=1..n} \alpha_i \, p_{wp}^{F,\gamma_i}. \tag{5.2}$$

In order to reduce the number of potential configurations, one may consider only maximal configurations, i.e., configurations γ such that there exists no configuration γ' satisfying:

For all $F \in \mathcal{F}, wp \in \mathcal{WP}$,

$$\varphi_{wp}^{F,\ell,\gamma} \leq \varphi_{wp}^{F,\ell,\gamma} \qquad \ell \in L \tag{5.3}$$

$$p_{wp}^{F,\gamma'} \leq p_{wp}^{F,\gamma} \tag{5.4}$$

i.e., no configuration that can offer less protection with more protection bandwidth requirement. But then, on the one hand, there would still be many potential configurations, and on the second hand, there is no guarantee that an optimal solution could be made of only maximal configurations, while maximizing protection bandwidth sharing and consequently minimizing the protection bandwidth requirements (see constraints (5.7) in the mathematical model). Pushing the idea of maximal configurations to its extreme, one could think about the definition of a configuration which supports the overall needed protected capacity. But then, the resulting optimization problem may be quite difficult to solve. Following those two observations, we decided to turn our attention to unit configurations.

Given a working path, a backup lightpath of it is called failure independent protection path if and only if any failure set that impacts on the working path does not disrupt that backup lightpath.

Definition 5.2. A unit FDPP configuration $\gamma = (\varphi, p)$ is represented by a pair of vectors φ and p such that $\varphi = (\varphi^{\ell}_{wp})$ and $p = (p_{wp})$, for $wp \in \mathcal{WP}$ and $\ell \in L$, where φ^{ℓ}_{wp} in $\{0, 1\}$ and ℓ cannot be shared for two working lightpaths wp_1 and wp_2 that can be broken simultanously.

Using unit configuration, we propose to set an optimization model where the protection structure will be defined by a combination of several unit configurations, with some unit configuration occurring more than one.

In order to compute the traffic flow values $\varphi^{F,\ell}_{wp}$ and the protected amounts p^{F}_{wp}, we use a network flow formulation that is presented in Section 5.2.2. Those values constitute the building blocks of the configurations.

We next have a closer look at the configurations. In order to be protected against failure F, on each link ℓ, we need a protection capacity that is equal to the sum of the protection capacities which are reserved for the traffic of each working path wp with respect to F:

$$\varphi^{F,\ell} = \sum_{wp \in \mathcal{WP}} \varphi^{F,\ell}_{wp} \qquad F \in \mathcal{F}, \ell \in L. \tag{5.5}$$

For a given set of values of variables $\varphi^{F,\ell}_{wp}$, the amount of protected capacity that configuration γ provides for the traffic of working path wp against failure F is as follows:

$$p^{F}_{wp} = \sum_{\ell \in \delta(v_s)} \varphi^{F,\ell}_{wp} \qquad F \in \mathcal{F}, wp \in \mathcal{WP}. \tag{5.6}$$

To apply the decomposition approach in a column generation method, we need to break the protection solution into several configurations. Note that the solution process consists of repeatedly solving the pricing problem and the restricted master problem (see Section 5.2 for the detailed definition of these problems), thus, in order to achieve a scalable decomposition model, a good performance trade-off between the pricing problem and the restricted master problem must be found. As configurations are generated by the pricing problem, we need to define a so-called basic configuration that can be easily generated by the pricing problem, and such that any configuration can be easily decomposed into an integer linear combination of basic configurations.

5.2 FDPP p-cycle decomposition model

The proposed optimization model establishes relationships among the configurations in order to satisfy the protection bandwidth requirements, as the configurations take care (throughout the pricing problems) of generating the protection paths against the various independent failure sets. It requires one set of variables defined as follows:

$z_\gamma \in \mathbb{Z}^+$ number of selected copies of configuration γ.

5.2.1 Master problem

The objective, which aims at minimizing the protection bandwidth requirements, can be written as follows:

$$\min \quad z^{\text{OBJ}} = \sum_{\gamma \in \Gamma} \text{COST}_\gamma \, z_\gamma \tag{5.7}$$

where $\text{COST}_\gamma = \sum\limits_{\ell \in L} x_\ell^\gamma$.

Constraints are expressed as follows:

$$\sum_{\gamma \in \Gamma} p_{wp}^\gamma \, z_\gamma \geq c_{wp} \qquad wp \in \mathcal{WP} \tag{5.8}$$

$$z_\gamma \in \mathbb{Z}^+ \qquad \gamma \in \Gamma \tag{5.9}$$

where c_{wp} the capacity carried by working lightpath wp. Notice that working paths that are not impacted by any failure set will not be included in that model.

5.2.2 Pricing problem

We first write the pricing problem for the classical shared path protection and extend it later to the p-cycle protection scheme.

In the undirected case, the pricing problem $\text{PRICING}(\text{INPUT} : u; \text{OUTPUT} : \varphi, p)$ has two sets of variables:

$\varphi_{wp}^\ell \in \{0,1\}$. Those unit flow variables define potential protection path(s) for a given working lightpath $wp \in \mathcal{WP}$, against any failure set that impacts on wp.

$p_{wp} \in \mathbb{Z}^+$. Those variables help to indicate the number of protected units with respect to protection against any failure impacted set F, for a given lightpath $wp \in \mathcal{WP}$.

We define $\delta(S)$ for $S \subset V$, as the cut induced by S, i.e., the set of edges incident to a node in S and another node in $V \setminus S$.

Let $\mathcal{WP}_F$ set of working lightpaths impacted by F, and $\mathcal{F}_{wp}$ the union of all failure sets that impact on wp.

For all $wp \in \mathcal{WP}$, v_s and v_d source and destination of wp we have:

$$\varphi_{wp}^{\ell} = 0 \qquad \ell \in \mathcal{F}_{wp} \tag{5.10}$$

$$\sum_{\ell \in \omega(v_s)} \varphi_{wp}^{\ell} = \sum_{\ell \in \omega(v_d)} \varphi_{wp}^{\ell} = p_{wp} \tag{5.11}$$

$$\sum_{\ell \in \omega(v)} \varphi_{wp}^{\ell} \leq 2 \qquad v \in V \setminus \{v_s, v_d\} \tag{5.12}$$

$$\sum_{\ell \in \omega(v) \setminus \{\ell'\}} \varphi_{wp}^{\ell} \geq \varphi_{wp}^{\ell'} \qquad \ell' \in \omega(v), v \in V \setminus \{v_s, v_d\} \tag{5.13}$$

$$p_{wp} \in \{0, 1, 2\} \tag{5.14}$$

$$\varphi_{wp}^{\ell} \in \{0, 1\} \tag{5.15}$$

The above constraints establish paths throughout a flow formulation, from a given source to a given destination, while forbidding the use of failing links.

Also, we need the following constraint to make sure that no link can be shared between lightpaths that may fail simultanously:

$$\sum_{wp \in \mathcal{WP}_F} \varphi_{wp}^{\ell} \leq 1 \qquad \forall F, \ell \tag{5.16}$$

In order to get a FDPP p-cycle protection scheme, we introduce the unit flow variables $x_\ell \in \{0, 1\}$, which enforce cycle shapes for supporting the protection paths, i.e., to guarantee that the two end points of each protection path are lying on a cycle.

We also need the following constraints:

$$x_\ell \geq \sum_{wp \in \mathcal{WP}} \varphi^\ell_{wp} \tag{5.17}$$

$$\sum_{\ell \in \omega(v)} x_\ell \leq 2 \qquad v \in V \tag{5.18}$$

$$\sum_{\ell \in \omega(v) \setminus \{\ell'\}} x_\ell \geq x_{\ell'} \ell' \in \omega(v), v \in V \tag{5.19}$$

$$\sum_{\ell \in \delta(S)} \varphi^\ell_{wp} \geq p_{wp} \quad S \subset V, 3 \leq |S| \leq |V| - 3,$$

$$v_s \in S, v_d \in V \setminus S, wp \in \mathcal{WP} \tag{5.20}$$

$$x_\ell \in \{0, 1\} \quad \ell \in L \tag{5.21}$$

Constraints (5.20) are subtour elimination constraints which eliminates cycles isolating the source node from the destination node of a given flow. Note that those constraints do not eliminate all subtours, but only those disconnected a source node to its corresponding destination node.

5.3 Solution enhancements

In this section we introduce two techniques to enhance the solution process. The first one is to speed up the pricing problem solving. The second one is to efficiently manage the program memory.

5.3.1 Speed up pricing problem

For FDPP p-cycle, a configuration $\gamma = (\varphi, p, x)$ includes: (i) the definition of one of several cycles throughout the flow variables of vectors φ and x where x is a flow vector defining the cycle(s) (there might be more than one) associated with the configuration, (ii) the number of protected units for each traffic flow between v_s and v_d against each failure set F, as identified by the variables of vector p. Moreover, different configurations can be associated with the same cycle or set of cycles.

In order to speed up the solution of the pricing problems, which are iteratively solved, we introduced a decomposition solution scheme, as in [Rocha *et al.*, 2012]. Let us denote by PRICING(INPUT : u; OUTPUT : φ, p, x) the current pricing problem

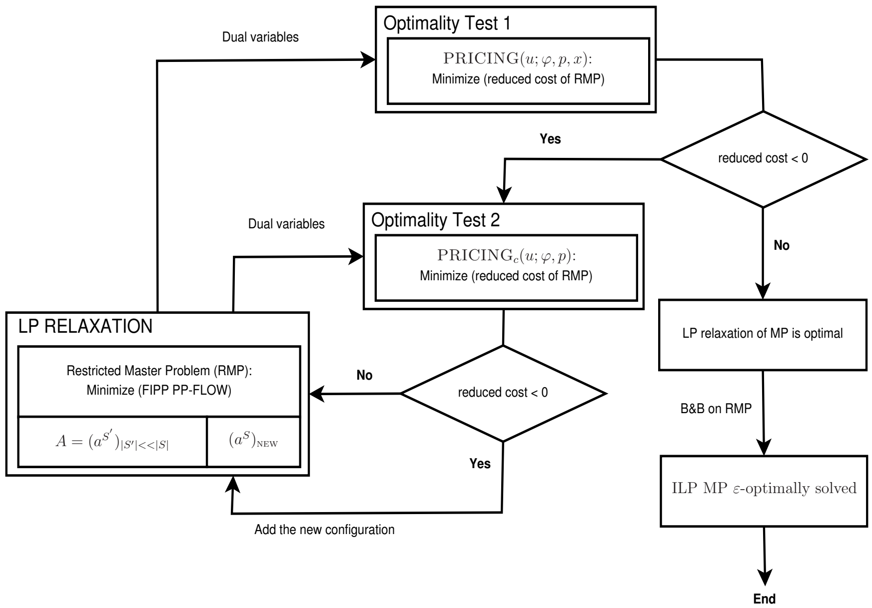

Fig. 5.1: ILP & column generation algorithm

to be solved, where u is the vector of the dual variables of the current RMP. Let C_γ be the set of cycles associated with configuration γ. We introduce the restricted pricing problem PRICING$_c(u;\varphi,p)$, for each cycle $c \in C_\gamma$, where constraints are identical to the constraints of PRICING(INPUT : u; OUTPUT : φ, p, x), except that a cycle is given (see Section 5.2.2 for more details). Before solving a new pricing problem PRICING$(u;\varphi,p,x)$, we first iterate solving restricted pricing problems PRICING$_c(u;\varphi,p)$, for all cycles $c \in C_\gamma$, until no more augmenting configuration can be generated with the set C of cycles generated so far, see Fig. 5.1 for a flowchart of the algorithm that is adapted from the original CG algorithm.

5.3.2 Memory management

Although column generation helps to significantly reduce the number of considered configurations, it may attain a quite huge value after a certain number of iterations, for e.g., up to tens of thousands of configurations. Keeping too many columns in the RMP leads to two possible problems. Firstly, memory is probably not enough to contain the RMP. Secondly, solving the master problem with a lot of columns at each step may take a nontrivial amount of time such that it results in an unacceptable performance of the solve process. In order to get over this difficulty, we use the following observation: the highest reduced cost column (most of the time, it is a non-basic column) is the one that has the highest probability of not being in the final solution. Thus, if the number of non-basic columns is greater than the one of basic columns, instead of adding the new column, we replace it with the highest reduced cost column in the RMP. By this way, we keep the rate of the RMP columns over the RMP basic columns under 2.0, such a rate varies from problem to problem. One may wonder why we do not eliminate all non-basic columns. The reason is that non-basic columns, which are not in the optimal relaxed solution, are possibly in the RMP integer solution. We see here the tradeoff between keeping the number of master columns reasonably small to guarantee an acceptable performance but reasonably big enough to produce a high quality final integer solution. A good upper bound on the non-basic/basic RMP columns is the key to the success of this approach. Readers are encouraged to see, e.g., [Chvatal, 1983] if not familiar with generalized linear programming concepts.

5.4 Insights into the proposed model

In this section, we study two aspects of the proposed model. Firstly, we show that our model, when it comes to single link failures, uses less spare capacity than the FIPP model proposed in [Rocha and Jaumard, 2012] (experimental evidences are given in Table 5.2). Secondly, we explain how the studied model can express a node failure by a multiple link failure.

5.4.1 Compare with the previously proposed model

The main advantage of our model lies at the fact that a backup cycle can protect a set of arbitrary working paths while, in the case of [Rocha and Jaumard, 2012], such a backup cycle is able to protect only a set of disjoint working paths. Fig. 5.2 represents backup cycle A-B-C-D-E-F-G-H with two working paths: $l_8 - l_9 - l_{10}$ and $l_{11} - l_9 - l_{12}$. In the previous model, one unit of the backup cycle provides either 2 backup units for the first working path or 2 backup units for the second working path (full-cycle protection for a straddle link). With the proposed model, besides two mentioned backup solutions, we have the third backup solution, drawn by dashed lines, that gives 1 backup units to each of working paths. Hence, less restrictions

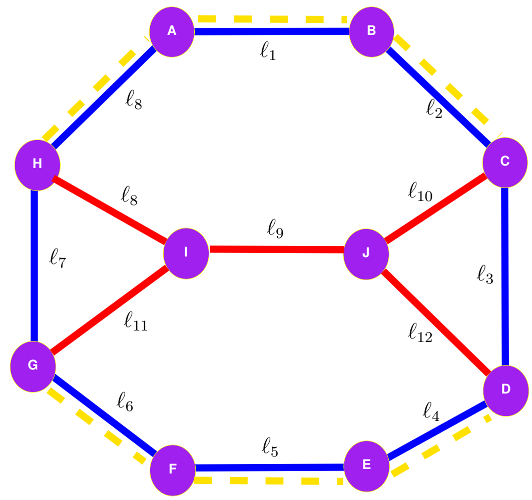

Fig. 5.2: A backup cycle

on which working paths are protected results in having more backup solutions, that means more spare capacity can be saved. For e.g., in Fig. 5.2, we want to protect 5 units of working path $l_8 - l_9 - l_{10}$ and 3 units of working path $l_{11} - l_9 - l_{12}$. The proposed model will reserve 4×8 (cycle size=8) spare capacity units while the previous model need 5×8 units.

5.4.2 As a node protection framework

A node failure makes its adjacent links out of service, therefore, we can replace this node failure by the failure of its adjacent links. For instance, in Fig. 5.3, if all links of link set $L = \{l_1, l_2, l_3, l_4\}$ fail simultaneously, then node A is isolated from other nodes in the network. This means node A is considered being failed. Evidently, multiple link failure set L represents node failure A. Considering node failures as multiple link failures makes our FDPP model more unified as a path-based protection framework.

In the literature, most studies simulate node failing by replacing the network topology by a directed graph in which links are represented by two opposite directed edges and network nodes by two vertices interconnected by a directed edge (see Fig. 5.4 where node A is splitted into node A^{in} and A^{out}). Not only such an approach increases the number of nodes in the network topology by a factor of two, but also it does not reduce the number of failure sets that we have to deal with. Computational complexity of node failure protection problem depends on the number of failure sets

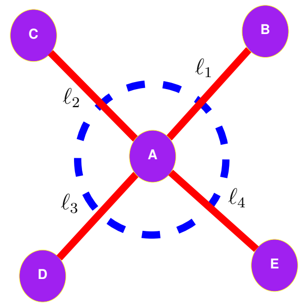

Fig. 5.3: A node failure

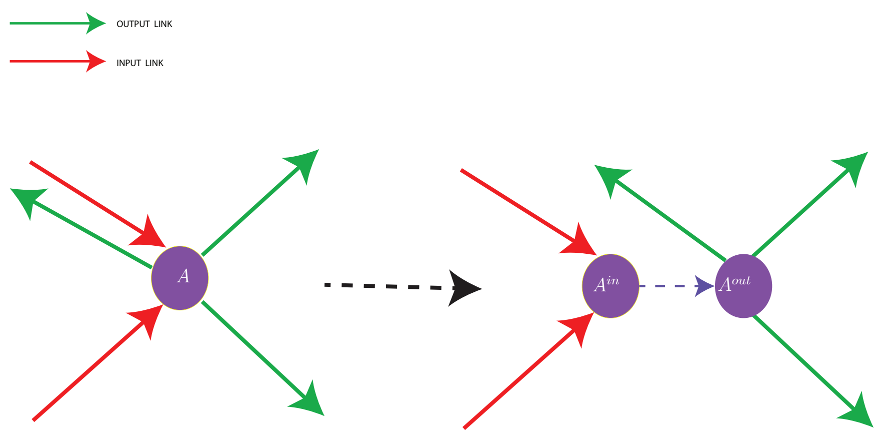

Fig. 5.4: Transformation of a node failure into a link failure

rather than their size. Thus, in comparison to the conventional way, our node failure formulation is more scalable.

5.4.3 An example where FDPP solution exists but FIPP solution does not

Fig. 5.5 is a simple network that has only one working path $S - V5 - V6 - D$ and two failure sets $S1 = \{L1, L2\}$ and $S2 = \{L2, L3\}$. A trivial FDPP solution can be easily found: using $S - V3 - V4 - D$ when failure set $S1$ occurs, and using $S1 - V1 - V2 - D$ when failure set $S2$ happens. It does not exist one backup lightpath that can protect $S - V5 - V6 - D$ against $S1$ as well as $S2$.

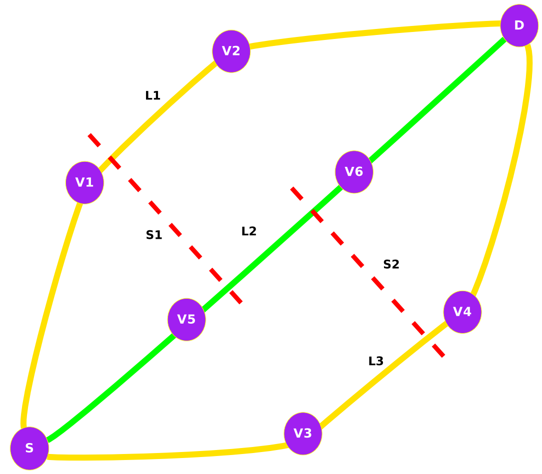

Fig. 5.5: FDPP vs FIPP

5.5 Numerical results

We implemented the model, called FDPP p-cycle model, developed in Section 5.2 for FDPP p-cycle. Algorithms were implemented in the OPL programming language and executed in [IBM, 2011b]. Programs were run on a 2.2 GHz AMD Opteron 64-bit processor with 16GB of RAM. For each instance, the running time was limited to 24 hours, which is satisfactory in the context of network planning.

The computation time restriction is determined from two factors: cost of running the solution process and how much solution improvement we get per solution step. We see that, after 24 hours, incumbent solutions get insignificantly improved, while the solution process, when it takes a long time, costs an expensive price (see Amazon EC2's prices) and could prematurely end with an out of memory error. Even if we can apply few memory management techniques to avoid such an error, those techniques significantly increase the runtime of the solution process in return. Hence, at some point we have to decide between paying for the solution process and the benefit of potential solutions that could be generated by such a process.

We next describe the network and data instances in Section 5.5.1, and then discuss performances of the FDPP p-cycle model in the cases of single link failures (Section 5.5.2) and of dual link failures (Section 5.5.3). Node protection experiments are conducted in Section 5.5.4. We also look at the increase of the bandwidth requirements when the number of protected pair of links increases. Section 5.5.5 investigates the scalability of the model when it comes to triple and quadruple link failures.

5.5.1 Network and data instances

We consider the benchmark network and data instances listed in Table 5.1 for our numerical experiments. They are all from [Orlowski *et al.*, 2007], except for the traffic matrice denoted by US14N21S, which are taken from [Rocha and Jaumard, 2012]. For each network, we provide the number of nodes ($|V|$), the number of undirected links ($|L|$), the average node degree (d), the number of node pairs with requests ($|\mathcal{SD}|$), and the overall flow value ($\sum_{\{v_s,v_d\}\in\mathcal{SD}} d_{sd}$).

Network & traffic instances	$\lvert V\rvert$	$\lvert L\rvert$	d	$\lvert\mathcal{SD}\rvert$	$\sum_{\{v_s,v_d\}\in\mathcal{SD}} d_{sd}$
POLSKA	12	18	3.0	66	9,943
NOBEL-US	14	21	3.0	91	5,420
US14N21S	14	21	3.0	91	2,710
ATLANTA	15	22	2.9	105	136,726

Table 5.1: Description of Network Instances

5.5.2 Performance of the FDPP p-cycle model: single link failure

As already mentioned in Section 5.4, the multiple failure model for FDPP p-cycle proposed in Section 5.2 differs from the previously proposed models for FIPP p-cycle ([Rocha and Jaumard, 2012; Jaumard *et al.*, 2007; Kodian and Grover, 2005]). It is indeed more general in the sense that it is less constrained. For instance, the so-called Z-case is allowed (see [Jaumard *et al.*, 2007] for its definition), and no restriction is made on disjointness of the working paths protected by a given FDPP p-cycle. The consequences, as illustrated by the results in Table 5.2, is some reduced bandwidth requirements.

Experiments reported in Table 5.2 have been made on the same network and traffic instances with exactly the same working paths (shortest paths). In comparison with [Rocha and Jaumard, 2012], we observed that the reduction in the bandwidth requirements for protection against single link failure range from 2.08% for the ATLANTA instance up to 14.85 % for the NOBEL-US instance, which is quite meaningful.

In addition, the optimality gaps, which measure the accuracy of the obtained solutions, are very comparable between the two models, see the two columns entitled "Gaps". As observed in other experiments in the literature, the gap is very small (between 0.09% and 1.39%), and indeed optimal from a practical point of view.

Instances	FIPP p-cycles. Model of [Rocha and Jaumard, 2012]		FDPP p-cycle model		Bandwidth Reduction (Percentage)
	z^{ILP}	Gaps	z^{ILP}	Gaps	
POLSKA	11,830	0.43	11,086	0.52	6.29
NOBEL-US	6,102	0.31	5,196	0.70	14.85
US14N21S	3,308	0.85	2,932	1.39	11.37
ATLANTA	109,698	0.03	107,455	0.09	2.08

Table 5.2: Comparison of FIPP p-cycle models vs. FDPP p-cycle models.

5.5.3 Performance of the FDPP p-cycle model: dual link failure

We first discuss the performance, i.e., solution accuracy and scalability, of the FDPP p-cycle model. We solved the FDPP p-cycle model for different values of dual failure rates (R_2), on different traffic and network instances of Table 5.1. We first looked at the accuracy of the solutions in Table 5.3, where we report the values of the optimality gaps. Those values are average values on the number of R_2 rate values (with a step size of 10) for which each particular instance was solved, within the time limit of 24 hours. Solutions have been obtained with a very small optimality gap for all network and traffic instances.

In Fig. 5.6, we look at the ratio of the number of generated over the number of selected configurations. Firstly, while there are a priori millions of possible configurations (i.e., overall number of cycles $\times$ number of combinations of cycles, while taking

Instances	Range of R_2	Gaps
ATLANTA	[0, 100]	0.1
NOBEL-US	[0, 100]	0.9
POLSKA	[0, 100]	0.8
US14N21S	[0, 100]	2.1

Table 5.3: Accuracy of the Solutions

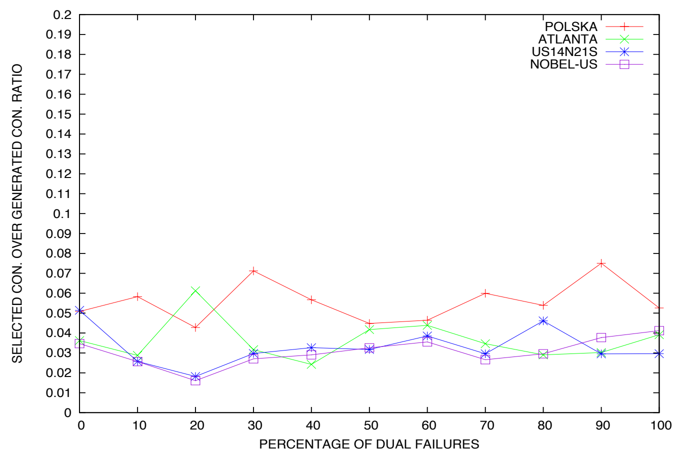

Fig. 5.6: Number of selected/generated configurations

into account the number of ways to protect the failure sets for each combination of cycles), only a very small number of them need to be generated, e.g., 7,584 in the case of the POLSKA instance for $R_2 = 100\%$ while 399 were indeed selected for the protection scheme. Secondly, what we see in Fig. 5.6, is that the number of selected configurations over the number of generated ones is quite small (less than 0.08 %). It means that: *(i)* the number of generated configurations which are not selected remains reasonable with respect to the number of selected configurations, taking into account that the most time consuming part of the solution process is the solution of the pricing problems, especially the PRICING$(u; \varphi, p, x)$ ones, *(ii)* Any improvement of the solution process should go with an attempt for reducing the number of generated configurations which do not belong to the final solution.

Fig. 5.7 shows us the relationship between the percentage R_2 of protected dual failures and the protection bandwidth over the working bandwidth ratio. Note that when R_2 is equal to zero, it corresponds to the classical FDPP p-cycle protection scheme

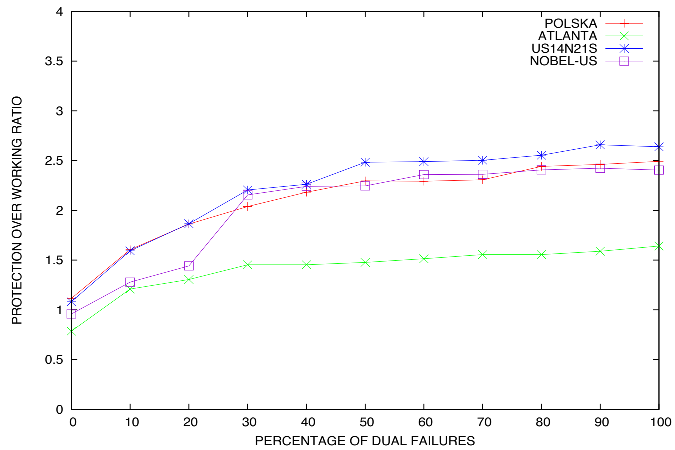

Fig. 5.7: R_2 ratio vs. capacity redundancy

with 100% protection against single failures. Depending on the network connectivity, the capacity redundancy ratio can vary from a range of 0.7 (ATLANTA topology with a nodal degree of 2.9) to 1.1 (POLSKA topology with a nodal degree of 3.0) for $\mathrm{R}_2 = 0\%$. When $\mathrm{R}_2 = 100\%$, we observe an increase of the redundancy ratio leading to a range of values between 1.6 for ATLANTA and 2.6 for US14N21S. Such values for the redundancy ratio are much smaller than what has been observed with a p-cycle link protection scheme, see [Sebbah and Jaumard, 2009], i.e., bandwidth redundancy ratio values ranging from 2 to 4 for $R_2 = 60$ % depending on the traffic instances.

Another conclusion we can draw from Fig. 5.7 is that most of significant increase of protection capacity with respect to working capacity happens when we raise the dual link failure percentage from 0 % to 40 %. After that point, the change of protection over working ratio is not heavily affected by that failure percentage anymore. It means that if we are ready to invest on dual link failure protection up to a certain level, we can even protect much more dual failures without spending a significant amount of capital.

5.5.4 FDPP p-cycle model: node protection

We investigate the quality of our solutions in case of one hundred percent protection against single node failures. Actually, if a node fails then we cannot protect any requests starting from or ending at that node. Thus, we ignore impossibly protected requests respecting to a certain node failure.

Table 5.4 shows the quality of our node protection solutions for the experimented instances. Column entitled "Bandwidth Increase" shows the difference in percentage between a node protection solution with its corresponding single link failure solution.

Instances	z^{ILP}	GAP	Bandwidth Increase (%)
ATLANTA	116,928	0.04	8.21
US14N21S	2,828	2.02	-3.68
NOBEL-US	5,207	0.44	0.21
POLSKA	11,146	0.43	0.54

Table 5.4: Node protection solutions

As we see in Table 5.4, in general we need more capacity to implement node protection scheme than single link failure protection one even through the capacity difference between two schemes is insignificant (less than 10%). US14N21S is an exception where the former uses less spare capacity than the latter. This is quite possible because in node protection, we need to ignore more traffic that is impossible to be protected.

5.5.5 FDPP *p*-cycle model: triple & quadruple link failure

In order to study the impact of triple and quadruple link failures on the spare capacity, we conduct experiments due to the scenario described in Table 5.5. Each cell in Table 5.6 contains the obtained spare capacity of an experiment on a network due to a certain scenario.

Scenario	Description
1	Single link failures
2	Node failures
3	100 % dual link failures
4	50 % dual link failures + 10 triple failures
5	50 % dual link failures + 20 triple failures + 10 quadruple failures

Table 5.5: High order link protection scenario description

From Table 5.6, we see that, for each instance, the obtained spare capacity can be clustered into two groups of nearly equal values: the first group consisting of scenario

Scenario	POLSKA	NOBEL-US	US14N21S	ATLANTA
1	11086	5196	2932	107326
2	11146	5207	2828	116928
3	24786	13033	7152	224385
4	23692	12575	6701	236913
5	25316	12978	6754	236950

Table 5.6: Higher order link protection scenario

1 and 2, the second group including scenario 3, 4, 5. Average value of the second group is about two times the one of the first group, indicating that there is a major shift in spare capacity for switching from single link/single node failure protection to higher link failure protection.

Since single node failure protection covers single link failure protection except for the links that are adjacent to the source and destination nodes of the considered working path, those two protections have similar spare capacities.

5.6 Conclusion

We proposed a new flow formulation for FDPP p-cycle for multiple failures, derived from a generic flow formulation for shared path protection, which resembles the model of [Orlowski and Pióro, 2011]. The new model compares favorably with the previously proposed ILP one for FIPP p-cycle [Rocha and Jaumard, 2012], i.e., it is at least as scalable with an equivalent precision, it also offers the very great advantage of dealing easily with multiple failures not necessarily restricted to dual link failures.

Future work will include a more thorough performance evaluation of the model against multiple failures, with improvement of the solution process of the pricing problems.

Chapter 6

Design of survivable virtual topologies against multiple failures

In IP-over-WDM networks, protection can be offered at the optical layer or at the electronic layer. Today, it is well acknowledged that synergies need to be developed between IP and optical layers in order to optimize the resource utilization and to reduce the costs and the energy consumption of the future networks.

In this chapter, we study the design of logical survivable topologies for service protection against multiple failures, including SRLG - Shared Risk Link Group - failures in IP-over-WDM networks. The problem we propose to capture in a scalable mathematical model is defined as follows. For given logical and physical directed topologies with physical capacity, checking whether the logical topology is survivable requires mapping logical links to physical paths, under the wavelength continuity assumption, and verifying whether, under any failure of either a single link, or a single node, or a set of links, there always exists a path linking the source to the destination of every logical link. If such a mapping exists, the objective is to find the mapping with the minimum cost, i.e., minimum bandwidth requirements as estimated by the sum, over the set of physical links, of the number of required wavelengths per physical link. However, a network may not be able to implement a certain mapping either due to lack of routing bandwidth or lack of spare capacity. As opposed to many studies, our model allows additional capacity to be added so that the capacity shortage is not a problem anymore.

For a network, only one survivable mapping will be selected as the final solution even though several ones may coexist simultaneously. Indeed, our mapping selection can be seen as a multiple criteria decision making that is described in the following objective list in decreasing order of priority.

1. Maximize the number of the routed lightpaths,
2. Minimize the additional bandwidth that need to be provided in order to support the routing traffic,
3. Minimize the number of unprotected lightpaths after a failure.

In our model, the difference in magnitude of the objective coefficients in the master problem is set to be significant in order to prioritizing those targets.

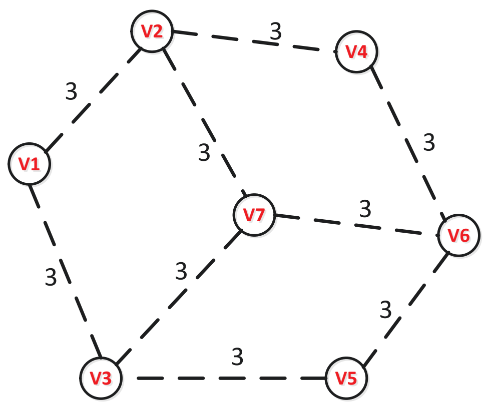

(a) Physical topology

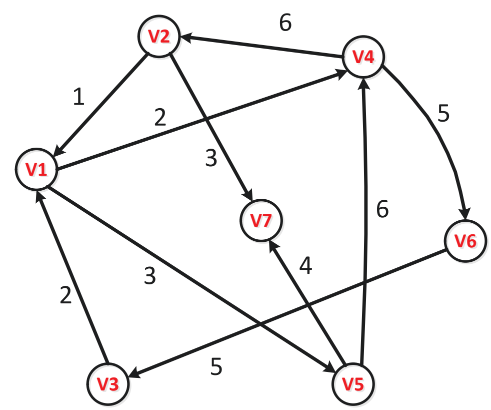

(b) Logical topology

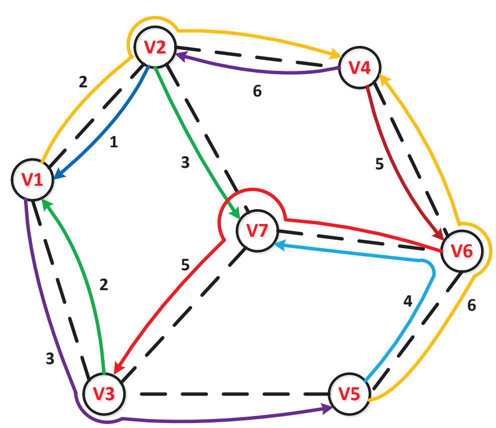

(c) Mapping

Fig. 6.1: A survivable mapping example

An illustration of the problem is depicted in Fig. 6.1. The physical network with its capacity is represented in Fig. 6.1(a), while the logical network with its demand is represented in Fig. 6.1(b). As shown in Fig. 6.1(a), three units are provided on each physical link at the outset. Let us consider the mapping represented in Fig. 6.1(c) where each physical lightpath (corresponding to a logical link) is represented by a solid line. For e.g., logical link $v_6 - v_3$ and $v_5 - v_4$ are mapped on $v_6 \rightarrow v_7 \rightarrow v_3$ and $v_5 \rightarrow v_6 \rightarrow v_4$, respectively.

Physical capacity provided at the outset may not be enough to support a certain mapping so that extra capacity need to be added. Extra capacity consists of additional routing capacity, which is added to cover working lightpaths, and additional protection capacity, which is added to cover restoration lightpaths. For e.g., as logical link $v_5 - v_4$ demands six units, the same amount of capacity is required on physical link $v_5 \rightarrow v_6$ as well as $v_6 \rightarrow v_4$. Yet, physical link $v_6 \rightarrow v_4$ has only three units at first meaning that this physical link need three more units of additional routing capacity. In the case of physical link $v_5 \rightarrow v_6$, as lightpath $v_5 \rightarrow v_6 \rightarrow v_7$ and $v_5 \rightarrow v_6 \rightarrow v_4$ (corresponding to logical link $v_5 \rightarrow v_7$ and $v_5 \rightarrow v_4$, respectively) pass through it, ten units (six units for the demand of logical link $v_5 \rightarrow v_7$ plus four units for the demand of logical link $v_5 \rightarrow v_4$) have to be provided. Obviously, after subtracting three units that are given at the beginning, physical link $v_5 \rightarrow v_6$ need seven units (additional routing capacity) in addition in order to fulfill the demand.

As opposed to additional routing capacity, the purpose of additional protection capacity is to support IP restoration. For e.g., let us consider a failure that occurs in physical span $v_2 - v_7$, meaning that we need to reroute the working traffic from v_2 to v_7 on logical links that do not be mapped on broken physical link $v_2 - v_7$. Suppose that logical path $v_2 \rightarrow v_1 \rightarrow v_5 \rightarrow v_7$ (corresponding to physical path $v_2 \rightarrow v_1 \rightarrow v_3 \rightarrow v_5 \rightarrow v_6 \rightarrow v_7$) is used after that failure. Hence, each physical link in that restoration path need three units to protect the disrupted traffic. Look at physical link $v_2 \rightarrow v_1$; since one unit is taken by the routing path $v_2 \rightarrow v_1$ we have two units left for IP restoration, consequently, we need one more unit of additional protection capacity in case of such a failure if we want to protect the three routing traffic units completely. For each physical link, because each failure follows by different amounts of addition protection capacity, thus the maximum of them is considered as the additional protection capacity needed in order to accommodate the

$\|E\|$	Routing	Additional
$v_1 \to v_2$	2	0
$v_2 \to v_1$	1	0
$v_1 \to v_3$	3	0
$v_3 \to v_1$	2	0
$v_4 \to v_2$	6	3
$v_2 \to v_4$	2	0
$v_7 \to v_2$	0	0
$v_2 \to v_7$	3	0
$v_4 \to v_6$	5	2
$v_6 \to v_4$	6	3
$v_7 \to v_6$	5	2
$v_6 \to v_7$	4	1
$v_7 \to v_3$	5	2
$v_3 \to v_7$	0	0
$v_3 \to v_5$	3	0
$v_5 \to v_3$	0	0
$v_5 \to v_6$	10	7
$v_6 \to v_5$	0	0

Table 6.1: Routing bandwidth and additional bandwidth

entire restoration traffic. Next, we explain how to compute additional protection capacity in a formal way.

The sum over additional capacity of protection as well as of routing is what we need to add to a network in order to make a corresponding mapping feasible. Table 6 shows the additional protection capacity per physical link of the mapping in Fig. 6.1(c).

Indeed, the concept of additional capacity comes from the fact that we can always upgrade, per link basis, a currently running network in order to accomodate a traffic that has been evolved.

We propose a new decomposition optimization model in Section 6.1. It is highly scalable and allows the exact solution of several benchmark instances, which were only solved with the help of heuristics so far. In case that no survivable mapping exists, we calculate the minimal amount of additional capacity that need to provide in order to get a survivable one in Section 6.1.6.

In the numerical experiments (Section 6.2), we investigate the number of multiple failures which can be recovered depending on the number of logical links, e.g., the number of VPN routes in a IP/MPLS network. In addition, larger instances than in previous studies can be solved as the proposed formulation avoids the explicit or implicit enumeration of cutsets (with respect to the much used minimum cut formulations), and concentrates on the implicit enumeration of augmenting paths only. Finally, Section 6.3 draws the conclusion.

6.1 The decomposition model

The next two sections introduce the definitions, notations and variables are used in our models. Section 6.1.3 and 6.1.4 describe the master problem and the pricing problem in our decomposition model, respectively. Since the proposed model is a multi-level objective optimization problem, we describe a multi-level objective solving process in Section 6.1.5.

6.1.1 Definitions and notation

Before we set our new scalable mathematical model, we need to introduce some definitions and notations.

Let the physical topology represented by a directed graph $G_{\text{P}} = (V_p, E_p)$ where V_p is the set of nodes, and E_p is the set of links indexed by ℓ (where each link is associated with a directional fiber link), and let the logical topology represented by a directed graph $G_{\text{L}} = (V_{\text{L}}, E_{\text{L}})$ where V_{L} is the set of nodes, and E_{L} is the set of logical links, indexed by ℓ'. Each logical link is associated with a unit demand, but we allow multiple logical links between any pair of source and destination in case of multi unit demands.

For a given logical link ℓ', let $\text{SRC}(\ell')$ be its source node, and $\text{DST}(\ell')$ be its destination node. We denote by $\omega^+_G(v)$ (resp. $\omega^-_G(v)$) the set of outgoing (resp. incoming) links of node v in graph G.

We denote by $\mathcal{F}$ the set of potential failure sets, indexed by F, where each set F is a set of edges (undirected links) which might fail at the same time (as in a SRLG - Shared Risk Link Group). In a study on 100% protection against single link failures, each set F contains a single physical edge (or *bidirectional* link), and $\bigcup_{F \in \mathcal{F}} F = E_{\text{L}}$. Indeed, if link $\ell \in E_{\text{P}}$ fails, then the physical directional link in the opposite direction of ℓ will also fail. In other words, for each link failure in the physical network, in order to avoid confusion, we should write *bidirectional link* failure or edge failure, but it is common understanding. Consequently, we will go on with the commonly accepted terminology.

The proposed model relies on the concept of configurations where a configuration is a one unit mapping on a given wavelength. This allows not only to easily take the wavelength continuity assumption into account, but also offers a decomposition scheme that entitled the use of decomposition techniques such column generation ones for solving it.

Let C be the overall set of configurations, indexed by c. Each configuration c is associated with a wavelength, say λ_c, and is defined by the list of logical links (a subset of E_{L}) routed on physical lightpaths associated with wavelength λ_c. More formally, a configuration is characterized by coefficients $f^c_{\ell\ell'}$ such that $f^c_{\ell\ell'} = 1$ if virtual link ℓ' is routed over a physical lightpath containing link ℓ in configuration c, 0 otherwise. For each logical link ℓ' covered by c, there exists a sequence of physical links defining a path from the source to the destination of ℓ', with λ_c assigned to each of those links, therefore defining a physical lightpath on which ℓ' is routed.

Let $a^c_{\ell'} = 1$ if one lightpath has been found in G_{P} in order to route logical link ℓ', 0 otherwise.

We propose to write the model in such a way that it always has a solution, whether or not there exists a survivable logical topology. To do so, we introduce high costs (penalties) for not being able to route or to protect a logical link. This way, we always output a logical topology, but which can be incomplete for either the routing of a logical link (no mapping to a physical path), or for the protection of the mapping of a logical link to a physical path. Moreover, we allow adding more bandwidth to cover not only the working traffic, but also the restoration traffic. We minimize the additional bandwidth added to fully support all working lightpaths and introduce a good heuristic to compute an additional bandwidth to cover all IP restoration paths (Section 6.1.6).

Such a formulation has the advantage of providing information when no survivable logical topology exists, i.e., tells us how many logical links have not been routed, or have been routed without any protection. Let PENAL^{NR} be the cost (penalty) of not routing a logical link, PENAL^{AR} be the cost of one unit of the additional routing bandwidth, and PENAL^{NP} be the cost (penalty) of not protecting the routing (mapping) of a logical link when a given failure (single link or single node or multiple links) occurs. As we may prefer unprotected routing with the minimum additional routing bandwidth over no routing, $\text{PENAL}^{\text{NR}} \gg \text{PENAL}^{\text{AR}} \gg \text{PENAL}^{\text{NP}}$. In the numerical experiments, we use $\text{PENAL}^{\text{NR}} = 10^{12}$, $\text{PENAL}^{\text{AR}} = 10^{8}$ and $\text{PENAL}^{\text{NP}} = 10^{4}$.

6.1.2 Variables

We introduce the sets of variables of the model in the following paragraph.

The first set of variables are decision ones: z_c for $c \in C$ such that $z_c = 1$ if configuration c is selected (i.e., a proposal for the mapping of a subset of logical links), 0 otherwise.

The second set of variables $(\varphi^F_{\ell'_1 \ell'_2})_{F \in \mathcal{F}; \ell'_1, \ell'_2 \in E_{\text{L}}}$ is used in order to take care of identifying a restoration logical path for each lightpath which has been selected for the mapping of a unit logical link when $\mathcal{F}$ occurs. Constraints satisfied by those variables are described in the next paragraph. Variable $\varphi^F_{\ell'_1 \ell'_2} \in \{0, 1\}$ is equal to 1 if the restoration logical path for protecting logical link ℓ'_1 goes through ℓ'_2, and 0 otherwise.

The third set of variables $(f_{\ell\ell'})_{\ell \in E_{\text{P}}, \ell' \in E_{\text{L}}} = 1$ if ℓ' is mapped on ℓ, and 0 otherwise. Indeed, those variables describe how the mapping is constructed. The fourth set of variables $(b^F_{\ell'})_{F \in \mathcal{F}, \ell' \in E_{\text{L}}}$ is equal to 1 if ℓ' need to be restored after F, and 0 otherwise. They tell us which logical link need to be restored.

Information of how much bandwidth the routing uses as well as how much additional routing bandwidth we need to provide is represented by variables $(r_{\ell\ell'})_{\ell \in E_{\text{P}}, \ell' \in E_{\text{L}}}$, which is the reserved working bandwidth within the capacity at the outset (CAP_ℓ), and variables $(\text{ADD}^R_\ell)_{\ell \in E_{\text{P}}}$, which is the additional routing bandwidth of ℓ, respectively.

The last two sets of variables, $(y_{\ell'})_{\ell' \in E_{\text{L}}}$ and $(x^F_{\ell'})_{\ell' \in E_{\text{L}}, F \in \mathcal{F}}$, take care of the possibly missing mappings or unprotected mappings, respectively. While they add some complexity to the solution of the model, they can be easily removed if one is only interested in a yes/no answer to whether there exists a survivable logical topology. Both sets of variables are defined as follows. Variable $x^F_{\ell'} = 1$ if logical link ℓ' cannot be protected when failure set F occurs, and 0 otherwise. Variable $y_{\ell'} = 1$ if logical link ℓ' cannot be routed on the physical layer, i.e., cannot be mapped to a physical path under the wavelength continuity assumption, and 0 otherwise.

6.1.3 Master problem

We aim at minimizing the cost of the logical topology throughout the sum, over the set of physical links, of the number of required wavelengths per physical link, and when only an incomplete logical topology can be found, at the number of missing mappings (routing of a logical link onto a lightpath) first, and then at the number of unprotected mappings.

$$\begin{aligned}\min \quad & \sum_{(\ell,\ell')\in E_{\mathrm{P}}\times E_{\mathrm{L}}} f_{\ell\ell'} \\ & + \sum_{\ell'\in E_{\mathrm{L}}} \textsc{penal}^{\mathrm{NR}}\, y_{\ell'} + \sum_{\ell\in E_{\mathrm{P}}} \textsc{penal}^{\mathrm{AR}}\, t_{\ell} + \sum_{(\ell',F)\in E_{\mathrm{L}}\times\mathcal{F}} \textsc{penal}^{\mathrm{NP}}\, x^{F}_{\ell'}. \end{aligned} \tag{6.1}$$

subject to:

$$\sum_{c \in C} a^c_{\ell'} \, z_c \geq 1 \qquad \ell' \in E_{\text{L}} \tag{6.2}$$

$$\sum_{c \in C} f^c_{\ell\ell'} \, z_c = f_{\ell\ell'} \qquad \ell \in E_{\text{P}}, \ell' \in E_{\text{L}} \tag{6.3}$$

$$r_{\ell\ell'} \leq f_{\ell\ell'} \qquad \ell \in E_{\text{P}}, \ell' \in E_{\text{L}} \tag{6.4}$$

$$r_{\ell\ell'} \leq 1 - y_{\ell'} \qquad \ell \in E_{\text{P}}, \ell' \in E_{\text{L}} \tag{6.5}$$

$$r_{\ell\ell'} \geq f_{\ell\ell'} - y_{\ell'} \qquad \ell \in E_{\text{P}}, \ell' \in E_{\text{L}} \tag{6.6}$$

$$\sum_{\ell' \in E_{\text{L}}} r_{\ell\ell'} \leq \text{CAP}_\ell \qquad \ell \in E_{\text{P}} \tag{6.7}$$

$$\sum_{\ell' \in E_{\text{L}}} f_{\ell\ell'} \leq \text{CAP}_\ell + \text{ADD}^R_\ell \qquad \ell \in E_{\text{P}} \tag{6.8}$$

$$b^F_{\ell'} \geq f_{\ell\ell'} \qquad F \in \mathcal{F}, \ell \in F, \ell' \in E_{\text{L}} \tag{6.9}$$

$$b^F_{\ell'} \leq \sum_{\ell \in F} f_{\ell\ell'} \qquad F \in \mathcal{F}, \ell' \in E_{\text{L}} \tag{6.10}$$

$$\varphi^F_{\ell'_1,\ell'_2} \leq 1 - b^F_{\ell'_2} \qquad \ell \in F, F \in \mathcal{F} \tag{6.11}$$

$$b^F_{\ell'_1} \geq 1 - x^F_{\ell'_1} \qquad F \in \mathcal{F}, \ell'_1 \in E_{\text{L}} \tag{6.12}$$

$$\sum_{\ell'_2 \in \omega^+_{G_{\text{L}}}(\text{SRC}(\ell'_1))} \varphi^F_{\ell'_1,\ell'_2} = \sum_{\ell'_2 \in \omega^-_{G_{\text{L}}}(\text{DST}(\ell'_1))} \varphi^F_{\ell'_1,\ell'_2} \tag{6.13}$$

$$= 1 - x^F_{\ell'_1} \qquad \ell'_1 \in E_{\text{L}}, F \in \mathcal{F} \tag{6.14}$$

$$\sum_{\ell'_2 \in \omega^+_{G_{\text{L}}}(v)} \varphi^F_{\ell'_1,\ell'_2} = \sum_{\ell'_2 \in \omega^-_{G_{\text{L}}}(v)} \varphi^F_{\ell'_1,\ell'_2} \qquad \ell'_1 \in E_{\text{L}}, F \in \mathcal{F}$$

$$v \notin \{\text{SRC}(\ell'_1), \text{DST}(\ell'_1)\} \tag{6.15}$$

$$\sum_{\ell'_2 \in \omega^-_{G_{\text{L}}}(v_s)} \varphi^F_{\ell'_1,\ell'_2} = \sum_{\ell'_2 \in \omega^+_{G_{\text{L}}}(v_d)} \varphi^F_{\ell'_1,\ell'_2} = 0 \qquad \ell'_1 \in E_{\text{L}}, F \in \mathcal{F} \tag{6.16}$$

$$z_c \in \{0, 1\} \qquad c \in C \tag{6.17}$$

$$\varphi^F_{\ell'_1\ell'_2} \in \{0, 1\} \qquad F \in \mathcal{F}, \ell'_1, \ell'_2 \in E_{\text{L}} \tag{6.18}$$

There are five constraint blocks that are introduced in the following paragraph.

The first block is made of constraints (6.2-6.3) and deals with the mapping of the logical links onto (physical) lightpaths. Constraints (6.2) ensure that each logical link is routed on the physical topology in at least one configuration, i.e., on a least one physical lightpath. Constraints (6.3) give us the amount of capacity that a logical link requires from a physical one.

The second block consists of constraints (6.4-6.6) and calculates the routing bandwidth that are supported by the physical capacity at the beginning. Actually, those constraints are a linear expression of the equality $r_{\ell\ell'} = f_{\ell\ell'}(1 - y_{\ell'})$ where the right term (so the left term) is the part of the demand of logical link ℓ' that does not need any additional routing bandwidth to be successfully routed.

The third block of constraints takes care of capacity limitation. Constraints (6.7) are transport capacity constraints, i.e., ensure that, for a given physical link $\ell \in E_{\text{P}}$, no more than CAP_ℓ lightpaths are routed on it, i.e., no more than its transport capacity in terms of number of wavelengths. Constraints (6.8), since they allow adding more bandwidth to physical link so that all logical links can be routed, are an extension of constraints (6.7) in a more flexible way.

In the fourth block, constraints (6.9-6.10) decide whether we need to reroute or not logical link ℓ' when failureset F occurs. In addition, constraints (6.11) indicate the availability of logical link ℓ'_2 in serving the restoration of ℓ'_1 after the happening of F.

The final block is, indeed, the network flow formulation. If failureset F has no impact on logical link ℓ'_1 then there is no need to protect ℓ'_1 against F, that is the purpose of constraints (6.12). Otherwise, logical link ℓ'_1 needs an alternate path if links of F fail. Consequently, there is a need for a unit flow from the source to the destination of ℓ'_1 in case F fails: this is the purpose of constraints (6.13) to (6.16), which computes a path in the logical graph G_{L} from $\text{SRC}(\ell'_1)$ to $\text{DST}(\ell'_1)$, for logical link ℓ'_1 if it is impacted by failure F. However, if due to a lack of network connectivity, such a path cannot be found, then $x^F_{\ell'_1} = 1$. Note that constraints (6.16) forbid to consider either incoming links for the source nodes, or outgoing links for the destination nodes.

As the sum of $x^F_{\ell'}$ appears in the objective, the program attempts to protect failed logical links as much as possible.

6.1.4 Pricing problem

The pricing problem looks for augmenting configurations. Its objective is defined by the so-called reduced cost, fed with the values of the dual variables of the constraints in which variable z_c appears.

Our pricing problem has two sets of variables. The first set is made of decision variables $(a_{\ell'})_{\ell' \in E_{\text{L}}}$ such that $a_{\ell'} = 1$ if logical link ℓ' is routed over a physical lightpath associated with λ_c, 0 otherwise. The second set of variables, $(f_{\ell\ell'})_{\ell \in E_{\text{P}}, \ell' \in E_{\text{L}}}$, is used for the establishment of lighpaths in the physical topology. They are defined as follows: $f_{\ell\ell'} = 1$, $\ell \in E_{\text{P}}$, $\ell' \in E_{\text{L}}$, if a unit flow of logical link ℓ' goes through physical link ℓ with λ_c assigned to it, 0 otherwise.

Note that, a priori, both sets of variables should be also indexed with c, i.e., the index of the configuration under construction. However, we did not add it to alleviate the notations, with the understanding that each pricing problem builds a single configuration. In addition, observe that, while $a_{\ell'}$ and $f_{\ell\ell'}$ are parameter values in the master problem (see Section 6.1.3), they are variables in the pricing model. Although there may be a slight abuse of notations, we refrain from introducing new notations, as to facilitate the understanding of the column generation techniques, i.e., the sequence of alternate solutions of the restricted problem and of the pricing problem, which are feeding each other (values of the dual variables for the pricing problem, configurations or columns for the restricted master problem), until an optimal solution of the linear relaxation of the master problem is found. The pricing problem is defined as follows.

$$\min - \sum_{\ell' \in E_{\text{L}}} u^{\text{D}}_{\ell'} a_{\ell'} + \sum_{\ell \in E_{\text{P}}} \sum_{\ell' \in E_{\text{L}}} u^{\text{C}}_{\ell\ell'} f_{\ell\ell'}$$

subject to:

$$\sum_{\ell \in \omega^-(v)} f_{\ell\ell'} \quad - \quad \sum_{\ell \in \omega^+(v)} f_{\ell\ell'} \quad = \quad \begin{cases} a_{\ell'} & \text{if } \textsc{src}(\ell') = v \\ -a_{\ell'} & \text{if } \textsc{dst}(\ell') = v \\ 0 & \text{otherwise} \\ & v \in V_{\text{L}}. \end{cases} \tag{6.19}$$

Where $u^{\text{D}}_{\ell} \geq 0$ (resp. $u^{\text{C}}_{\ell\ell'} \geq 0$) are the values of the dual variables associated with constraints (6.2) (resp. (6.3)).

There is only one set of constraints, which are multi-flow constraints, in order to route as many logical links as possible on routes to which wavelength λ_c is assigned. Indeed, a one unit logical link ℓ' is mapped to a route in the physical network if a route (flow) can be found from $\textsc{src}(\ell')$ to $\textsc{dst}(\ell')$.

6.1.5 Solving multi-level ILP objective

Magnitudes of $\textsc{penal}$ in the master objective reflect the priorities of the optimized terms. $\textsc{penal}^{\mathrm{NR}}$, as the greatest coefficient, implies that we try to route as much logical links as possible within the bandwidth capacity at the outset (CAP_{ℓ}). Similarly, among the mappings that provide such a maximum number of routed logical links, the ones with the smallest amount of working bandwidth are selected thanks to the second greatest coefficient: $\textsc{penal}^{\mathrm{AR}}$. Finally, with help of $\textsc{penal}^{\mathrm{NP}}$ which is the coefficient of the lowest priority term, a mapping with a minimum number of unprotected logical links is chosen as the solution.

Theoretically, we can directly solve the master problem with $\textsc{penal}$s, however, those coefficients are extremely large numbers so that the optimization process may result in numerical inaccuracy. In order to get over that difficulty, we divide the Master objective into multi parts where the part with the highest priority is optimized first, the one with the second priority is solved subsequently, and so on. A part, after being solved to the optimality, is used to generate new constraints that are included to the current set of constraints in order to force that this part of whatever a solution can not be worse than the optimal one. Let us see the following example.

$$\min z + \textsc{penal}^1 y + \textsc{penal}^2 x$$

$$\textsc{s.t.} \qquad Az = b \tag{6.20}$$

with assumption that $\textsc{penal}^2 \gg \textsc{penal}^1$. First, we solve the following ILP.

$$\min x$$

$$\textsc{s.t.} \qquad Az = b. \tag{6.21}$$

Suppose that $x = \bar{x}$ at the optimality, we consider the next ILP:

$$\min y$$

$$\textsc{s.t.} \qquad Az = b \tag{6.22}$$

$$x \leq \bar{x}. \tag{6.23}$$

Notice that constraints (6.25) are added in order to guarantee the optimality of x. Let $y = \bar{y}$ the solution of that ILP. The last ILP that need to be solved is the following:

$$\min z$$

$$\text{S.T.} \qquad Az = b \tag{6.24}$$

$$x \leq \bar{x} \tag{6.25}$$

$$y \leq \bar{y} \tag{6.26}$$

Our implementation applied this techniques in order to avoid the numerical inaccuracy caused by extremely large coefficients. As we solve those ILP by Column Generation, we may not be able to find the optimal solution, but a quasi-optimal solution (with a very tiny GAP) in each step of the above process is good enough for getting a high quality solution.

6.1.6 Computing the required spare capacity for a successful IP restoration

In this section, we propose an algorithm to calculate additional capacity that is required to guarantee the existence of a survivable mapping. We also define the way we calculate the redundancy ratio.

Let CAP_ℓ the original bandwidth (number of wavelength) available on physical link ℓ, CAP_ℓ^P the bandwidth used by IP restoration and CAP_ℓ^R the bandwidth reserved for routing, respectively. Let ADD_ℓ^P the additional protection capacity needed to be added to ℓ for a successful IP restoration. We have:

$$\text{ADD}_\ell^P = \max(0, \text{CAP}_\ell^P - \max(\text{CAP}_\ell - \text{CAP}_\ell^R, 0)). \tag{6.27}$$

Since CAP_ℓ is the input parameter and CAP_ℓ^R is the obtained result of the decomposition model in the previous sections.To get ADD_ℓ^P, we only need to determine CAP_ℓ^P. Let CAP_ℓ^F the spare capacity that is required on ℓ in order to ensure a successful IP restoration against failureset F. Such CAP_ℓ^P are obtained by the following algorithm.

For all $F \in \mathcal{F}$ **do**

Let L^F be the list of logical links which fail,

following a failure of the links of F

For all $\ell \in L$, $\text{CAP}_\ell^F \leftarrow 0$ **EndFor**

For all $\ell' \in L_F$ do

Compute $\text{RP}_{\ell'}$, the IP recovery path

Compute $\text{PP}_{\ell'}$, the physical recovery path underlying $\text{RP}_{\ell'}$

For all $\ell \in \text{PP}_{\ell'}$, $\text{CAP}_\ell^F \leftarrow \text{CAP}_\ell^F + 1$ **EndFor**

EndFor

EndFor

Let $\text{CAP}_\ell^P = \max\limits_{F \in \mathcal{F}} \text{CAP}_\ell^F$

Redundancy ratio is defined as the fraction of the spare capacity over the working bandwidth, thus, is given in the following formula:

$$\frac{\sum\limits_{\ell \in L} \text{CAP}_\ell^P}{\sum\limits_{\ell \in L} \left(\text{CAP}_\ell + \text{ADD}_\ell^R\right)}.$$

6.2 Numerical results

Section 6.2.1 introduces the network topologies that we use for the experiments. Section 6.2.2 explains how network traffic is generated in detail. We report the quality of solutions obtained by our model in Section 6.2.3. Discuss on network performance is given in Section 6.2.4.

Programs were developed using the OPL language and the (integer) linear programs were solved using Cplex 12.2 [IBM, 2011b]. We use computers with 4-cores 2.2 GHz AMD Opteron 64-bit processor to run the programs.

6.2.1 Data instances

We conducted experiments on the same four different physical topologies as in [Todimala and Ramamurthy, 2007], i.e., NJLATA, NSF, EURO and 24-NET, which are described in Table 6.2. As in [Todimala and Ramamurthy, 2007], we used randomly generated degree k regular undirected graphs and m-edge general undirected graphs as virtual topologies, and assumed that $V_{\text{L}} = V_{\text{P}}$. Undirected graphs were converted to directed graphs by replacing each edge with two links between the same node pair, but of opposite directions.

Topologies	# nodes	# edges = (# links)/2	Average nodal degree	Reference
NJLATA	11	23	4.2	[Singh *et al.*, 2008]
NSF	14	21	3.0	[O'Mahony *et al.*, 1995]
EURO	19	37	3.9	[Grover]
24-NET	24	43	3.4	[Todimala and Ramamurthy, 2007]

Table 6.2: Network Topologies

6.2.2 Transport capacity and link dimensioning

In order to set meaningful transport capacity, some basic (physical) link dimensioning is needed. We therefore computed the shortest path routing of all logical links (forgetting about wavelength continuity), and then computed the transport capacities required for such a routing and mapping of the logical links onto the shortest physical paths. Let $\textsc{cap}_\ell^E$ the resulting required estimated transport capacity for each physical link ℓ. We then set

$$\textsc{cap}_\ell = \textsc{alea}[\textsc{cap}_\ell^E - 20\%, \textsc{cap}_\ell^E + 20\%],$$

where $\textsc{alea}[a, b]$ is a function which randomly generates a value of the set (a, b).

Although most network designers use a shortest path routing for working lighpaths, we aim at simulating the mapping of logical links onto physical links in a context where existing transport capacities does not necessarily allow a shortest path routing, due to, e.g., the evolution of the traffic.

As will be seen in the experiments in the forthcoming sections, we computed the minimum additional transport capacity that is required in order to: *(i)* route all demands (additional routing capacity), and *(ii)* ensure enough capacity for a successful IP restoration at the logical layer (additional protection capacity).

Instances	Logical topologies	Configurations # generated	Configurations # selected	$\tilde{z}_{\text{ILP}}$	Optimality gaps	# Wavelengths per link $\mu(W)$	# Wavelengths per link $\sigma(W)$
NJLATA	degree 3	71	34	46	< 0.001	1.0	0.9
	20-edge	99	40	69	< 0.001	1.5	1.5
	40-edge	201	80	131	< 0.001	2.8	2.4
	70-edge	505	140	242	< 0.001	5.3	4.6
NSF	21-edge	114	42	90	< 0.001	2.2	1.3
	25-edge	128	50	103	< 0.001	2.5	1.3
	50-edge	480	100	220	< 0.001	5.2	2.3
	80-edge	757	160	348	< 0.001	8.3	3.1
EURO	degree-3	373	58	131	< 0.001	1.8	1.2
	30-edge	228	60	150	< 0.001	2.0	1.8
	35-edge	268	70	169	0.3	2.3	1.9
	70-edge	690	140	331	0.8	4.5	3.2
	90-edge	1162	180	418	< 0.001	5.6	3.9
24-NET	40-edge	508	80	233	< 0.001	2.7	1.9
	70-edge	782	140	401	< 0.001	4.7	3.2
	90-edge	1159	180	528	0.9	6.1	3.9
24-NET $\lvert V_{\text{P}}\rvert = 1/2\lvert V_{\text{L}}\rvert$	40-edge	457	80	229	0.4	2.7	2.5
	90-edge	1000	180	556	< 0.001	6.5	6.0
	120-edge	1425	240	717	0.3	8.3	7.9

Table 6.3: Performance of the decomposition model

Instances	Logical Topologies	# Non survivable logical links		Bandwidth		
				Routing	Protection	
		%	# failure sets	To be added (%)	To be added (%)	Redundancy ratio
NJLATA	degree-3	0.0	0.0	0.0	89.5	1.8
	20-edge	10.0	2.5	1.0	133.3	2.0
$V_P = V_L$	40-edge	0.0	0.0	1.3	353.2	4.4
	70-edge	0.0	0.0	3.0	777.0	8.8
NSF	21-edge	14.3	1.7	0.0	153.5	2.1
	25-edge	12.0	1.0	0.0	187.2	2.5
$V_P = V_L$	50-edge	0.0	0.0	2.1	249.6	2.8
	80-edge	0.0	0.0	1.9	421.4	4.6
EURO	degree-3	31.0	1.1	0.6	168.6	2.2
	30-edge	48.3	1.4	0.0	149.2	2.2
$V_P = V_L$	35-edge	28.6	1.4	0.0	239.0	3.2
	70-edge	20.7	1.1	1.3	510.8	5.9
	90-edge	14.4	1.0	2.2	612.3	6.8
24-NET	40-edge	32.5	1.8	0.7	258.4	3.3
$V_P = V_L$	70-edge	0.0	0.0	2.0	527.4	6.0
	90-edge	0.0	0.0	3.2	564.7	6.2
24-NET	40-edge	10.0	1.2	0.4	316.3	3.8
$\lvert V_P \rvert = 1/2 \lvert V_L \rvert$	90-edge	0.0	0.0	6.5	822.8	8.5
	120-edge	0.0	0.0	7.8	1115.1	11.2

Table 6.4: Existence and dimensioning of a survivable logical topology (single-link failures)

6.2.3 Quality of solutions

We now discuss the performance of the column generation model proposed in Section 6.1 in the context of 100% against single link failures, i.e., when $\mathcal{F} = \{F_e = \{e\}, e \in E\}$ where E is the set of protection edges in the physical network (edges are undirected links between two nodes). Results that are reported in Table 6.3 come from a set of randomly generated virtual topologies with some degree k regular undirected graphs and some m-edge general undirected graphs.

The number of generated configurations as well as the number of selected configurations in the integer solutions are given in the third and fourth column, respectively. Those numbers clearly show that a very small number of configurations out of the overall number of potential configurations is needed in order to reach the optimal solution of the linear relaxation of the master problem on the one hand, and a nearly optimal integer solution on the other hand. The next three columns contain the characteristics of the ILP solutions:

(i) optimal value $z^{\star}_{\text{LP}}$ of the linear relaxation of the master problem, *(ii)* integer value $\tilde{z}_{\text{ILP}}$ of the optimization model, and *(iii)* optimality gap.

We can observe that all optimality gaps are less than 2 percent, some even less than 0.001, meaning that the integer solutions are nearly optimal ones. The last two columns provide the mean (μ) and the variance (σ) of numbers of reserved wavelengths on a physical link.

Comparing with the transport capacity values selected by [Todimala and Ramamurthy, 2007], 6 wavelengths for NJLATA and 8 for NSF (values are not available for EURO and 24-NET), we can conclude that it is more than enough. Indeed, the average wavelength requirements ($\pm$ the corresponding variance) on the physical links are 1.0 ± 0.9 (degree-3 logical network) and 1.5 ± 1.5 (20-edge logical network) for NJLATA, 2.1 ± 1.3 (21-edge logical network) and 2.5 ± 1.3 (25-edge logical network) for NSF with variance values such that the 6 and 8 threshold values are unlikely to be exceeded.

In conclusion, the proposed solution process is very efficient, as practical optimal solutions are obtained very often (solution with a gap smaller than 0.1% can be considered optimal ones for practical purposes), which allow the proper identification of the existence of a survivable logical topology.

6.2.4 Networking performances

The first set of experiments (Table 6.4) is again with single link failures only. In Table 6.4, we report:

(i) the percentage of logical links which cannot survive the link failure of at least one failure set,

(ii) for the logical links of *(i)*, the average number of failure sets they cannot survive,

(iii) the additional bandwidth (% with respect to the initial transport capacities) which is required in order to be able to map all logical links,

(iv) the additional bandwidth (% with respect to the adjusted transport capacities after the routing/mapping of all logical links onto the physical links) which need to be added in order to completely support IP restoration,

(v) the redundancy ratio assuming enough spare capacity is provided in order to allow a successful IP restoration for all (physical) link failures.

In Table 6.4, we notice that redundancy ratio increases rapidly with number of physical edges. That ratio is very high when number of physical edges becomes significant, for e.g., is 6.8 in case of EURO network with 90 edges. The reason for such a high ratio comes from the fact that: we maximize number of protected logical links, not dimensioning protection capacity. See Fig. 6.2 where solid lines are logical links while dash lines are their routed physical lightpaths. Label of each physical lightpath consists of its name and its length covered by a parenthesis. Suppose that logical link $v_1 \rightarrow v_3$ fails, there are two options to restore that logical link: we route the traffic either on logical path $v_1 \rightarrow v_2 \rightarrow v_3$ or on $v_1 \rightarrow v_4 \rightarrow v_5 \rightarrow v_3$. As our model maximizes only number of protected links, thus, the two choices are the same. If logical path $v_1 \rightarrow v_2 \rightarrow v_3$ is selected, then the spare capacity is 10. Otherwise, if the alternative path is used, the spare capacity is just 3, i.e., three times smaller than in the case of the precedent path which is the shorter one in logical layer. So, as we see, not dimensioning could waste a meaningful amount of capacity, hence leads to significantly large redundancy ratios.

Comparing our results with those of [Todimala and Ramamurthy, 2007], we need to be cautious as our randomly logical topologies are arbitrary ones (no special structures), those generated by [Todimala and Ramamurthy, 2007] have the planar cycle property.

In the next set of experiments, we look at multiple failure scenarios (1-5) as

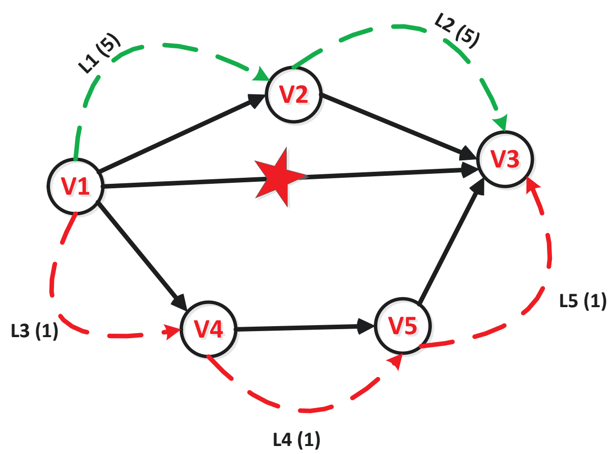

Fig. 6.2: Explain why redundancy ratio is a significantly large number.

described in Table 6.5. We conducted the experiments on several topologies and reported the result in Table 6.6.

Scenarios	Comments
1	only single link failure sets
2	single sets + 7% dual sets
3	single sets + 7% dual sets + 7% triple sets
4	single sets + 10% dual sets + 10% triple sets
5	single sets + 10% dual sets + 10% triple sets + 5% quadruple sets

Table 6.5: Multiple failure set scenarios

Instances	Logical Topologies	Failure Scenarios	# Non survivable logical links		Bandwidth		
					Routing	Protection	
			%	# failure sets	To be added (%)	To be added (%)	Redundancy ratio
NJLATA	20 edge	2	10.0	3.2	1.0	171.9	2.5
		3	50.0	1.9	1.0	214.6	3.1
		4	57.5	2.0	1.0	225.0	3.3
		5	57.5	2.7	1.0	209.4	3.1
NJLATA	70 edge	2	0.0	0.0	3.0	862.8	9.7
		3	8.6	1.0	3.0	908.9	10.3
		4	8.6	1.0	3.0	917.5	10.4
		5	8.6	1.0	3.0	987.4	11.1
EURO	90 edge	2	14.4	1.5	2.2	584.4	6.5
		3	14.4	3.2	2.2	570.8	6.3
		4	17.8	4.4	2.2	605.3	6.7
		5	17.8	4.4	2.2	664.6	7.3
24-NET	90 edge	2	2.8	1.0	3.2	591.9	6.5
		3	2.8	1.0	3.2	526.5	5.8
		4	2.8	1.0	3.2	453.1	5.0
		5	2.8	1.0	3.2	450.3	5.0
24-NET $\lvert V_{\rm P}\rvert = 1/2\lvert V_{\rm L}\rvert$	120 edge	2	18.3	1.1	7.8	1097.5	11.1
		3	18.3	1.1	7.8	1187.6	11.9
		4	18.8	1.1	7.8	1153.0	11.6
		5	17.5	1.2	7.8	1287.3	12.9

Table 6.6: Existence and dimensioning of a survivable logical topology (multiple-link failures & $|V_{\rm P}| = 1/2|V_{\rm L}|$)

6.3 Conclusion

We proposed a first scalable ILP model for the design of survivable logical topologies, which allow the exact solution of most of the data instances considered so far in the literature. In addition, not only the proposed model allows checking whether a survivable logical topology exists or not, but, when none exists, it still constructs the largest possible survivable logical topology, with indication on an appropriate dimensioning of the physical links.

In this work, we do not dimension protection capacity, only maximize the amount of protected links, thus it results in a very high redundancy ratio. That means a significant amount of protection capacity can be waste if network dimensioning does not be taken into account. A possible extension of this work is to combine protected capacity with protection one.

In future work, we will investigate how to improve the solution of the proposed model with heuristics in order to solve larger data instances (including data instances with multi-unit logical links), closer to the ones encountered in the current IP-over-WDM networks. We believe that there is a lot of room for improving the current solution scheme and for combining it with heuristics in order to speed it up.

Another direction for this study is to consider node failure in the physical layer. To deal with physical node failures, we simulate a failing node by the failure of the links that are adjacent to that node.

Chapter 7

Design of a multirate optical network architecture

New high capacity optical devices such as 40Gbps and 100Gbps regenerators are powerful tools to deal with the continuous traffic growth. However, economic incentives make network operators deploy those new devices with minimum capital investment. As completely upgrading the current backbone network with new devices is impossible due to their expensive price, a cost-effective dimensioning plan where equipment of heterogeneous optical rates co-exist in a network (mixed line rate WDM networks) is necessary.

When it comes to regenerators, besides transmission reach and capacity, maximum number of hops (because of physical impairment) and maximum number of sites where regenerators can be deployed have to be taken into account. Additionally, limitation on wavelength capacity per fiber and per node must be considered according to reality. The design problem becomes even more complicated when grooming criteria is included, hence it is quite difficult to develop a general solution.

By applying a decomposition methodology with a novel formulation of hierarchical pricing sub-problems, an exact and scalable algorithm is proposed in our work. Since no ad-hoc requirements are needed in our solution, new physical criteria can be easily included thanks to the generality of our formulation.

Numerical results in Section 7.5 show that, firstly, the percentage distribution of transceivers grouped by MTD is stable while the traffic volume grows. Secondly, we see that 10Gbps transceivers takes the major part in the optimal solution in contrast to the minor part of 100Gbps and 40Gbps. But such a difference is reduced with the evolution of traffic. Moreover, number of 100 Gbps transceivers grows faster than the one of 40Gbps transceiver. Thirdly, we witness a huge impact of maximum regenerable site constraint on the transceiver cost. The main idea of restricting the maximum number of regenerable sites is to gather regenerators to few sites in order to take advantage of sharing support devices, such as cooling systems. By that way, we can reduce the operating cost (OPEX). In return, we have pay more CAPEX. Thus, our result helps network designer to make a trade-off between OPEX and CAPEX when planing such a system.

Section 7.1 introduces the problem that this research addresses. Cost information of optical equipment is given in Section 7.2. We propose our decomposition model in Section 7.3. The flexibility of our model shows in Section 7.3.5 where we can easily adapt it to undirected network. Since our solution process has minor differences to the general multi-pricing decomposition algorithm that Section 2.4.2 describes, we explain in detail our computational approach in Section 7.4. Section 7.5 reports the numerical result that we got. Conclusions are draw in Section 7.6.

7.1 Problem description

Next three paragraphs present the network architecture, the assumption constraints, and the cost objective, respectively.

Network architecture

The study considers backbone networks with the following architecture.

Node structure in our backbone network is an OXC that supports three basic operations. First, it can let a lightpath pass through without being regenerated by using an optical bypass. Second, a lightpath can be regenerated in order to improve its optical quality that is degraded during the transmission. Third, it can add or drop a wavelength that means finishing a single-hop lightpath or starting a new one from the electrical layer.

We work with multiple rate networks, meaning that an optical link contains different wavelengths at different bit-rates.

A lightpath, also called single-hop lightpath, is an optical path without any regeneration, otherwise it is called multi-hop lightpath. Actually, a multi-hop lightpath is a sequence of several single-hop lightpaths. Moreover, a single-hop lightpath operates at only one bit-rate.

Actually, we do no consider grooming capacity in our model as it is performed in the electrical layer. Node cost in our model consists of transceivers costs and regenerator costs. We assume that regenerators are deployed only at nodes. On other words, there is no in-line regenerator. Network cost is simply the sum of all node costs.

Node equipment is a function of bit-rate capacity and maximum distance reach which is defined as the maximal possible length of a single-hop lightpath. Certainly, there is a limitation to the length of a multi-hop lightpath, but this can be easily approximated by setting a constraint on the number of regenerators. Information about those costs are given in Table 7.1.

Fig. 7.1 shows a simple multirate network. Let TR_D^B be the cost of transceiver TX + RX of bandwidth B and maximum distance reach D. Those parameters are defined in Table 7.1. The total network cost consists of the transceiver cost between A and B ($2\times\mathrm{TR}_{1000}^{40}+2\times\mathrm{TR}_{1000}^{100}$), the transceiver cost between B and C ($2\times\mathrm{TR}_{750}^{40}+2\times\mathrm{TR}_{750}^{100}$) and the one between A and C ($2\times\mathrm{TR}_{1750}^{10}$). Then, the whole transceiver cost of the example in Fig. 7.1 is

$$2\times\mathrm{TR}_{1000}^{40}+2\times\mathrm{TR}_{750}^{40}+2\times\mathrm{TR}_{750}^{100}+2\times\mathrm{TR}_{1000}^{100}+2\times\mathrm{TR}_{1750}^{10}.$$

Line cost (such as amplifiers) is not considered here because it is not impacted by optimization process.

Assumptions

In order to avoid the expensive cost of wavelength converters, we consider wavelength continuity assumption in the sense that in a single hop lightpath, a same wavelength is used for every link. We also assume that there is a limited number of available wavelengths in a link.

In our model, one important constraint is applied: we limit the number of nodes where regenerators are deployed. The rationale comes from the fact that, in practice, regenerators are gathered in few nodes for being effectively managed as well as minimizing the overall cost of supporting equipment such as cooling systems.

We also take into account a constraint that implies a limit on the number of hops

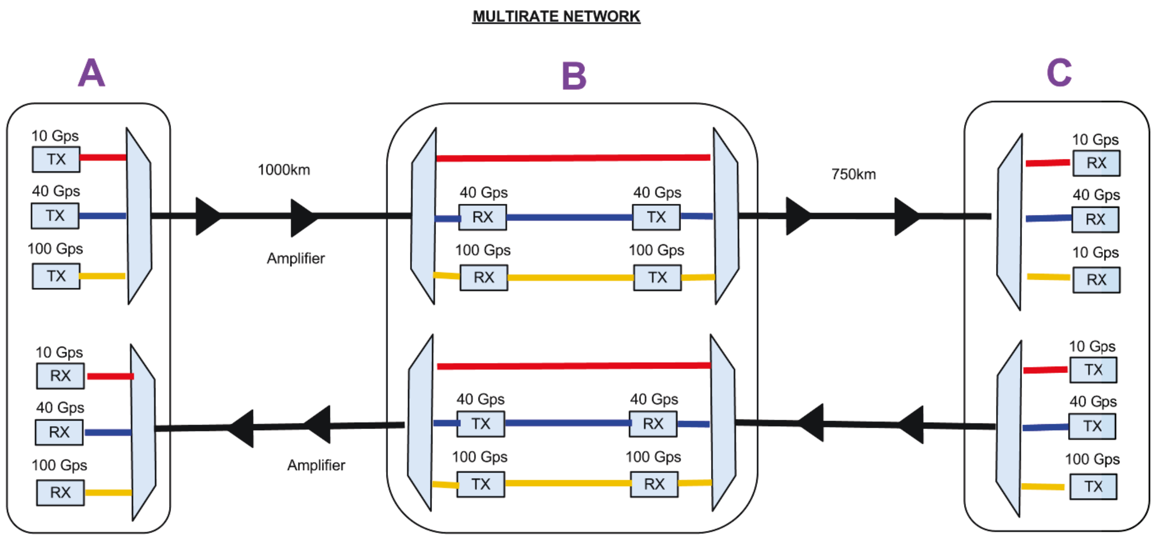

Fig. 7.1: A simple multirate optical network

of a multi-hop lightpaths. This constraint is applied to prevent the delay between optical channels from being too large.

Objective

With a given network topology, traffic demands, and cost distribution of different kinds of transceivers and regenerators, we design a network that satisfies all demands at minimum transceiver cost while satisfying the previously described constraints.

7.2 Cost model

In this section, we propose a model that evaluates the transceiver cost of a network. Our numbers are taken from [Huelsermann *et al.*, 2008]. However, [Huelsermann *et al.*, 2008] does not contain informations about 40 Gbps transceivers and regenerators at 3000 km - MTD (Maximum Transmission Distance), nor any information about 100 Gbps transceivers and regenerators. One way to get an idea about missing information is to use the cost formulation given in [Simmons, 2005] to calculate the transceiver costs and use back-to-back (B2B) regenerators whose prices are two times the cost of a transceiver. The amplifier costs are exactly the same as in [Huelsermann *et al.*, 2008]. We were surprised that, in [Huelsermann *et al.*, 2008], the dispersion cost depends on MTD and bit-rate, thus, we decided to assume the dispersion cost is 0.01

(thousand dollars) which is the average of the values given in [Huelsermann *et al.*, 2008].

We decided to build the traffic of a network topology such that its bandwidth demand between two cities are in proportion of their populations. We use the formulation (27-29) given in [Batayneh *et al.*, 2011a] to produce such a traffic. The population of a city is easily found in Internet [Brinkhoff, 2014].

In Table 7.1, cost unit is a thousand dollars.

	Transceiver $\text{COST}^{\text{TR}}_{\text{MTD}(p),r}$		Regenerator $\text{COST}^{\text{REG}}_{\text{MTD}(p),r}$		Amplifier $\text{COST}^{\text{AP}}_{\text{MTD}(p),r}$	Dispersion $\text{COST}^{\text{DS}}_{\text{MTD}(p),r}$
References	[Simmons, 2005] (*)	[Huelsermann *et al.*, 2008] (**)	**	B2B	**	**
MTD (km)	$r = 10$ Gbs					
750 LH	1	1	1.4	2	1.92	0.01
1,500 ELH	1.25	1.25	1.75	2.5	2.77	0.01
3,000 ULH	1.56	1.67	2.34	3.12	3.45	0.01
MTD (km)	$r = 40$ Gbs					
750	3	3.75	5.25	6	1.92	0.01
1,500	3.75	5.17	7.24	7.5	2.77	0.01
3,000	4.68			9.36	3.45	0.01
MTD (km)	$r = 100$ Gbs					
750	5			10	1.92	0.01
1,500	6.25			12.5	2.77	0.01
3,000	7.8			15.6	3.45	0.01

Table 7.1: Cost model (MTD = Maximum Transmission Distance).

7.3 Decomposition model

We formulate a column generation model with two pricing problems. One pricing problem generates wavelength configurations while the other generates a multi-hop path configurations. We introduce our definitions and notations in Section 7.3.1. Then, the master (Section 7.3.2) and the two pricing problems (Section 7.3.3 and

7.3.4) are detailed. Section 7.3.5 explains how to adapt the decomposition model to undirected networks.

7.3.1 Definitions and notations

We explain our notations and variables in this section. Definition of wavelength configuration and of multi-hop path configuration are given in the next paragraphs. Such configurations are generated by the two pricing problems that we introduce in the sequel.
So let:

- s : source.
- d : destination.
- D^r_{sd}: number of demand units between v_s and v_d, with rate r.
- $\mathcal{SD} = \{\{v_s, v_d\} : D^r_{sd} > 0$ for at least one $r \in R\}$
- r : granularity/rate (10 Gbps, 40 Gbps, 100 Gbps).
- n_{REG}: maximum number of nodes where regeneration can occur

Also, we have:

- $G = (V, L)$ where
  - V is the set of nodes (generic index v), and
  - L is the set of (directed) links (generic index ℓ)
- W : maximum number of available wavelengths.
- REG_v : maximum number of regenerator ports at node v.

Variables of our model are as follows.

- z_γ : number of times configuration γ is selected.
- n^r_{ij} : number of lightpaths with bit-rate r between v_i and v_j, which belong to the set of selected wavelength configurations.
- y_π : number of selected copies of multi-hop path configuration π.
- x_v : 1 if node v is used for regeneration, 0 otherwise.

Wavelength configurations

The optimization model relies on a set of potential wavelength configurations, which are defined as follows.

A wavelength configuration γ is a set of disjoint single-hop lightpaths, all routed on the same wavelength.

- Γ: set of configurations (generic index γ)
- $\textsc{cost}_\gamma$: cost of configuration γ (defined in equation (7.1))
- P set of lightpaths with
  - $P = \bigcup\limits_{(v_i,v_j) \in V \times V} P_{ij}$
  - P_{ij}: set of (single-hop) lightpaths from v_i to v_j (generic element p)
  - characteristic vector: $\delta_{\ell p} = 1$ if ℓ belongs to p, 0 otherwise.
- Characteristic vector of a wavelength configuration $\gamma \in \Gamma$: for $p \in P$

$$a^\gamma_{pr} = \begin{cases} 1 & \text{if wavelength configuration } \gamma \text{ contains} \\ & \text{lightpath } p \in P \text{ with bit-rate } r \\ 0 & \text{otherwise.} \end{cases}$$

Multi-hop path configurations

A multi-hop path configuration, denoted by π is a wavelength route defined as a sequence of lightpaths, where all the lightpaths have the same bit-rate. Notice that the lightpaths belonging to a given multi-hop path configuration can be associated with different wavelengths. Let Π denote the set of all possible multi-hop path configurations with

$$\Pi = \bigcup_{(v_s,v_d) \in V \times V} \bigcup_{r \in R} \Pi^r_{sd},$$

where Π^r_{sd} is the set of multi-hop path configurations between v_s and v_d and bit rate r.

Characteristic vectors of a multi-hop path configuration $\pi \in \Pi^r_{sd}$: for $(v_i, v_j) \in$

$V \times V$

$$b_{ij}^{\pi} = \begin{cases} 1 \text{ if multi-hop path configuration } \pi \text{ contains} \\ \quad \text{a lightpath with bit-rate } r \text{ from } v_i \text{ to } v_j, \\ 0 \text{ otherwise} \end{cases}$$

$$e_v^{\pi} = \begin{cases} 1 \text{ if } v \text{ is a regeneration node of } \pi \\ 0 \text{ otherwise} \end{cases}$$

7.3.2 Master model

The objective of the optimization model is to minimize the network cost, as estimated by the regenerator costs, as well as the transceiver/receiver, amplifier and dispersion equipment costs. The model is expressed as follows.

$$\min \quad \sum_{\gamma \in \Gamma} \text{COST}_{\gamma} z_{\gamma}$$

where

$$\text{COST}_{\gamma} = \sum_{p \in P} \sum_{r \in R} \text{COST}^{\text{REG}}_{\text{MTD}(p),r} \, a^{\gamma}_{pr} \tag{7.1}$$

with $\text{COST}^{\text{REG}}_{\text{MTD}(p),r}$ being the regenerator cost of path p with rate r. Values can be found in Table 7.1 for various parameters. The master problem is subject to following constraint:

Limited number of available wavelengths

$$\sum_{\gamma \in \Gamma} z_{\gamma} \leq W \tag{7.2}$$

Computation of the number of lightpaths with bit-rate r from v_i and v_j

$$n_{ij}^{r} = \sum_{\gamma \in \Gamma} \sum_{p \in P_{ij}} a^{\gamma}_{pr} \, z_{\gamma} \quad r \in R, (v_i, v_j) \in V \times V \tag{7.3}$$

Bandwidth demands

$$\sum_{\pi \in \Pi_{sd}^{r}} y_{\pi} = D_{sd}^{r} \qquad r \in R, (v_s, v_d) \in \mathcal{SD} \tag{7.4}$$

Do not use more than the number of available lightpaths belonging to the selected multi-hop path π configurations

$$\sum_{\pi \in \Pi^r} b_{ij}^{\pi}\, y_{\pi} \leq n_{ij}^{r} \qquad r \in R, (v_i, v_j) \in V \times V \tag{7.5}$$

Limit on the number of regenerator ports at node v

$$\sum_{\pi \in \Pi} e_v^{\pi}\, y_{\pi} \leq x_v \mathrm{REG}_v \quad v \in V \tag{7.6}$$

Limit on the number of nodes with regeneration equipment

$$\sum_{v \in V} x_v \leq n_{\text{REG}}. \tag{7.7}$$

7.3.3 Pricing I: generation of wavelength configurations (γ)

The first pricing problem is to generate wavelength configurations and is defined as follows.

INPUT: Dual values of constraints (7.2) ($\rightsquigarrow u^0$), (7.3) ($\rightsquigarrow u_{ijr}^1$), and set of pre-enumerated single-hop lightpaths.

OUTPUT: An improving configuration $\gamma \in \Gamma$ described by its characteristic vector $(a_{pr}^{\gamma})_{p \in P, r \in R}$.

The formal formulation is expressed as:

$$\min \quad \overline{\text{COST}}^{\gamma} = \text{COST}_{\gamma} - u^0 - \sum_{r \in R} \sum_{(v_i, v_j) \in V \times V} \sum_{p \in P_{ij}} u_{ijr}^1 a_{pr}$$

subject to:

Link disjointness requirement

$$\sum_{r \in R} \sum_{p \in P} \delta_{\ell p}\, a_{pr} \leq 1 \quad \ell \in L \tag{7.8}$$

Reach vs. rate

$$a_{pr} r \leq r_{\text{LH}} \qquad p \in P : \text{LEN}(p) \geq p_{\text{LH}} \tag{7.9}$$

$$a_{pr} r \leq r_{\text{ELH}} \qquad p \in P : \text{LEN}(p) \geq p_{\text{ELH}} \tag{7.10}$$

$$a_{pr} r \leq r_{\text{ULH}} \qquad p \in P : \text{LEN}(p) \geq p_{\text{ULH}} \tag{7.11}$$

Domain of the variables

$$a_{pr} \in \{0, 1\} \qquad p \in P, r \in R. \tag{7.12}$$

7.3.4 Pricing II: generation of multi-hop path configuration (π)

The second pricing problem is to generate mutli-hop path configurations and is defined as follows.

INPUT: Dual values of constraints (7.4) ($\rightsquigarrow u^{2k}_{sdr}$), (7.5) ($\rightsquigarrow u^{3k}_{ijr}$) (7.6) ($\rightsquigarrow u^{4k}_{v}$) ; bit rate r ; pair of source and destination nodes $\{v_s, v_d\}$
OUTPUT: An improving configuration $\pi \in \Pi^r_{sd}$ described by its characteristic vector $(b^{\pi}_{ij})_{v_i, v_j \in V \times V}$ and e^{π}_v.

The formal formulation is expressed as:

$$\min \quad \overline{\text{COST}}^{\pi} = -u^{2k}_{sdr} - \sum_{ij} b_{ij} u^{3k}_{ijr} - \sum_{v} u^{4k}_{v} e_v$$

subject to:

1. Flow Conservation

$$\sum_{(v_i, v_j) \in w^+(v)} b_{ij} = \sum_{(v_i, v_j) \in w^-(v)} b_{ij} = e_v \qquad (v \neq s, d) \tag{7.13}$$

2. In/Out Source Destination Flow

$$\sum_{(v_i, v_j) \in w^+(s)} b_{ij} = \sum_{(v_i, v_j) \in w^-(d)} b_{ij} = 1 \tag{7.14}$$

7.3.5 Adaptation to undirected model

The presented model can be easily converted to undirected one by using undirected topology, undirected path, and undirected link instead of directed ones. In that case, Master as well as Wavelength Configuration Pricing keep being the same as in the directed case. We only need to replace Eq. (7.13) and (7.14) by new undirected versions for Multi-hop Path Configuration Pricing as follows.

1. Flow Conservation

$$\sum_{(v_i,v_j)\in w^(v)} b_{ij} = 2e_v \qquad (v \neq s, d) \tag{7.15}$$

2. In/Out Source Destination Flow

$$\sum_{(v_i,v_j)\in w^(s)} b_{ij} = \sum_{(v_i,v_j)\in w^(d)} b_{ij} = 1 \tag{7.16}$$

7.4 Solution of the models

The outline of the solution process is depicted in the flow chart Fig. 7.2. We start with a restricted master problem (RMP) which is made of an artificial solution consisting of several dummy columns. The objection of such an solution is far from the optimal one that we have to obtain through a repeat process.

Step 1 The RMP is optimally solved to get the corresponding dual values which are the input parameters of the first pricing problem (wavelength pricing problem).

Step 2 Searching for the solution of the wavelength pricing problem whose reduced cost is negative. If such a solution is found then it will be added back to the RMP since the pricing solution is the augmented column to the RMP and Step 1 is repeated. Otherwise, we continue to Step 3.

Step 3 The second pricing problem (multi-hop pricing problem) is solved with a same set of dual values in Step 2 in order to find a solution with negative reduced cost. If such a solution exists, it is added back to the RMP and the process is repeated from Step 1. Otherwise, we jump to Step 4

Step 4 Solve the RMP with all integer constraints to get the final ILP solutions since we know that the relax incumbent solution after Step 3 is the optimal RMP solution.

Each step is either an integer programming problem (Step 2,3,4) or a linear programming problem (Step 1). Those problems are implemented in OPL, an optimization programming language, and are solved by using software IBM ILOG CPLEX Optimization Studio 12.5.

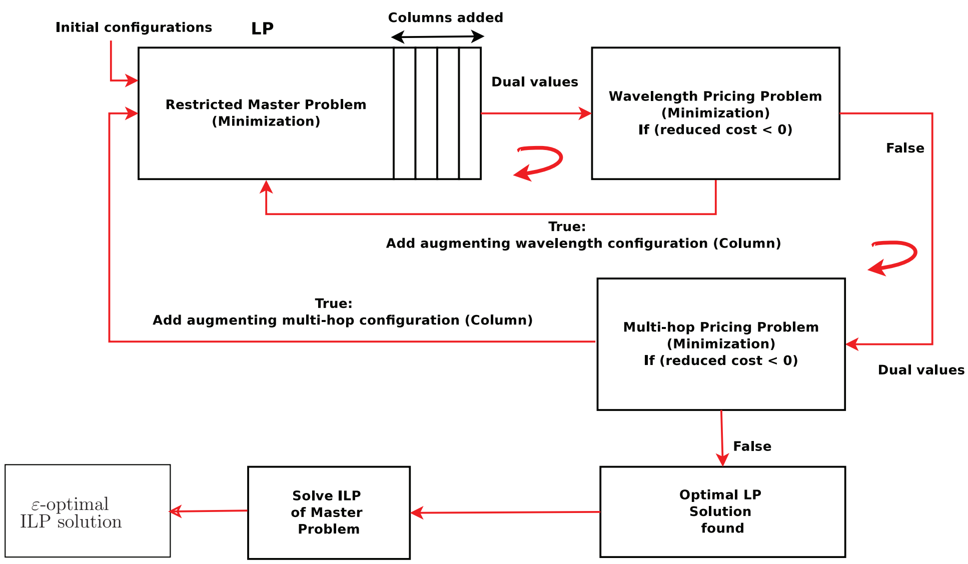

Fig. 7.2: Outline of the solution process

7.5 Numerical experiments

Our plan of experiments consists of two parts. The first part is to solve the problem for different traffic volumes in order to acknowledge the importance of high capacity transceivers (100 Gbps transceivers) in reducing CAPEX of WDM networks. The second part is to investigate the impact of maximum available regenerable sites. We would like to discover the relationship between that constraint with the network cost so that network designers can have some ideas when taking into account such a constraint.

Section 7.5.1 introduces how we prepare network traffic between cities in order to reflect the real life situation. Section 7.5.2 describes our analysis about the impact of traffic and of maximum regenerable site constraint in detail.

7.5.1 Data instances

We conducted experiments on the US-24 network with 24 nodes and 84 directed links (see Fig. 7.4) [Batayneh *et al.*, 2011a]. We use the same traffic generation as in [Batayneh *et al.*, 2011a]. Traffic is generated on every node pair where each node corresponds to a city, and the traffic is a function of the population in the cities associated with the endpoints. Bandwidth demand on a node pair corresponds to the product of population of the two end nodes. Actually, such a demand of a node pair is calculated as follows.

co	coefficient for generating traffic.
pop_i	population in city i
totpop	total population $= \sum_i \text{pop}_i$
demand_{ij}	traffic demand from city i to city j

Traffic demand from city i to city j is computed as follows.

$$\text{demand}_{ij} = \text{co} \times \frac{\text{pop}_i \times \text{pop}_j}{\text{totpop} \times \text{totpop}} \times \frac{\text{pop}_i}{\text{pop}_i + \text{pop}_j} \text{ (Gbps).} \tag{7.17}$$

We then derive granularity bandwidth demands (grooming) from demand_{ij} by the following simple scheme.

$$D_{sd}^{100} = \left\lfloor \frac{\text{demand}_{sd}}{100} \right\rfloor$$

$$D_{sd}^{40} = \left\lfloor \frac{\text{demand}_{sd} - 100 \times D_{sd}^{100}}{40} \right\rfloor$$

$$D_{sd}^{10} = \left\lceil \frac{\text{demand}_{sd} - 100 \times D_{sd}^{100} - 40 \times D_{sd}^{40}}{10} \right\rceil$$

where co (Eq. 7.17) represents the traffic volume. In our experiments (as in [Batayneh *et al.*, 2011a]), co varies from 2,048 up to 20,480 in order to simulate traffic volume patterns at different peek intervals. Hereby, we define traffic load over the network as the sum of all traffic demands between node pairs:

$$\text{traffic load} = \sum_{ij} \text{demand}_{ij}.$$

Traffic load represents the traffic volume that takes place in network. Table 7.2 shows the correspondence between co and traffic load.

co	2,048	4,096	6,144	8,192	10,240	12,288	14,336	16,384	18,432	20,480	22,528	24,576
traffic load (Gbps)	957	1,915	2,873	3,830	4,787	5,745	6,703	7,660	8,617	9,575	10,533	11,490

Table 7.2: Traffic load vs. co

Fig. 7.3 shows the traffic demand distributions per node pair with respect to different traffic load. Such a distribution is formed by sorting the node pair traffic demands in descending order of their demand. In Fig. 7.3, X-axis indicates node pair index (ranked by traffic demand) which spreads from 1 to 552 while Y-axis presents the corresponding demand. It turns out that, firstly, the form of our traffic patterns remains the same with our traffic generated model, and secondly, 36% of node pairs contributes 76% of network traffic while 18% of node pairs occupies 56% of network traffic.

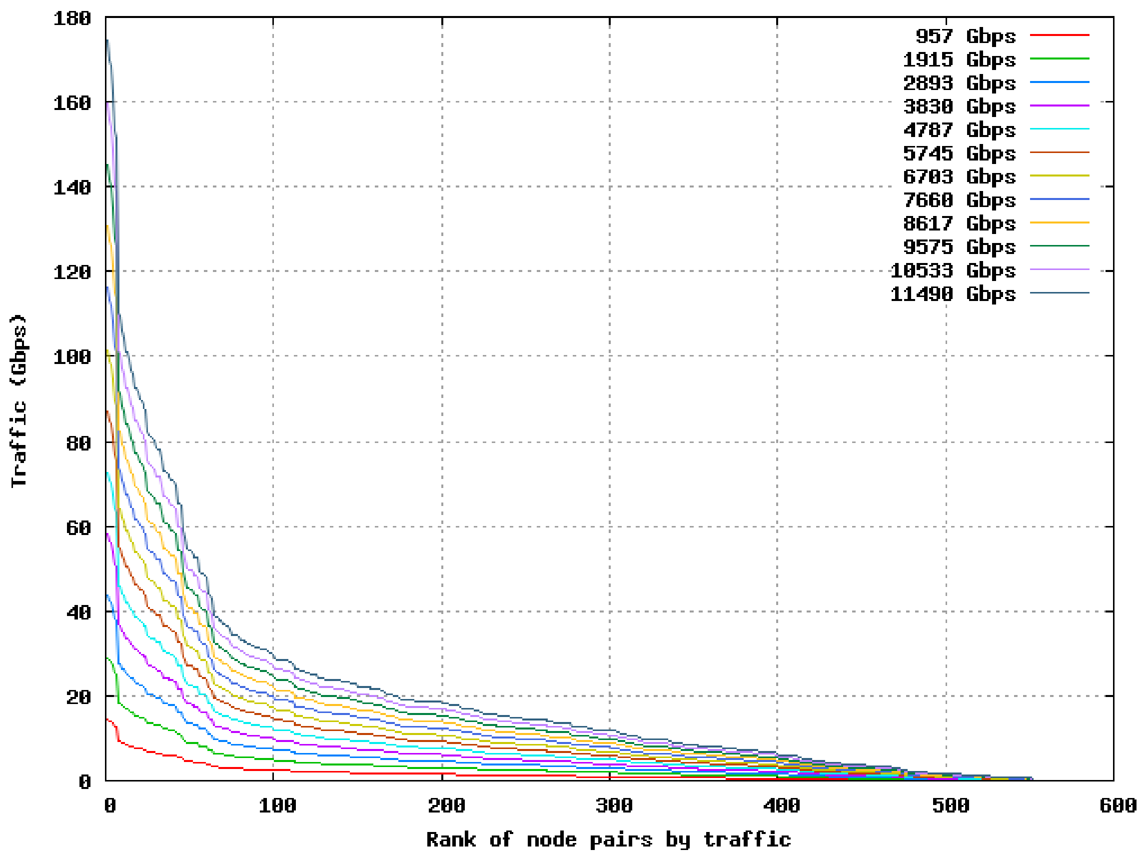

Fig. 7.3: Traffic demand distribution

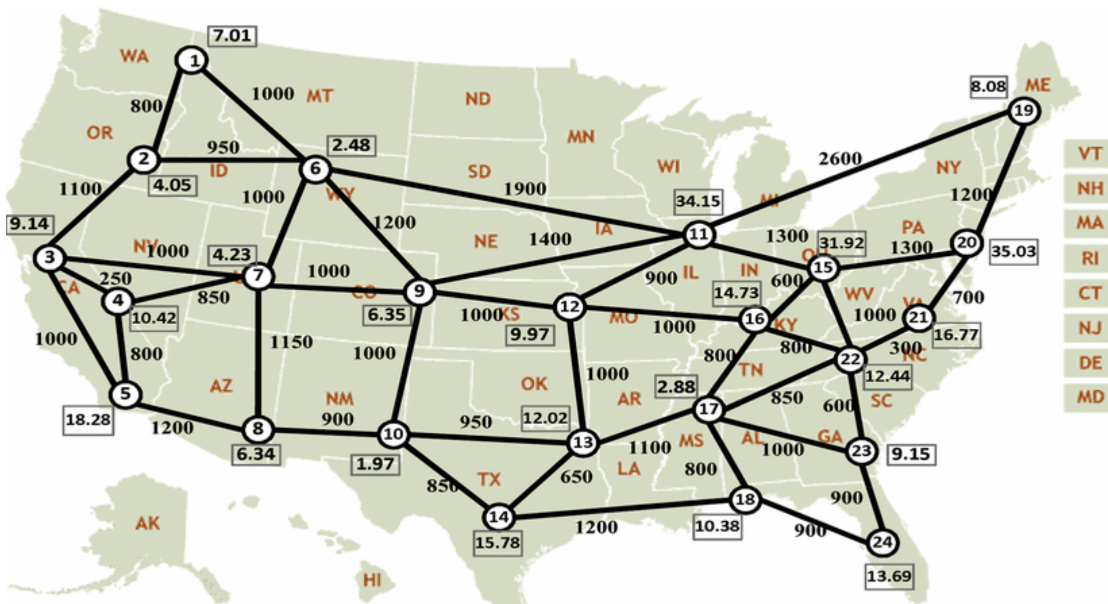

Fig. 7.4: US-24 network

7.5.2 Impact of traffic volume and physical constraints on CAPEX

Percentage pattern of transceivers grouped by MTD

Fig. 7.5 reports the evolution of the average percentage of transceivers by 750km, 1,500km and 3,000km against traffic load. For each traffic load, such an average is defined as follows:

$$\text{AVG}(percentage) = \frac{percentage_{12} + percentage_{18} + percentage_{24}}{3}$$

where $percentage_x$ is the percentage of a kind of transceiver (750km, 1500km or 3000km) in the quasi-optimal solution of the problem whose amount of regenerable sites is x. We did the linear regression ($f(x) = a \times x + b$) on the set of average percentage for each kind of transceiver (classified by MTD) and displayed the obtained a and b on the top right of Fig. 7.5.

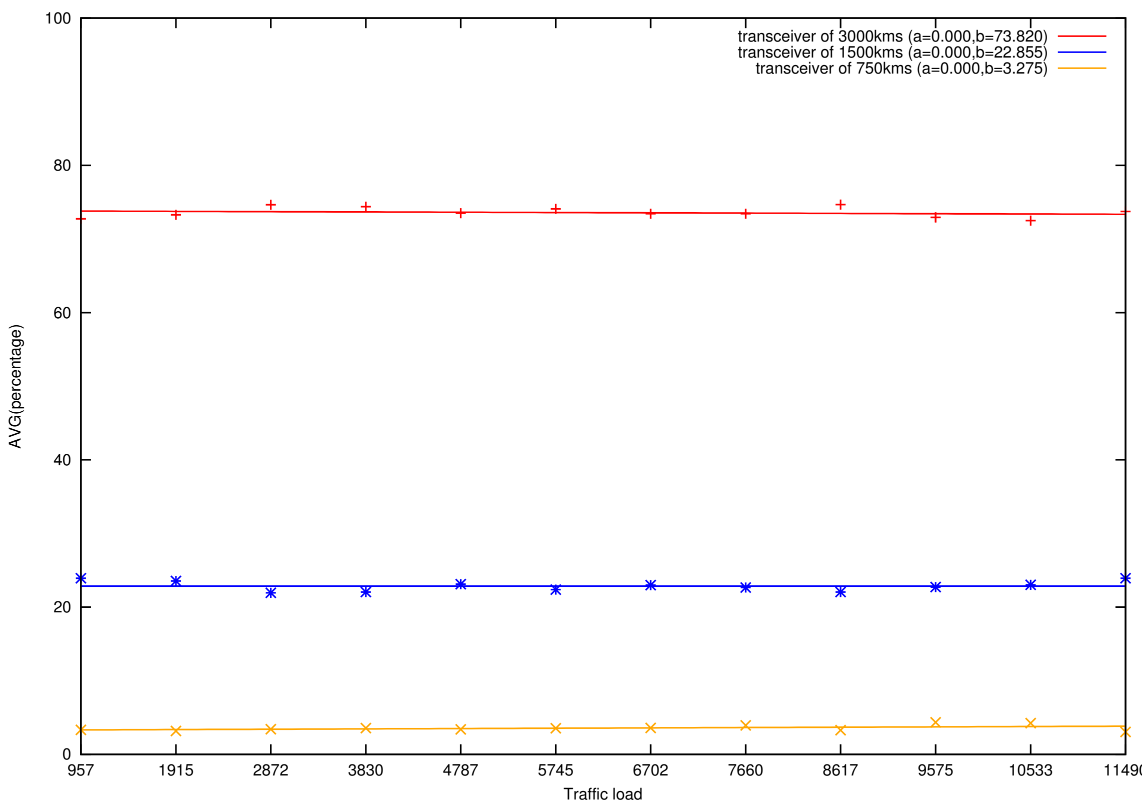

Fig. 7.5: Average of transceiver percentages of 750km, 1500km and 3000km

MTD	Mean	Standard Deviation
3000km	[71.4-75.6]	[0.7-2.0]
1500km	[21.4-24.9]	[0.3-2.0]
750km	[02.8-04.8]	[0.3-1.0]

Table 7.3: Statistics of the percentage average

Table 7.3 shows the mean and the standard deviation of the set of AVG($percentage$) with different traffic load for each MTD.

It turns out that transceivers of 3000km takes the largest part in the quasi-optimal solution (∼73%), then transceiver of 1500km takes about 23% and the ones of 750km takes the smallest part (∼4%). This fact makes sense since it is obvious that using long distance transceivers reduces the need of regenerators.

Fig. 7.5 shows that traffic evolution has no significant impact on the average percentage distribution of the set of transceivers grouped by MTD since parameter a keeps being 0 despite traffic increase.

Percentage pattern of transceivers grouped by bit-rate

Fig. 7.6 is similar to Fig. 7.5, except that its transceivers are classified by bit-rate instead of MTD. We also fit the data with the linear regression ($f(x) = a \times x + b$).

This figure shows clearly that transceivers of 10Gbps has the largest percentage (>50%) while other kinds of transceivers (40Gbps and 100Gbps) takes the rest. Moreover, transceiver percentage of 10Gbps slowly decreases with the evolution of traffic load ($a = -0.0015 < 0$) while transceiver percentages of 40Gbps and 100Gbps increase ($a = 0.0010$ and $a = 0.0006$).

The increasing momentum of transceivers of 100Gbps ($a = 0.0010$) is higher than the one of transceivers of 40Gbps ($a = 0.0006$). It means, in comparison with the percentage of transceivers of 40Gbps, the percentage of transceivers of 100Gbps is increasing in accordance with traffic load increment. However, when the traffic load is relatively small, both percentages have a meaningless difference.

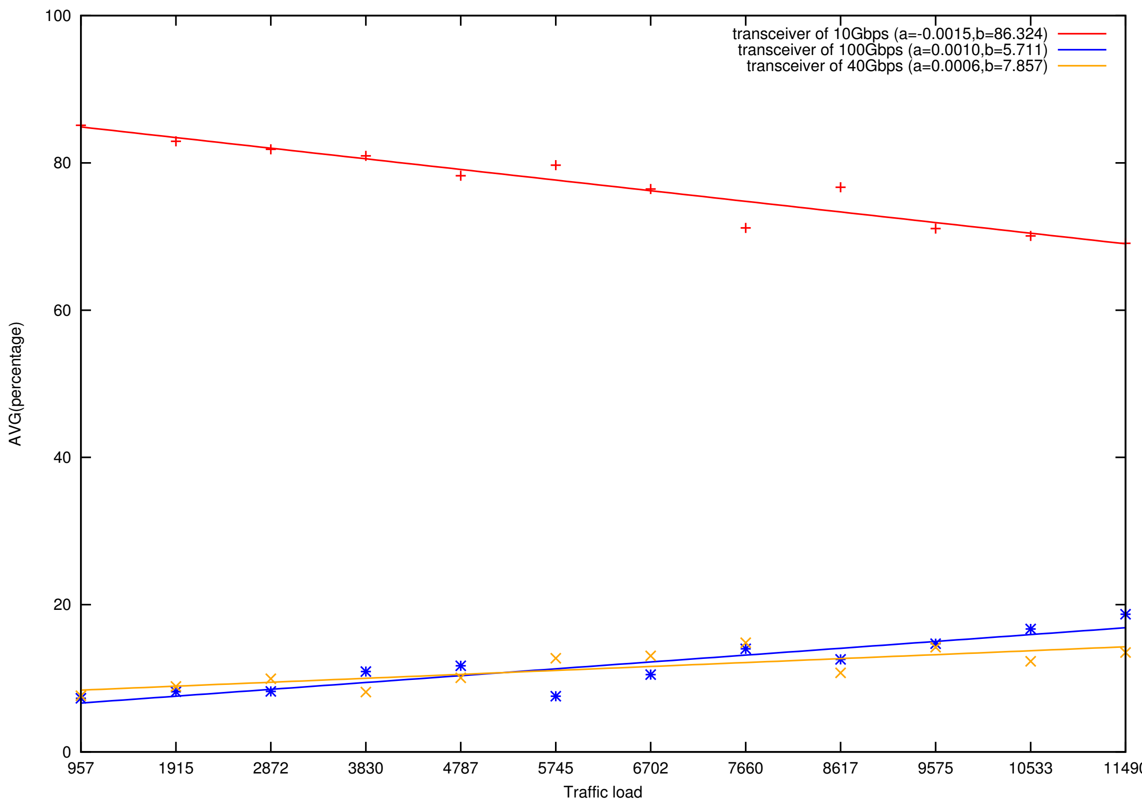

Fig. 7.6: Average of transceiver percentages of 10Gbps, 40Gbps and 100Gbps

Impact of constraint of maximum regenerable sites over transceiver distribution (grouped by bit-rate)

Fig. 7.7 compares two extreme cases where maximum amount of regenerable sites are 12 and 24. The former case is when such an amount is half number of nodes while the latter case means that every node can be a regenerable site. In Fig. 7.7, the dash lines are for the 12 regenerable sites case while the solid lines are for the 24 regenerable sites case. Blue and red indicates transceiver of 10 Gbps and 100 Gbps, respectively.

Obviously, in the case of maximum 12 regenerable sites, the optimal solution uses more transceivers of 100Gbps and less transceivers of 10Gbps than in the case of maximum 24 regenerable sites. It makes sense since the first case has fewer choices of node to deploy regenerators than the second case has. We conclude that when such a constraint gets stricter, the optimal design has to deploy more and more transceivers of high capacity (100Gbps).

Fig. 7.7 also confirms the trend of using less transceivers of 10Gbps and more of 100Gbps as the traffic load increases. The next paragraph makes a quantitative comparison about the impact of maximum regenerable sites on the deployment cost.

Since we do not consider grooming, the number of transceivers of a specific bit-rate at the end nodes of working paths is constant; consequently we can pre-calculated their numbers. However, the number of transceivers that are deployed at intermediate nodes depends on the maximum number of regeneration sites.

Impact of constraint of maximum regenerable sites over the deployment cost (CAPEX)

The main idea of restricting the maximum number of regenerable sites is to gather regenerators to few sites in order to take advantage of sharing support devices, such as cooling systems. By that way, we can reduce the operating cost (OPEX). As shown in previous paragraphs, such a constraint results in requiring more 100Gbps and 40Gbps transceivers, in the other words, increasing the deployment cost (CAPEX).

Fig. 7.8 shows the dependency of the transceiver costs on the maximum available regenerable sites. E.g., the transceiver cost in the case of 24 regenerable sites over the one of 12 regenerable sites may vary from 21.4% to 50.3%.

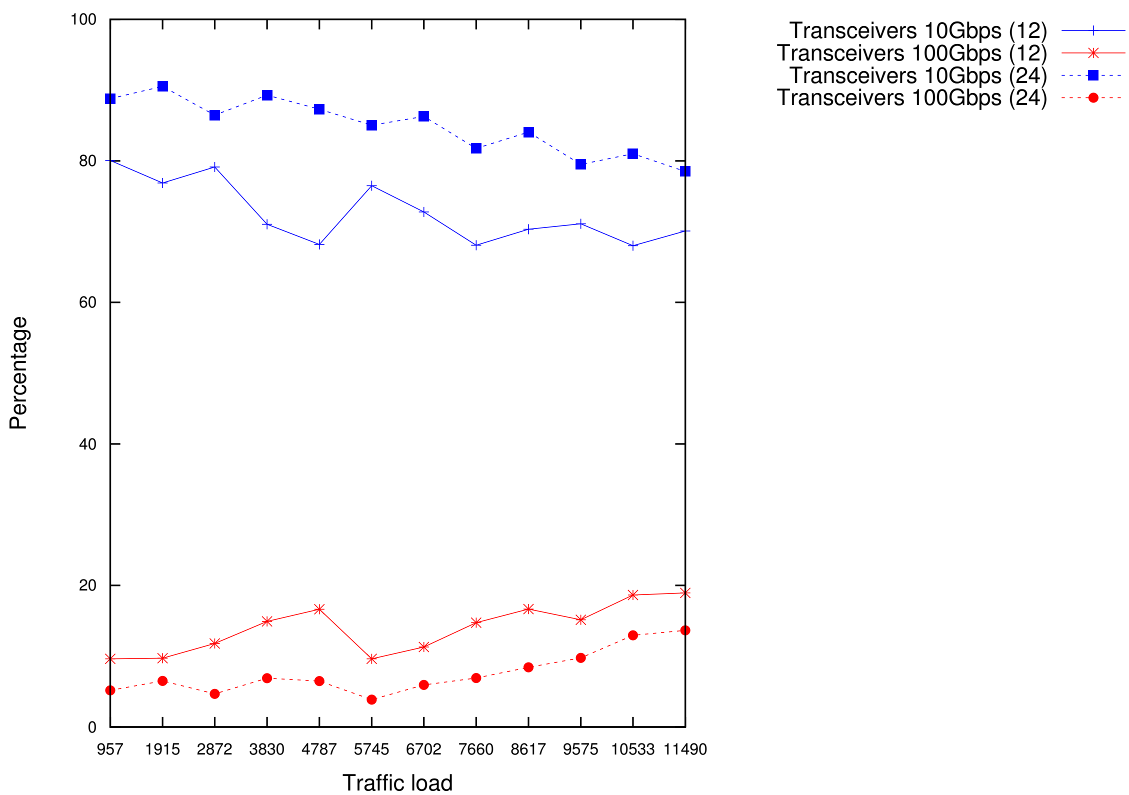

Fig. 7.7: Comparison of percentages of transceivers grouped by bit-rate that is made between the case of maximum 12 regenerable sites and of maximum 24 regenerable sites

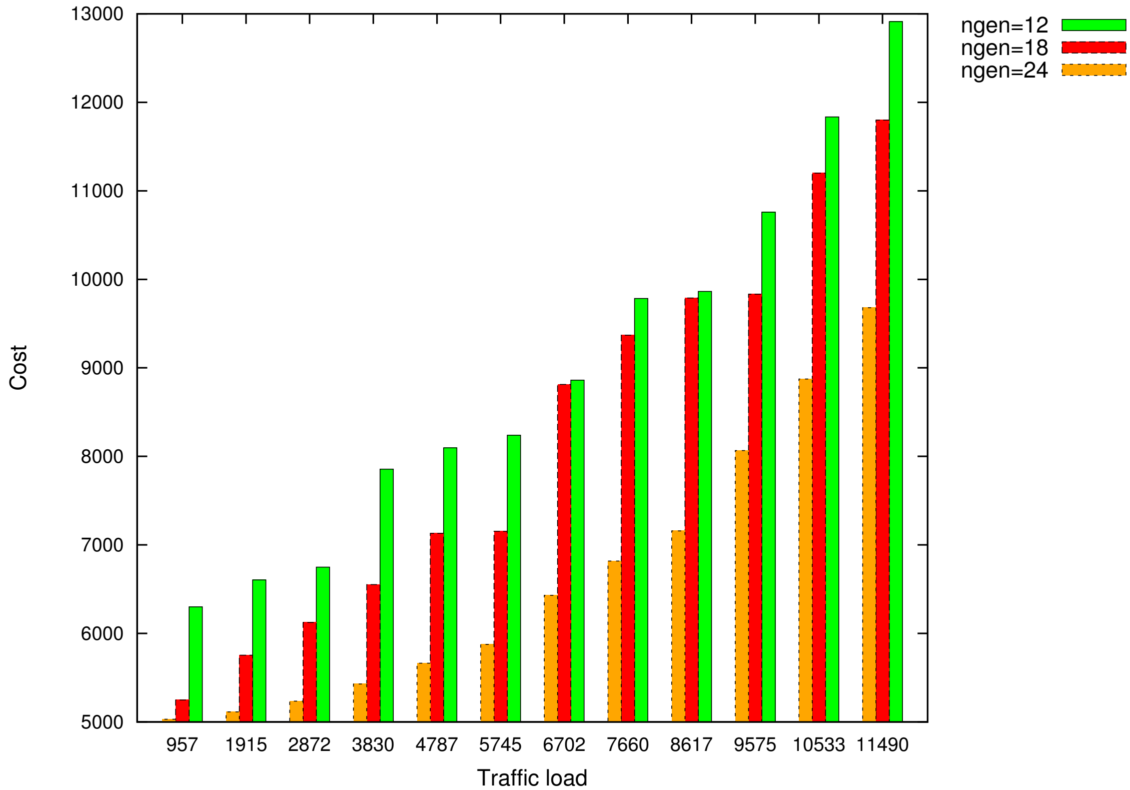

Fig. 7.8: Cost comparison between different amount of maximum regenerable sites

7.6 Conclusion

We develop a decomposition method to solve the multi-rate design problem taking into account the constraint of maximum regenerable sites which, to the best of our knowledge, has not been considered in literature. We discover that the traffic evolution has almost no impact on the percentage distribution of transceiver grouped by MTD. When we group transceivers by bit-rate, when the traffic grows we see the percentage of 100Gbps transceivers increases fastest, then the one of 40Gbps transceiver, as opposed to the reduction of the percentage of 10Gbps. Those points could be hints to develop a high scalable heuristic for huge networks where such an extract method is intractable.

We study the restriction on maximum regenerable sites and see a huge impact on the deployment cost. For US-24 network, when reducing the number of regenerable sites from 24 to 12, we can see that the increase in deployment cost is between 21.4% and 50.3%. Based on such information, a network designer can make a appropriate compromise between OPEX and CAPEX.

7.7 Future work

Our proposed models are for a network with a general pattern of traffic. In this section, we assume that we are given different traffic matrices, where each traffic matrix corresponds to the traffic over a given time period within the time horizon under study. The goal is then to find a network design that allows the provisioning of the traffic for all time periods, at minimum cost. We next explain how to modify the model presented in the previous section. We re-use the same notations and variables, except for few exceptions, which are next described. In future, we will do the experiments with networks that have multiple traffic matrices.

Notations

T	Set of time periods within the time horizon (generic index t)
D_{sd}^{rt}	Number of demand units from v_s to v_d, with rate r during time period t.

Variables y_π are replaced by:

y_π^t number of selected copies of multi-hop path configuration π during period t.

The objective function remains unchanged while constraints (7.4), (7.5) and (7.6) are modified as follows:

$$\sum_{\pi \in \Pi_{sd}^r} y_\pi^t = D_{sd}^{rt} \qquad r \in R, v_s, v_d \in \mathcal{SD}, t \in T \tag{7.4'}$$

Do not use more lightpaths that the number of available lightpaths belonging to the selected multi-hop path configurations

$$\sum_{\pi \in \Pi^r} b_{ij}^\pi \, y_\pi^t \leq n_{ij}^r \qquad r \in R, (v_i, v_j) \in V \times V, t \in T \tag{7.5'}$$

Restriction on the number of regenerator ports at node v

$$\sum_{\pi \in \Pi} e_v^\pi \, y_\pi^t \leq x_v \mathrm{REG}_v \quad v \in V, t \in T \tag{7.6'}$$

It is possible, but not straightforward, to apply our proposed formulation to elastic optical networks. As indicated in [Gerstel *et al.*, 2012], two important properties of elastic optical networks are: firstly, the optical spectrum can be divided up flexibly and secondly, the transceivers can generate elastic optical paths (EOPs); that is, paths with variable bit rates. The first property implies that we do not have a fixed number of wavelengths and bit-rate per wavelength is variable. In order to implement those conditions, we can remove the constraint on the maximum number of wavelengths and the integer granularity on wavelength bit-rate. We denote, in that case, wavelength bit-rates by a set of float variables. The second property means that we have to take into account grooming in our formulation. So, even it is possible to extend our proposed model to elastic optical networks, it need to invest serious effort.

Chapter 8

Conclusion and future works

8.1 Conclusion

Scalability and quality estimation are two important aspects of a network design solution. Achieving both of those characteristics are difficult for heuristics. Decomposition techniques allow to obtain such criteria if we have a proper mathematical decomposition.

This thesis developed several innovative decomposition models for various network design problem and, consequently, get very good results in terms of performance and solution quality for some basic optimization planning problems arising in the design of optical networks. This work explores four principal aspects.

Firstly, with help of large-scale decomposition model, the impact of wavelength continuity assumption on the ε-optimal solutions of p-cycle and FIPP network designs is investigated. Our numerical results shows that, when it comes to p-cycle and FIPP designs, a fair amount of money can be saved by implying wavelength continuity constraint. Such a constraint simplifies the network design complexity as well, thus allows us to explore larger instances than previous studies and, at the same time, combine working and protection capacities in an objective.

Secondly, a scalable multi-pricing column generation algorithms is proposed for FDPP p-cycles subject to multiple link failures that delivers ε-optimal solutions. Such a algorithm reconfirms that FDPP design has a better redundancy ratio over FIPP designs. Moreover, we formally show that, by using our proposed framework, node failure is just a special case of multiple link failure.

Thirdly, a network-flow based column generation is also successfully applied to the survivability logical topology design problem. Thanks to the network flow formulation, such a problem is solved at a large scale and subject to multiple link failures that can not be obtained with other existed studies which follows the cut-set based approach. The flexibility of that network-flow based CG algorithm allows us to explorer several options to a survivability logical mapping, for e.g., what is an optimal amount of spare capacity should be added in order to guarantee a successful restoration against a certain network failure. Since we do not optimize the protection capacity, we got very high redundancy ratios. That means a meaningful amount of protection capacity may be wasted.

Fourthly, we attacked multirate cross-layer design problem by introducing a multiple pricing CG algorithm that helps us to investigate on the impact of various physical constraints, for e.g., number of available regenerator sites, maximum number of slots in optical switches, etc. By formulating the optical layer and the physical layer into two separate pricing problems, a great flexibility of introducing physical and optical constraints is obtained since the inter-dependent between those layers are moved into the master problem. When studying the restriction on maximum regenerable sites, we see a huge impact of such a constraint on the deployment cost. Our proposed model gave an exact value on the deployment cost according to each constraint setting. Based on such information, a network designer can make a appropriate compromise between OPEX and CAPEX.

The thesis is a successful story of applying large-scale decomposition methodology to telecommunication network design. It shows that, when dealing with current industrial optical networks, scalability, solution quality as well as model flexibility are very possibly archived with CG methodology if we can come up with an effective decomposition.

8.2 Future works

The work in this thesis can be extended in three directions.

Firstly, our proposed decomposition models solve larger instances than the ones that have been studied in the literature. We also consider complicated constraints, for e.g., multiple link/node failures, that are often ignored in many studies. In our thesis, we solve up to 24-nodes networks. Such a limitation is set by the current computational power that is available to us. In order to improve the scalability, several heuristics, such as warm start, parallel computing, lazy constraints, and ad-hoc speciality algorithms (shortest path, network flow, bender decomposition..) can be applied to both master and price problems. Those techniques will improve the solution process in order to meet the computational challenging coming from future hypothetical large-scale optical networks, i.e, CORONET Global Network (see [Chiu *et al.*, 2009]) which is an hypothetical optical network with 100 nodes and 136 links. The next generation decomposition models should be able to solve such a large-scale network within few hours.

Secondly, our decomposition algorithms are implemented by CPLEX OPL which is a general purpose optimization language. In order to avoid re-invent CG implementation every time, an universal CG framework should be developed so that network designer can focus more on the design rather than on implementation. An universal CG framework should be implemented in C++ as well as in multi-threading platform in order to gain as much performance as possible.

Thirdly, up to two network layers are considered in our thesis. Beyond two layer designs are impossible for our current CG implementations due to the computing limitation. In order to attack more than two layers in network design, we can focus on developing heuristics that speed up the solving process of the pricing problem and/or build a good initial set of columns in the master problem.

Bibliography

[Barnhart *et al.*, 1998] Barnhart, C.; Johnson, E.L.; Nemhauser, G.L.; Savelsbergh, M.W.P., and Vance, P.H. Branch-and-Price: Column Generation for Solving Huge Integer Programs. *Operations Research*, 46(3):316–329, 1998.

[Batayneh *et al.*, 2006] Batayneh, M.; Zhu, H.; Song, L., and Mukherjee, B. Cost-efficient WDM mesh network design with line cards of multiple ports. In *IEEE Global Telecommunications Conference - GLOBECOM*, pages 1 –5, 2006.

[Batayneh *et al.*, 2008] Batayneh, M.; Schupke, D.A.; Hoffmann, M.; Kirstaedter, A., and Mukherjee, B. Optical network design for a multiline-rate carrier-grade Ethernet under transmission-range constraints. *Journal of Lightwave Technology*, 26:121–130, January 2008.

[Batayneh *et al.*, 2011a] Batayneh, M.; Schupke, D.A.; Hoffmann, M.; Kirstadter, A., and Mukherjee, B. On routing and transmission-range determination of multi-bit-rate signals over mixed-line-rate WDM optical networks for carrier ethernet. *IEEE/ACM Transactions on Networking*, 19(5):1304–1316, October 2011a.

[Batayneh *et al.*, 2011b] Batayneh, M.; Schupke, D.A.; Hoffmann, M.; Kirstaedter, A., and Mukherjee, B. Reliable multi-bit-rate VPN provisioning for multipoint carrier-grade ethernet services over mixed-line-rate WDM optical networks. *IEEE/OSA Journal of Optical Communications and Networking*, 3(1):66–76, January 2011b.

[Brinkhoff, 2014] Brinkhoff, Thomas. Population statistics for countries, administrative areas, cities and agglomerations. `http://www.citypopulation.de/`, 2014. (*last visited on 21 April 2014*).

[Chiu *et al.*, 2009] Chiu, A.L.; Choudhury, G.; Clapp, G.; Doverspike, R.; Gannett, J.W.; Klincewicz, J.; Li, Guangzhi; Skoog, R.A.; Strand, J.; Von Lehmen, A., and Xu, Dahai. Network design and architectures for highly dynamic next-generation ip-over-optical long distance networks. *Journal of Lightwave Technology*, 27(12):1878–1890, 2009.

[Choi *et al.*, 2002] Choi, H.; Subramaniam, S., and Choi, H.A. On double-link failure recovery in WDM optical networks. In *IEEE Annual Joint Conference of the IEEE Computer and Communications Societies - INFOCOM*, volume 2, pages 808–816, 2002.

[Cholda and Jajszczyk, 2007] Cholda, P. and Jajszczyk, A. Reliability assessment of optical p-cycles. *IEEE/ACM Transactions on Networking*, 15(6):1579–1592, December 2007.

[Cholda and Jajszczyk, 2010] Cholda, P. and Jajszczyk, A. Recovery and its quality in multilayer networks. *Journal of Lightwave Technology*, 28(4):372–389, 2010.

[Chu *et al.*, 2003] Chu, X.; Li, B., and Chlamtac, I. Wavelength converter placement under different RWA algorithms in wavelength-routed all-optical networks. *IEEE Transactions on Communications*, 51(4):607 – 617, April 2003.

[Chvatal, 1983] Chvatal, V. *Linear Programming*. Freeman, 1983.

[Cisco, 2013] Cisco, . Cisco Visual Networking Index: Forecast and Methodology, 2012-2017. `http://www.cisco.com/c/en/us/solutions/collateral/service-provider/ip-ngn-ip-next-generation-network/white_paper_c11-481360.html`, 2013. (*last visited on 21 April 2014*).

[Clouqueur and Grover, 2005a] Clouqueur, M. and Grover, W.D. Mesh-restorable networks with enhanced dual-failure restorability properties. *Photonic Network Communications*, 9(1):7–18, January 2005a.

[Clouqueur and Grover, 2005b] Clouqueur, M. and Grover, W.D. Availability analysis and enhanced availability design in p-cycle-based networks. *Photonic Network Communications*, 10(1):55–71, 2005b.

[Dantzig and Wolfe, 1960] Dantzig, G.B. and Wolfe, P. Decomposition Principle for Linear Programs. *Operations Research*, 8(1):101–111, 1960.

[Eiger *et al.*, 2012] Eiger, M.I.; Luss, H., and Shallcross, D.F. Network restoration under dual failures using path-protecting preconfigured cycles. *Telecommunication Systems*, 49(3):271–286, 2012.

[Eira *et al.*, 2012] Eira, A.; Pedro, J., and Pires, J. Cost-optimized dimensioning of translucent WDM networks with mixed-line-rate spectrum-flexible channels. In *IEEE 13th International Conference on High Performance Switching and Routing (HPSR)*, pages 185–190, 2012.

[Eshoul and Mouftah, 2009] Eshoul, A.E. and Mouftah, H.T. Survivability approaches using *p*-cycles in WDM mesh networks under static traffic. *IEEE/ACM Transactions on Networking (TON)*, 17(2):671–683, April 2009.

[Gerstel *et al.*, 2012] Gerstel, O.; Jinno, M.; Lord, A., and Yoo, S.J.B. Elastic optical networking: a new dawn for the optical layer? *IEEE Communications Magazine*, 50(2):12–20, February 2012.

[Grover and Doucette, 2002] Grover, W. D. and Doucette, J. Advances in optical network design with *p*-cycles: Joint optimization and pre-selection of candidate *p*-cycles. In *Proc. IEEE LEOS Summer Topical Meetings*, pages 49–50, July 2002.

[Grover and Stamatelakis, 1998] Grover, W. D. and Stamatelakis, D. Cycle-oriented distributed preconfiguration: Ring-like speed with mesh-like capacity for self-planning network restoration. In *IEEE International Conference on Communications - ICC*, pages 537–543, June 1998.

[Grover] Grover, W.D. `http://www.ece.ualberta.ca/grover/book/protected-material/`. Last visit on July 2011.

[Grue and Grover, 2007] Grue, A. and Grover, W. Comparison of *p*-cycles and *p*-trees in a unified mathematical framework. *Photonic Network Communications*, 14(2):123–133, 2007.

[Guangzhi *et al.*, 2012] Guangzhi, L.; Dongmei, W.; Gallivan, T., and Doverspike, R. On shared risk link group optimization [invited]. *IEEE/OSA Journal of Optical Communications and Networking*, 4(11):B52–B57, 2012.

[Higginbotham] Higginbotham, S. Verizon Delivers 100G Speeds to U.S. Internet Backbone. `http://gigaom.com/2011/03/30/verizon-delivers-100g-speeds-to-u-s-internet-backbone/`. (*last visited on 9 June 2013*).

[Houmaidi and Bassiouni, 2006] Houmaidi, M.E. and Bassiouni, M.A. Dependency-based analytical model for computing connection blocking rates and its application in the sparse placement of optical converters. *IEEE Transactions on Communications*, 54 (1):159–168, 2006.

[Huang *et al.*, 2007] Huang, C.C.; Li, M.Z., and Srinivasan, A. A scalable path protection mechanism for guaranteed network reliability under multiple failures. *IEEE Transactions on Reliability*, 56:254–267, June 2007.

[Huelsermann *et al.*, 2008] Huelsermann, R.; Gunkel, M.; Meusburger, C., and Schupke, D.A. Cost modeling and evaluation of capital expenditures in optical multilayer networks. *Journal of Optical Networking*, 7:814–833, 2008.

[IBM, 2011a] *IBM ILOG CPLEX 11.0 Optimization Studio*. IBM, 2011a.

[IBM, 2011b] *IBM ILOG CPLEX 12.0 Optimization Studio*. IBM, 2011b.

[Jaumard *et al.*, 2007] Jaumard, B.; Rocha, C.; Baloukov, D., and Grover, W. D. A column generation approach for design of networks using path-protecting *p*-cycles. In *Proceedings of IEEE/VDE Workshop on Design of Reliable Communication Networks - DRCN*, pages 1–8, October 2007.

[Jaumard *et al.*, 2009] Jaumard, B.; Meyer, C., and Thiongane, B. On column generation formulations for the RWA problem. *Discrete Applied Mathematics*, 157:1291–1308, March 2009.

[Javed *et al.*, 2007] Javed, M.; Thulasiraman, K., and Xue, G.L. Lightpaths routing for single link failure survivability in IP-over-WDM networks. *Journal of Communications and Networks*, 9(4):394, 2007.

[Javed *et al.*, 2006] Javed, M.S.; Thulasiraman, K.; Gaines, M.A., and Xue, G. Survivability aware routing of logical topologies: On Thiran-Kurant approach, enhancements and evaluation. In *IEEE Global Telecommunications Conference - GLOBECOM*, pages 1 –6, December 2006.

[Kan *et al.*, 2009] Kan, D.D.-J.; Narula-Tam, A., and Modiano, E. Lightpath routing and capacity assignment for survivable IP-over-WDM networks. In *Workshop on Design of Reliable Communication Networks - DRCN*, pages 37–44, oct. 2009.

[Kodian and Grover, 2005] Kodian, A. and Grover, W.D. Failure-independent path-protecting p-cycles efficient and simple fully preconnected optical-path protection. *Journal of Lightwave Technology*, 23(10):3241–3259, October 2005.

[Kodian *et al.*, 2005] Kodian, A.; Grover, W.D., and Doucette, J. A disjoint route sets approach to design of failure-independent path-protection p-cycle networks. In *Proceedings of IEEE/VDE Workshop on Design of Reliable Communication Networks - DRCN*, October 2005. 8pp.

[Korotky, 2012] Korotky, S.K. Traffic Trends: Drivers and Measures of Cost-Effective and Energy-Efficient Technologies and Architectures for Backbone Optical Networks. In *Optical Fiber Communication Conference*, pages 1–3. Optical Society of America, 2012.

[Kurant and Thiran, 2005] Kurant, M. and Thiran, P. On survivable routing of mesh topologies in IP-over-WDM networks. In *Annual Joint Conference of the IEEE Computer and Communications Societies - INFOCOM*, volume 2, pages 1106 – 1116, 2005.

[Kurant and Thiran, 2006] Kurant, M. and Thiran, P. Survivable routing in IP-over-WDM networks in the presence of multiple failures. In *EuroNGI Workshop on Traffic Engineering, Protection and Restoration for NGI*, pages 1–8, AGH University of Science and Technology, Krakow, Poland, 2006.

[Kurant and Thiran, 2007] Kurant, M. and Thiran, P. Survivable routing of mesh topologies in IP-over-WDM networks by recursive graph contraction. *IEEE Journal on Selected Areas in Communications*, 25(5):922 –933, 2007.

[Lasdon, 1970] Lasdon, L.S. *Optimization Theory for Large Systems.* MacMillan, New York, 1970.

[Li and Wang, 2004] Li, Tianjian and Wang, Bin. Cost effective shared path protection for wdm optical mesh networks with partial wavelength conversion. *Photonic Network Communications*, 8(3):251–266, 2004. ISSN 1387-974X.

[Lin *et al.*, 2011] Lin, T.; Zhou, Z., and Thulasiraman, K. Logical topology survivability in IP-over-WDM networks: Survivable lightpath routing for maximum logical topology capacity and minimum spare capacity requirements. In *Workshop on Design of Reliable Communication Networks - DRCN*, pages 1–8, 2011.

[Liu and Ruan, 2006a] Liu, C. and Ruan, L. Dynamic provisioning of survivable services using path-segment protecting p-cycles in WDM networks. In *International Conference on Computer Communications and Networks - ICCCN*, pages 275–280, October 2006a.

[Liu and Ruan, 2006b] Liu, C. and Ruan, L. p-Cycle design in survivable WDM networks with shared risk link groups (SRLGs). *Photonic Network Communications*, 11(3): 301–311, 2006b.

[Liu and Ruan, 2007] Liu, C. and Ruan, L. A new survivable mapping problem in IP-over-WDM networks. *IEEE Journal of Selected Areas in Communications*, 25(4):25–34, April 2007.

[Liu *et al.*, 2011] Liu, M.; Tornatore, M., and Mukherjee, B. Efficient shared subconnection protection in Mixed-Line-Rate optical WDM networks. In *Optical Fiber Communication Conference and Exposition (OFC/NFOEC), 2011 and the National Fiber Optic Engineers Conference*, pages 1–3. IEEE, 2011.

[Lübbecke and Desrosiers, 2005] Lübbecke, M.E. and Desrosiers, J. Selected topics in column generation. *Operations Research*, 53:1007–1023, 2005.

[Markopoulou *et al.*, 2008] Markopoulou, A.; Iannaccone, G.; Bhattacharyya, S.; Chuah, C.-N.; Ganjali, Y., and Diot, C. Characterization of failures in an operational IP backbone network. *IEEE/ACM Transactions on Networking*, 16(4):749–762, August 2008.

[Mauz, 2003] Mauz, C. p-Cycle protection in wavelength routed networks. In *IEEE International Conference on Optical Network Design and Management - ONDM*, Budapest, Hungary, February 2003.

[Modiano and Narula-Tam, 2001] Modiano, E. and Narula-Tam, A. Survivable routing of logical topologies in WDM networks. In *Annual Joint Conference of the IEEE Computer and Communications Societies - INFOCOM*, pages 348 – 357, 2001.

[Modiano and Narula-Tam, 2002] Modiano, E. and Narula-Tam, A. Survivable lightpath routing: a new approach to the design of WDM-based networks. *IEEE Journal of Selected Areas in Communications*, 20(4):800–809, 2002.

[Mukherjee *et al.*, 2006] Mukherjee, D. S.; Assi, C., and Agarwal, A. An alternative approach for enhanced availability analysis and design methods in p-cycle-based networks. *IEEE Journal on Selected Areas in Communications*, 24:23–34, December 2006.

[Nag *et al.*, 2010] Nag, A.; Tornatore, M., and Mukherjee, B. Optical network design with mixed line rates and multiple modulation formats. *Journal of Lightwave Technology*, 28(4):466–475, 2010.

[Nguyen *et al.*, 2006] Nguyen, H.N.; Habibi, D.; Phung, V.Q.; Lachowicz, S.; Lo, K., and Kang, B. Joint optimization in capacity design of networks with p-cycle using the fundamental cycle set. In *IEEE Global Telecommunications Conference - GLOBECOM*, 2006.

[Nguyen *et al.*, 2010] Nguyen, H.N.; Habibi, D., and Phung, V.Q. Efficient optimization of network protection design with p-cycles. *Photonic Network Communications*, 19 (1):22–31, 2010.

[O'Mahony *et al.*, 1995] O'Mahony, M.J.; Simeonidu, D.; Yu, A., and Zhou, J. The design of the European optical network. *Journal of Ligthwave Technology*, 13(5):817–828, 1995.

[Orlowski and Pióro, 2011] Orlowski, S. and Pióro, M. On the complexity of column generation in survivable network design with path-based survivability mechanisms. *Networks*, 2011. to appear.

[Orlowski *et al.*, 2007] Orlowski, S.; Pióro, M.; Tomaszewski, A., and Wessäly, R. SNDlib 1.0–Survivable Network Design Library. In *Proceedings of the 3rd International Network Optimization Conference (INOC 2007), Spa, Belgium*, April 2007.

[Pinto-Roa *et al.*, 2013] Pinto-Roa, D.P.; Baran, B., and Brizuela, C.A. A multi-objective approach for routing and wavelength converter allocation under uncertainty. In *20th International Conference on Telecommunication*, pages 1–5, 2013.

[Ramamurthy *et al.*, 2003] Ramamurthy, S.; Sahasrabuddhe, L., and Mukherjee, B. Survivable WDM mesh networks. *Journal of Lightwave Technology*, 21(4):870–883, 2003.

[Ramasubramanian and Chandak, 2008] Ramasubramanian, S. and Chandak, A. Dual-link failure resiliency through backup link mutual exclusion. *IEEE/ACM Transactions on Networking*, 16(1):539–548, 2008.

[Ramaswami *et al.*, 2009] Ramaswami, R.; Sivarajan, K.N., and Sasaki, G.H. *Optical Networks - A Practical Perspective*. Morgan Kaufmann, 3nd edition edition, 2009.

[Rocha and Jaumard, 2012] Rocha, C. and Jaumard, B. Efficient computation of FIPP p-cycles. *to appear in Telecommunications Systems*, 2012.

[Rocha *et al.*, 2012] Rocha, C.; Jaumard, B., and Stidsen, T. A hierarchical decomposition method for efficient computation of path-protecting p-cycles. *to appear in Telecommunications Systems*, 2012.

[Santos *et al.*, 2012] Santos, J.; Pedro, J.; Monteiro, P., and Pires, J. Optimization Framework for Supporting 40 Gb/s and 100 Gb/s Services over Heterogeneous Optical Transport Networks. *Journal of Networks*, 7(5), 2012.

[Schupke *et al.*, 2002] Schupke, D.A.; Gruber, C.G., and Autenrieth, A. Optimal configuration of p-cycles in WDM networks. In *IEEE International Conference on Communications - ICC*, volume 5, pages 2761 – 2765, 2002.

[Schupke *et al.*, 2003] Schupke, D.A.; Scheffel, M.C., and Grover, W.D. Configuration of p-Cycles in WDM Networks with Partial Wavelength Conversion. *Photonic Network Communications*, 6(3):239–252, 2003.

[Schupke *et al.*, 2004] Schupke, D.A.; Grover, W.D., and Clouqueur, M. Strategies for enhanced dual failure restorability with static or reconfigurable p-cycle networks. In *IEEE International Conference on Communications - ICC*, volume 3, pages 1628– 1633, June 2004.

[Sebbah and Jaumard, 2009] Sebbah, S. and Jaumard, B. Dual failure recovery in WDM networks based on p-cycles. In *International Conference on Optical Networking Design and Modeling - ONDM*, Braunschweig, Germany, 2009.

[Sebbah and Jaumard, 2010] Sebbah, S. and Jaumard, B. Design of survivable WDM networks using pre-configured protection structures with unrestricted shapes. *Photonic Netowrk Communications*, 9(1):9–21, 2010.

[Shah-Heydari and Yang, 2004] Shah-Heydari, S. and Yang, O. Hierarchical protection tree scheme for failure recovery in mesh networks. *Photonic Network Communications*, 7(2):145–149, 2004.

[Shen *et al.*, 2005] Shen, L.; Yang, X., and Ramamurthy, B. Shared risk link group (srlg)-diverse path provisioning under hybrid service level agreements in wavelength-routed optical mesh networks. *IEEE/ACM Transactions on Networking*, 13:918 – 931, August 2005.

[Simmons, 2005] Simmons, J.M. On determining the optimal optical reach for a long-haul network. *Journal of Lightwave Technology*, 23(3):1039–1048, march 2005.

[Singh *et al.*, 2008] Singh, P.; Sharma, A.K., and Rani, S. Minimum connection count wavelength assignment strategy for WDM optical networks. *Optical Fiber Technology*, 14(2):154 – 159, 2008.

[Stidsen and Thomadsen, 2004] Stidsen, T. and Thomadsen, T. Joint optimization of working and *p*-cycle protection capacity. Technical report, Technical Univ. of Denmark, 2004.

[Strand *et al.*, 2001] Strand, J.; Chiu, A.L., and Tkach, R. Issues for routing in the optical layer. *IEEE Communications Magazine*, 39(2):81–87, feb 2001.

[Subramaniam *et al.*, 1999] Subramaniam, S.; Azizoglu, M., and Somani, A.K. On optimal converter placement in wavelength-routed networks. *IEEE/ACM Transactions on Networking*, 7(5):754–766, 1999.

[Szigeti and Cinkler, 2011] Szigeti, J. and Cinkler, T. Evaluation and estimation of the availability of p-cycle protected connections. *Telecommunication Systems*, pages 1–16, 2011.

[Tapolcai *et al.*, 2013] Tapolcai, J.; Ho, P.-H.; Babarczi, P., and Ronyai, L. On signaling-free failure dependent restoration in all-optical mesh networks. *IEEE/ACM Transactions on Networking*, PP(99):1–12, 2013.

[**Hoang Hai Anh** and Jaumard, 2011] **Hoang Hai Anh**, and Jaumard, Brigitte. **RWA and p-Cycles**. In *Ninth Annual Communication Networks and Services Research Conference (CNSR)*, pages 195–201, May 2011.

[Thulasiraman *et al.*, 2009a] Thulasiraman, K.; Javed, M.; Lin, T., and Xue, G. Logical topology augmentation for guaranteed survivability under multiple failures in IP-over-WDM optical network. In *IEEE 3rd Int'l Symposium on Advanced Networks and Telecommunication Systems*, pages 1 –3, December 2009a.

[Thulasiraman *et al.*, 2009b] Thulasiraman, K.; Javed, M.S., and Xue, G. Circuits/cutsets duality and a unified algorithmic framework for survivable logical topology design in IP-over-WDM optical networks. In *Annual Joint Conference of the IEEE Computer and Communications Societies - INFOCOM*, pages 1026 –1034, april 2009b.

[Thulasiraman *et al.*, 2010] Thulasiraman, K.; Javed, M., and Xue, G. Primal meets dual: A generalized theory of logical topology survivability in IP-over-WDM optical networks. In *Second International Conference on Communication Systems and Networks (COMSNETS)*, pages 1–10, 2010.

[Tianjian and Bin, 2006] Tianjian, L. and Bin, W. On Optimal p-Cycle-Based Protection in WDM Optical Networks With Sparse-Partial Wavelength Conversion. *IEEE Transactions on Reliability*, 55(3):496–506, 2006.

[Todimala and Ramamurthy, 2007] Todimala, A. and Ramamurthy, B. A scalable approach for survivable virtual topology routing in optical WDM networks. *IEEE Journal of Selected Areas in Communications*, 23(6):63–69, August 2007.

[Tran and Killat, 2008] Tran, P.N. and Killat, U. An exact ilp formulation for optimal wavelength converter usage and placement in wdm networks. In *IEEE Global Telecommunications Conference*, pages 1–6, 2008.

[Vanderbeck, 1994] Vanderbeck, F. *Decomposition and Column Generation for Integer Programs.* PhD thesis, Universite Catholique de Louvain, 1994.

[Wu *et al.*, 2010a] Wu, B.; Yeung, K.L., and Ho, P.-H. ILP formulations for non-simple p-cycle and p-trail design in WDM mesh networks. *Computer Networks*, 54(5): 716–725, 2010a.

[Wu *et al.*, 2010b] Wu, Bin; Yeung, Kwan L., and Ho, Pin-Han. ILP Formulations for P-cycle Design Without Candidate Cycle Enumeration. *IEEE/ACM Transactions on Networking*, 18(1):284–295, February 2010b. ISSN 1063-6692.

[Wu and Lau, 1992] Wu, T.H. and Lau, R.C. A class of self-healing ring architectures for SONET network applications. *IEEE Transactions on Communications*, 40(11): 1746–1756, 1992.

[Xi *et al.*, 2005] Xi, K.; Arakawa, S., and Murata, M. How many wavelength converters do we need? In *Conference on Optical Network Design and Modeling*, pages 347–358, 2005.

[Xiao and Leung, 1999] Xiao, G. and Leung, Y.W. Algorithms for allocating wavelength converters in all-optical networks. *IEEE/ACM Transactions on Networking*, 7(4): 545 – 557, August 1999.

[Xiao *et al.*, 2004] Xiao, G.; Lu, K., and Chlamtac, I. An evaluation of distributed wavelength provisioning in WDM optical networks with sparse wavelength conversion. *Journal of Lightwave Technology*, 22(7):1668 – 1678, July 2004.

[Xie *et al.*, 2012] Xie, W.; Jue, J.P.; Wang, X.; Zhang, Q.; She, Q.; Palacharla, P., and Sekiya, M. Regenerator site selection for mixed line rate optical networks with flexible routing. In *16th International Conference on Optical Network Design and Modeling (ONDM)*, pages 1–6, 2012.

[Yuan and Wang, 2011] Yuan, S. and Wang, B. Highly available path routing in mesh networks under multiple link failures. *IEEE Transactions on Reliability*, 60(4): 823–832, 2011.

[Zhao *et al.*, 2013] Zhao, J.; Subramaniam, S., and Brandt-Pearce, M. QoT-aware Grooming, Routing, and Wavelength Assignment (GRWA) for Mixed-Line-Rate translucent optical networks. *China Communications*, 10(1):17–30, 2013.

[Zheng and Mouftah, 2004] Zheng, J. and Mouftah, H. *Optical WDM Networks.* Wiley Interscience, 2004.